

1993

Microfabric Analysis of the Northern Part of the Pelham Dome, Central Massachusetts

Robert M. Reed
University of Massachusetts Amherst

Follow this and additional works at: <https://scholarworks.umass.edu/theses>

Reed, Robert M., "Microfabric Analysis of the Northern Part of the Pelham Dome, Central Massachusetts" (1993). *Masters Theses 1911 - February 2014*. 3526.
<https://doi.org/10.7275/8m2k-b416>

This thesis is brought to you for free and open access by ScholarWorks@UMass Amherst. It has been accepted for inclusion in Masters Theses 1911 - February 2014 by an authorized administrator of ScholarWorks@UMass Amherst. For more information, please contact scholarworks@library.umass.edu.

**MICROFABRIC ANALYSIS OF THE NORTHERN PART OF THE PELHAM
DOME, CENTRAL MASSACHUSETTS**

A Thesis Presented

by

Robert M. Reed

Approved as to style and content by:

Dr. Michael L. Williams, Chair _____

Dr. George E. McGill, Member _____

Dr. Peter Robinson, Member _____

**Dr. George E. McGill, Department Head
Department of Geology and Geography**

**MICROFABRIC ANALYSIS OF THE NORTHERN PART OF THE PELHAM
DOME, CENTRAL MASSACHUSETTS**

A Thesis Presented

by

ROBERT M. REED

**Submitted to the Graduate School of the
University of Massachusetts in partial fulfillment
of the requirements for the degree of**

MASTER OF SCIENCE

February 1993

Department of Geology and Geography

ACKNOWLEDGMENTS

Field work for this project was partially funded by two grants-in-aid from Sigma Xi, the Scientific Research Society, and the Department of Geology and Geography of the University of Massachusetts at Amherst.

I would like to thank my advisor Dr. Michael Williams for his unflagging support during this project. In addition to serving on my committee, Dr. Peter Robinson originally brought this project to my attention. Dr. George McGill proved especially helpful on technical aspects of editing the thesis.

Of the students at the University of Massachusetts, I would especially thank David Snoeyenbos whose help was invaluable. I would also thank Ginny, Jon, Jenny, Ali, Frank, George, Pete, Mike, Dave E., Vinny and especially Jim for help in various facets of the research process.

Dr. Donald U. Wise provided much needed moral guidance. Dr. Ronald Lavigne of the Department of Plant and Soil Sciences provided employment for a longer period of time than any other source during the study. Members of my Ph.D. committee at the University of Texas at Austin were extraordinarily patient with me during the period in which I was finishing this thesis.

Almost all of the figures in this thesis were drawn or redrawn with Adobe Illustrator.

ABSTRACT

MICROFABRIC ANALYSIS OF THE NORTHERN PART OF THE PELHAM DOME, CENTRAL MASSACHUSETTS

FEBRUARY 1993

ROBERT M. REED, B.S., UNIVERSITY OF TEXAS AT AUSTIN

M.S., UNIVERSITY OF MASSACHUSETTS

Directed by: Professor Michael L. Williams

A microfabric study conducted in the northern part of the Pelham gneiss dome, central Massachusetts, has shown that the dome fabric is dominated by a relatively homogeneous, pervasive top-to-the-south shearing. Evidence consists of numerous kinematic indicators including: S-C fabrics, asymmetric winged porphyroclasts, asymmetric strain shadows, asymmetrically-boudinaged pegmatites, and asymmetric folds. Shear-related fabrics are present throughout the exposed section, from the lowest exposed gneissic rocks to the uppermost units in the cover section. Some textural evidence exists to suggest that this shearing diminishes slightly in intensity with structural depth. Reconnaissance indicates that shear fabrics are present throughout the Pelham dome and perhaps in adjacent areas of the Bronson Hill anticlinorium.

Porphyroblasts within pelitic units contain inclusion trails which preserve evidence for at least one, and probably two, previous foliations occurring at a high angle to the shear fabric. Both the shear fabric and the one certain previous fabric seem to have formed at similar amphibolite-grade metamorphic conditions. Kyanite,

the peak metamorphic mineral present in these assemblages, seems to have formed both before and after the shearing, with the majority overgrowing the shear-related foliation.

Fabrics within the Pelham dome are inconsistent with the Pelham dome having formed through solid-state diapirism. The concentric, oval foliation and shallow N-S lineation are clearly associated with top-to-the-south subhorizontal shearing. Several alternative mechanisms for dome formation have been examined, and none has proven completely satisfactory. The most likely mechanism is that the Pelham dome is a low-strain pod within a very large ductile shear regime.

Interpretations of the tectonics of the deformation seen here are complicated by uncertainty over the age of deformation. It is probable that some component of the deformation is Pennsylvanian in age (Gromet and Robinson, 1990), but other elements are probably Acadian. Serious questions about timing, style of deformation, and direction of shear undermine the direct correlation of shearing in the Pelham dome and shearing in the Willimantic dome suggested by Getty (1990).

TABLE OF CONTENTS

	<u>Page</u>
ACKNOWLEDGEMENTS	iii
ABSTRACT	iv
LIST OF FIGURES	x
LIST OF PLATES	xiv
 Chapter	
1. INTRODUCTION	1
The Pelham Dome	1
Purpose of This Study	3
Geologic Setting	7
Stratigraphy	7
Structural Geology	15
Tectonics	20
Location of Study	21
Methods of Study	22
2. MICROFABRICS AND KINEMATIC INDICATORS	23
Descriptions of Microfabrics	23
Foliation	23
Lineation	24
Kinematic Indicators	26
Porphyroclast/Porphyroblast Systems	27
Asymmetric Recrystallized Tails	27
Asymmetric Pressure or Strain Shadows	29
Quarter Structures	39
S-C Fabrics	39
Foliation or Mica Fish	45
Micro-scale Asymmetric Folds	47
Extensional Crenulation Cleavages	51
Broken Grains or Asymmetric Pull-aparts	53

Non-Kinematic Microfabrics	55
Crystallographic Preferred Orientation	55
Deformation, Recovery, and Recrystallization	
Features in Minerals	55
Quartz Features	58
Feldspar Features	59
Post-Shearing Microfabrics	61
Kinematic Indicators in Outcrop	63
Asymmetric Folds	63
Asymmetrically-boudinaged Pegmatites	65
Analysis of Shear Fabrics	68
Extent of Shearing in the Pelham dome	68
Possible Extent of Shearing in the Bronson	
Hill Anticlinorium	70
Quantification of Shear Strain	74
Relative Magnitude of Shear Strain	78
Textural Criteria for Shear Development	79
Feldspar Textures	79
Preferred Orientation of Quartz C-Axes	81
Foliation Development	83
Recrystallized Grain Size	83
Shear Intensity in the Poplar Mountain Gneiss	83
Shear Intensity in Quartzites	85
Shear and Previously Documented Deformational Phases	87
3. RELATIVE TIMING OF METAMORPHISM AND DEFORMATION .	92
Introduction	92
Metamorphic Events in the Pelham Dome Area	92
Fabric/Porphyroblast Relations	96
Formation of Inclusion Trails in Porphyroblasts	97
Formation of Curved Inclusion Trails	97

Fabric/Porphyroblast Relations in the Pelham Dome	102
Fabric/Porphyroblast Relations of Garnets	104
Fabric/Porphyroblast Relations of Staurolites	110
Fabric/Porphyroblast Relations of Kyanites	119
Fabric/Porphyroblast Relations of Biotites	123
Fabric/Porphyroblast Relations of Plagioclases	125
Fabric/Porphyroblast Relations of Amphiboles	126
Summary of Inclusion Fabrics	127
Relative Timing of Mineral Growth	131
Relationship of Inclusion Fabrics to Deformational Events	136
Peak of Metamorphism	138
Timing of Other Metamorphic Events	139
Relict Sillimanite-Potassium Feldspar Metamorphism	139
Retrograde Metamorphism	142
4. FORMATION MECHANISM OF THE PELHAM DOME	146
Introduction	146
Definition of a Mantled Gneiss Dome	146
Relationship of Ductile Shearing and Dome Formation in the Pelham Dome	148
Dome Formation Mechanisms	149
Solid-State Gravitational Models	152
Refolded Folds	154
Sheath Folds	155
Thrust Fault Associated Folding	159
Mega-Boudinage	160
Summary and Conclusions	163
5. REGIONAL TECTONICS	166
Timing of Deformation	166
Suggested Correlations with Avalonian and Alleghanian Events	167
Possible Correlation with Avalonian Rocks	167
Suggested Deformational Correlation with the Willimantic dome	169

	Absolute Timing of Deformation: Evidence From Fabrics	170
	Possible Alleghanian Tectonic Correlations	173
6.	CONCLUSIONS	174
	BIBLIOGRAPHY	180

LIST OF FIGURES

Figure	Page
1.1. Major geological features of central Massachusetts and adjacent areas.	2
1.2. Metamorphic zones of central Massachusetts.	4
1.3. Map of the northern part of the Pelham dome, showing the location of the thesis field area.	5
1.4. Stratigraphic column for the Pelham dome.	8
1.5. Cartoon of the sequence of major deformations in the Bronson Hill anticlinorium and Merrimack belt, central Massachusetts and adjacent New Hampshire.	17
2.1. Regional map showing representative orientation and distribution of backfold- and dome-stage lineations across central Massachusetts.	25
2.2. Kinematic indicators seen in the northern part of the Pelham dome that involve asymmetries around porphyroclasts or porphyroblasts.	28
2.3. Asymmetric recrystallized tails from the northern part of the Pelham dome.	30
2.4. Asymmetric strain (pressure) shadows occurring on porphyroblasts from the northern part of the Pelham dome.	36
2.5. Photomicrograph of a quarter structure developed on a garnet indicating top-to-the-south sense of shear.	40
2.6. Kinematic indicators seen in the northern part of the Pelham dome that involve asymmetries of foliation and/or layering.	42
2.7. S-C fabrics from the northern part of the Pelham dome.	43
2.8. Photomicrograph of a mica fish indicating top-to-the-south sense of shear.	46

LIST OF FIGURES

Figure	Page
1.1. Major geological features of central Massachusetts and adjacent areas.	2
1.2. Metamorphic zones of central Massachusetts.	4
1.3. Map of the northern part of the Pelham dome, showing the location of the thesis field area.	5
1.4. Stratigraphic column for the Pelham dome.	8
1.5. Cartoon of the sequence of major deformations in the Bronson Hill anticlinorium and Merrimack belt, central Massachusetts and adjacent New Hampshire.	17
2.1. Regional map showing representative orientation and distribution of backfold- and dome-stage lineations across central Massachusetts.	25
2.2. Kinematic indicators seen in the northern part of the Pelham dome that involve asymmetries around porphyroclasts or porphyroblasts.	28
2.3. Asymmetric recrystallized tails from the northern part of the Pelham dome.	30
2.4. Asymmetric strain (pressure) shadows occurring on porphyroblasts from the northern part of the Pelham dome.	36
2.5. Photomicrograph of a quarter structure developed on a garnet indicating top-to-the-south sense of shear.	40
2.6. Kinematic indicators seen in the northern part of the Pelham dome that involve asymmetries of foliation and/or layering.	42
2.7. S-C fabrics from the northern part of the Pelham dome.	43
2.8. Photomicrograph of a mica fish indicating top-to-the-south sense of shear.	46

2.9.	Asymmetric micro- and macro-folds from the northern part of the Pelham dome.	48
2.10.	Photomicrograph of a poorly-developed extensional crenulation cleavage or shear band in a pelitic rock indicating top-to-the-south sense of shear.	52
2.11.	Sense of shear determination from asymmetrical pull-aparts or broken grains.	54
2.12.	Photomicrograph showing a broken plagioclase grain.	56
2.13.	Photomicrograph showing preferred orientation of quartz c-axes.	57
2.14.	Photomicrograph showing brittle deformation cross-cutting shear-related fabrics.	62
2.15.	Asymmetrically-boudinaged pegmatites from the northern part of the Pelham dome.	66
2.16.	Equal-area stereographic plots of mineral lineations from the Belchertown Intrusive Complex and the country rock surrounding it.	72
2.17.	Angular shear of a deformed pegmatite from the Dry Hill Formation	75
2.18.	Photomicrograph showing zoned development of tartan twinning in a microcline porphyroclast.	82
2.19.	Sketch from Onasch (1973) showing supposedly rotated amphibolite lens in the Biotite Member of the Dry Hill Gneiss.	88
2.20.	Shear of reverse sense from the Poplar Mountain Quartzite.	89
2.21.	Development of reverse sense shears in the northern part of the Pelham dome.	91
3.1.	AFM diagram showing phase relations of pelitic units in the northern part of the Pelham dome.	94

3.2.	Classic diagnostic forms for porphyroblast inclusion patterns with regard to time and deformation.	98
3.3.	The six steps of progressive foliation development through tightening of a differentiated crenulation cleavage.	101
3.4.	Model showing the progressive development of spiral-shaped (helicoïdal) inclusion trails in a garnet porphyroblast	103
3.5.	Photomicrograph of a garnet with sigmoidal crenulated inclusion pattern.	105
3.6.	Photomicrograph of two garnets with helicoïdal inclusion fabrics.	105
3.7.	Garnets with straight inclusion patterns from the northern part of the Pelham dome.	108
3.8.	Photomicrograph of a garnet that truncates the dominant foliation.	111
3.9.	Staurolites with sigmoidal inclusion fabrics from the northern part of the Pelham dome.	112
3.10.	Staurolites with straight inclusion trails from the northern part of the Pelham dome.	114
3.11.	Photomicrograph of two garnets included in a large staurolite which also has fine graphite inclusion trails.	118
3.12.	Kyanites with straight inclusion fabrics from the northern part of the Pelham dome.	120
3.13.	Photomicrograph of a biotite with crenulated graphite-inclusion pattern.	124
3.14.	Common porphyroblast inclusion geometries seen in the northern part of the Pelham dome.	128
3.15.	Timing of growth of major porphyroblastic minerals from pelitic rocks in the Pelham dome area.	132

3.16.	Post-shearing garnet overgrowth in the northern part of the Pelham dome.	133
3.17.	Photomicrograph of a garnet from a calc-silicate pod from the Poplar Mountain Quartzite.	140
3.18.	Muscovite replacing a staurolite? porphyroblast in the Littleton Formation from the northern part of the Pelham dome.	143
4.1.	Some possible mechanisms of dome formation.	150
4.2.	Cross-section of an experimentally-derived strain grid for an immature diapiric structure model.	153
4.3.	Structural features of a large sheath fold forming a domal structure in outcrop.	156
4.4.	Shear senses along the edges of boudins during extension or pure shear.	161
4.5.	Patterns of strain in a rock undergoing heterogeneous shear with the development of low strain pods and shear-dominated high strain zones.	161
5.1.	Direction of shearing within the Pelham and Willimantic domes.	168

LIST OF PLATES

Plate	Page
1. Sample Locations and Geologic Map of Metamorphic Rocks: Northern Part of the Pelham Dome.	In pocket

CHAPTER 1

INTRODUCTION

The Pelham Dome

The Bronson Hill anticlinorium of the New England Appalachians consists of a series of en-echelon mantled gneiss domes (Eskola, 1949; Billings, 1956; Thompson and others, 1968) (Figure 1.1). These domes typically consist of a core of predominantly gneissic rocks, mainly Late Ordovician plagioclase gneisses, with a mantle of Late Ordovician to Early Devonian metamorphosed sedimentary and volcanic cover rocks (Thompson and others, 1968; Robinson and Hall, 1980).

The Pelham gneiss dome is located on the western edge of the Bronson Hill anticlinorium just to the east of the Mesozoic Connecticut Valley border fault (Figure 1.1). The dome is defined by an elongate north-south trending foliation arch with a well developed, shallowly-plunging, north-south trending mineral lineation. The Pelham dome is atypical for gneiss domes in the Bronson Hill anticlinorium in that, in addition to Ordovician plagioclase gneiss, it contains gneisses of late Proterozoic age (Naylor and others, 1973; Zartman and Naylor, 1984; Tucker and Robinson, 1990). The Pelham dome area has been affected by several phases of deformation (Ashenden, 1973; Onasch, 1973; Laird, 1974; Robinson, 1979; Michener, 1983) but the deformational fabric is dominated by a single strong foliation and a mineral lineation that were apparently produced during a major late-tectonic shearing event (Reed and

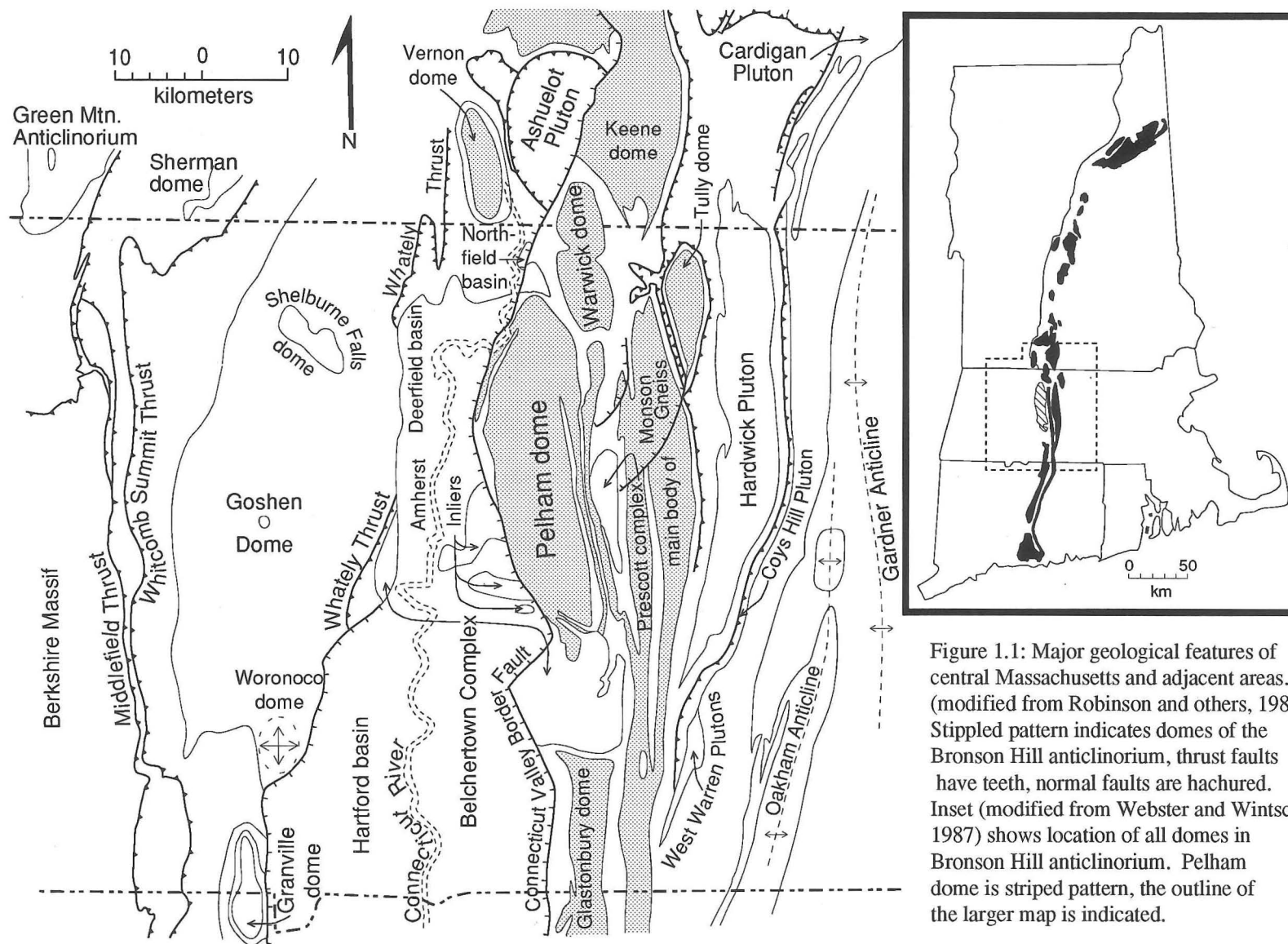


Figure 1.1: Major geological features of central Massachusetts and adjacent areas. (modified from Robinson and others, 1986) Stippled pattern indicates domes of the Bronson Hill anticlinorium, thrust faults have teeth, normal faults are hachured. Inset (modified from Webster and Wintsch, 1987) shows location of all domes in Bronson Hill anticlinorium. Pelham dome is striped pattern, the outline of the larger map is indicated.


Williams, 1989). The dominant regional metamorphism reached the amphibolite facies with kyanite-staurolite-biotite-garnet assemblages present in some pelitic rocks (Zone Ik of Robinson, 1983; Figure 1.2). Evidence for a relict granulite facies metamorphism is preserved in the Mt. Mineral Formation, originally assigned to the Proterozoic (Roll, 1987).

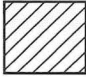
Purpose of This Study

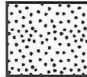
Very little work has previously been done on microfabrics and associated kinematic indicators in the Pelham dome. The main purpose of this study is to identify and to describe ductile microfabrics present in rocks of the northern part of the Pelham dome (Figure 1.3), especially those fabrics associated with the ductile shearing. Extent and intensity of the ductile top-to-the-south shearing have been documented. Porphyroblast inclusion geometries have been interpreted to determine relative timing of deformation and metamorphism. The relationship between the shear fabrics and microfabrics produced by other deformational phases has been examined for clues to relative timing. The study has also incorporated the ductile shearing more fully into the structural interpretation of the Pelham dome. Finally it is hoped that the study has shed light on the overall processes involved with gneiss dome formation and the role of gneiss domes in the evolution of an orogenic belt.

Metamorphic Zones

- VI Garnet-Cordierite-Sillimanite-K-feldspar
- V Sillimanite-K-feldspar
- IV Sillimanite-Muscovite-K-feldspar
- III Sillimanite-Muscovite
- II Sillimanite-Staurolite-Muscovite
- I_k Kyanite-Staurolite-Muscovite
- G Garnet
- B Biotite
- C Chlorite

 Zones of thorough retrograde metamorphism at New Salem and Quabbin Hill

 Probable extent of relict Sillimanite-K-feldspar metamorphism within the core of the Pelham dome

 Mesozoic sedimentary and volcanic rocks

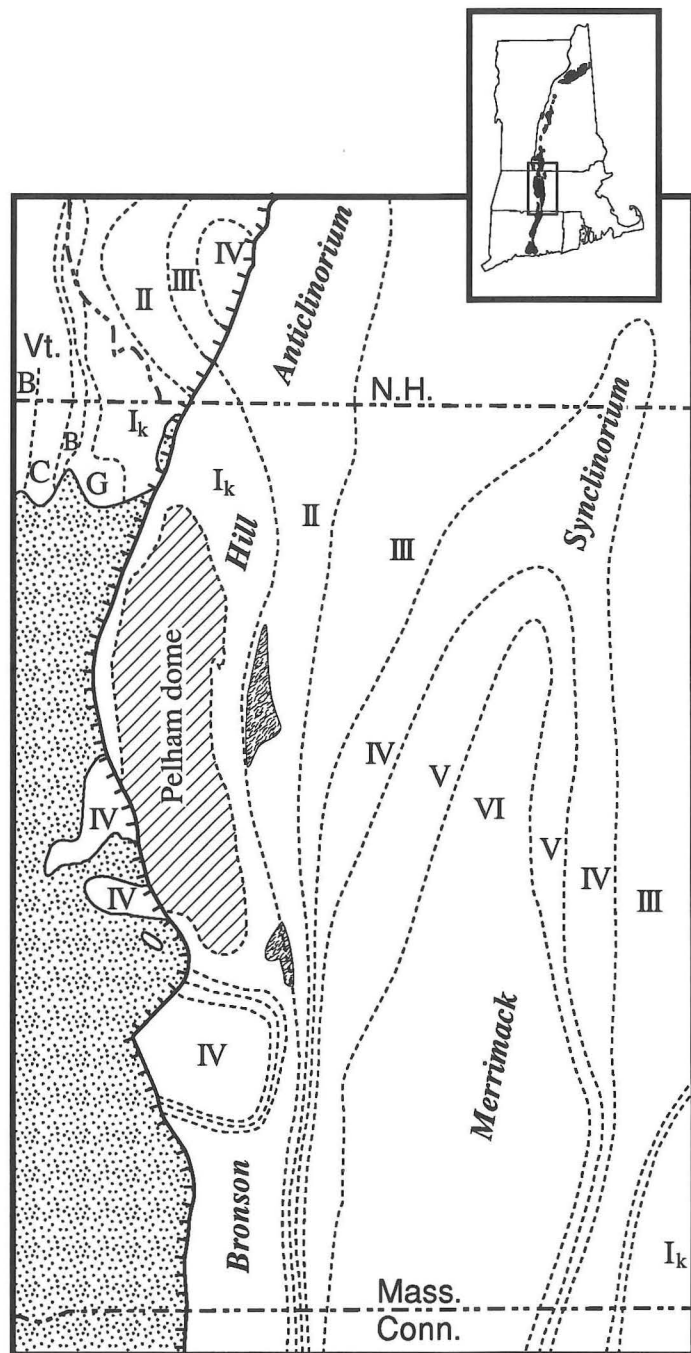


Figure 1.2. Metamorphic zones of central Massachusetts. (Modified from Robinson, 1983) Inset map shows domes of Bronson Hill anticlinorium and the area of the larger map.

Explanation

Silurian and Devonian

 Erving, Littleton and Clough Formations

Ordovician


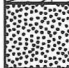
 Partridge Formation and Ammonoosuc Volcanics





 Fourmile Gneiss

Silurian, Ordovician and possibly late Proterozoic

 Mt. Mineral Formation

Late Proterozoic

 Poplar Mountain Gneiss
 Gneiss Member and Undifferentiated
Quartzite Member

 Dry Hill Gneiss
 Pelham Quartzite Member
 Biotite Member
 Hornblende Member

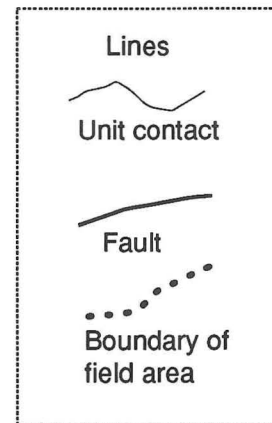
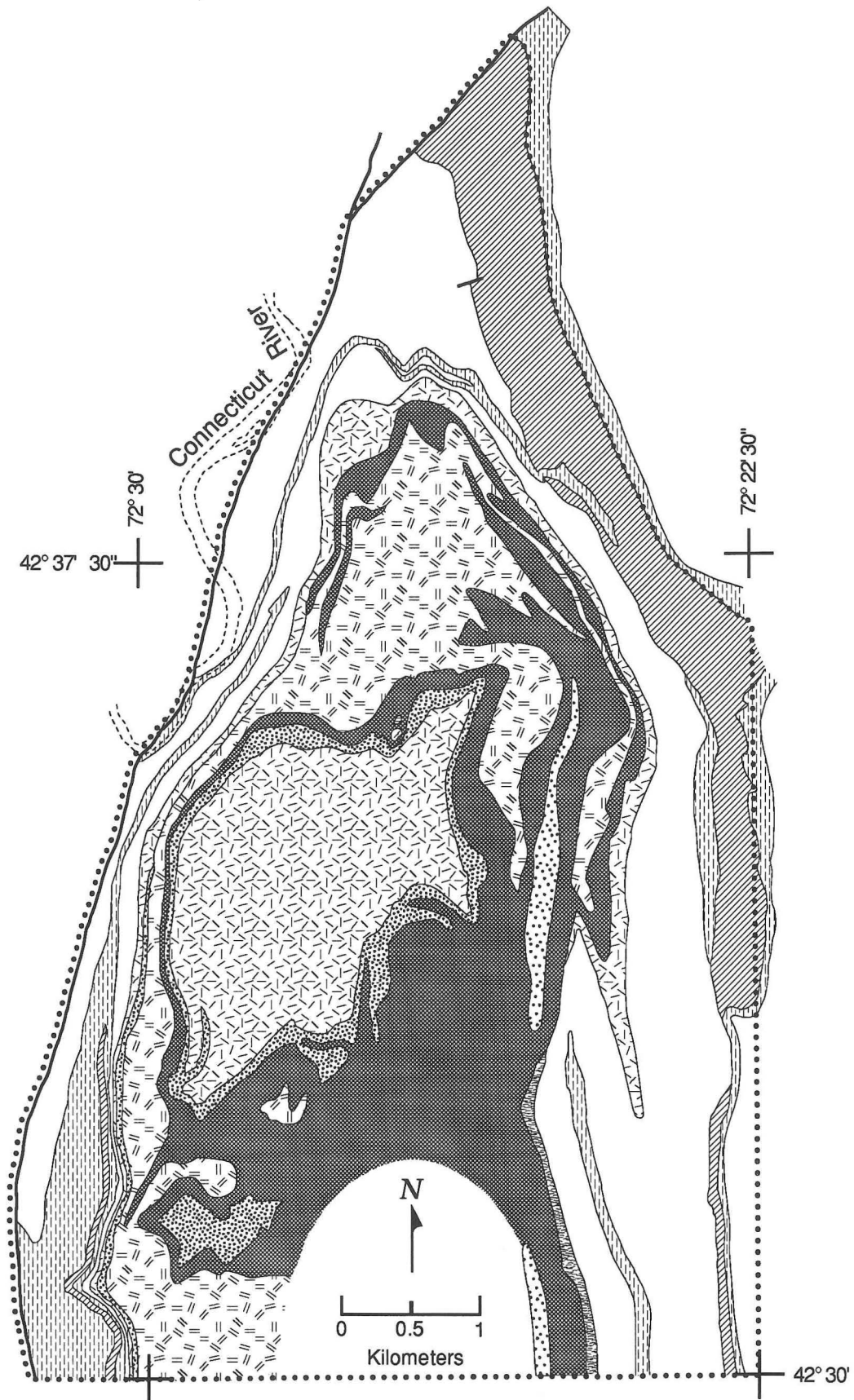


Figure 1.3: Map of the northern part of the Pelham dome, showing the location of the thesis field area. Based on original maps of Robinson (1963, 1967), Onasch (1973), Ashenden (1973), Laird (1974), Michener (1983), and Robinson, Ashenden, and Onasch (unpublished).



Geologic Setting

The Pelham dome is part of a larger structural province known as the Bronson Hill anticlinorium which occupies a central position in the New England Appalachians. This anticlinorium contains deformed sedimentary and volcanic rocks of two major depositional belts, the Connecticut Valley belt and the Merrimack belt (Hatch and others, 1984), as well as Ordovician and Proterozoic rocks which had previously been minorly involved in the Taconian orogeny. Located immediately to the west of the anticlinorium is the Acadian Connecticut Valley-Gaspé synclinorium. The Connecticut Valley-Gaspé synclinorium contains a series of domes somewhat similar to those found in the Bronson Hill anticlinorium (Figure 1.1). Further west, across the probable Taconian suture (Stanley and Ratcliffe, 1985) are the rocks of the Berkshire massif and the Taconic allochthons. Directly to the east of the synclinorium is the Merrimack belt (Kearrsarge-Central Maine synclinorium). Late Triassic to Early Jurassic rifting has superimposed the Northfield, Deerfield, and Hartford basins onto the Connecticut Valley synclinorium and the western edge of the Bronson Hill anticlinorium.

Stratigraphy

The stratigraphic sequence in the Pelham dome area is complex and somewhat controversial. In general, the sequence consists of gneissic units in the core, overlain by metamorphosed sedimentary and volcanic cover rocks (Figure 1.4). In the northern

Figure 1.4. Stratigraphic column for the Pelham dome.
[Radiometric ages from Tucker and Robinson (1990)]

Lower Devonian Erving Fm. **Deg**: interlayered granular feldspar-biotite rock and biotite-garnet-staurolite-kyanite schist **Dea**: epidote amphibolite

Lower Devonian Littleton Fm. **Dl**: graphitic muscovite-biotite-garnet-staurolite schist

Silurian Clough Quartzite **Sc**: muscovitic quartzite, commonly conglomeratic

Ordovician Partridge Fm. **Ops**: rusty-weathering quartz-biotite-muscovite-garnet schist with minor quartzite, amphibolite, and felsic gneiss

Ordovician Ammonoosuc Volcanics **Oa**: amphibolites and felsic gneiss

Ordovician Four Mile Gneiss **Ofm**: biotite-quartz-feldspar and hornblende-plagioclase gneisses **Ofmq**: feldspathic quartzite

Late Proterozoic Poplar Mountain Gneiss **Zpmg**: gneiss member, gray feldspar-quartz-biotite gneiss with large microcline megacrysts **Zpmq**: quartzite member, basal feldspathic quartzite **Zpmjh**: Jerusalem Hill member, pink felsic gneiss with hornblende and feldspar megacrysts **Zpmqr**: zone of interlayered gneiss member and quartzite

Late Proterozoic ? Mount Mineral Fm. **?Zmm**: Zpmg was previously correlated with Zmm: quartz-biotite-garnet-aluminosilicate schist with amphibolite and quartzite, but recent reassignment of part of this formation to the Silurian has made southern extension of the Zpmg uncertain.

Late Proterozoic Dry Hill Gneiss **Zdh**: hornblende member, foliated pink quartz-feldspar-hornblende gneiss, with feldspar megacrysts and biotite **Zdb**: biotite member, foliated pink quartz-feldspar-biotite gneiss, with feldspar megacrysts **Zdhs**: biotite-tourmaline schist **Zpq**: Pelham quartzite member, feldspathic quartzite with actinolite

Stratigraphy of the Pelham dome

North

South

Devonian	interlayered Deg and Dea	
Devonian	DI	
Silurian	Sc	
Ordovician 449+3/-2 Ma	Ops	<div>Oa</div>
Ordovician 454+3/-2 Ma	Ofm	<div>Ofmq</div>
late Proterozoic	<div><div>Zpmqr</div><div>? Zpmjh ?</div><div>Zpmg</div></div>	?Zmm
	<div>Zpmq</div>	
late Proterozoic 613 ±3 Ma	<div>Zdb</div>	
	Zdh	
	<div>Zpq</div>	<div>Zpq</div> <div>Zdhs</div>

part of the dome, the core rocks are divided into three predominantly gneissic units (Ashenden, 1973; Onasch, 1973): the late Proterozoic Dry Hill Gneiss, the late Proterozoic Poplar Mountain Gneiss, and the Late Ordovician Fourmile Gneiss.

The Dry Hill Gneiss is the oldest of the gneissic units exposed in the dome. U-Pb analysis of zircons from this gneiss have recently given radiometric ages of 613 ± 3 million years (Tucker and Robinson, 1990) or the late Proterozoic (Proterozoic Z). The unit is divided into two main members; the Biotite Member and the Hornblende Member, with other, more minor, lithologies present in both (Ashenden, 1973). The Biotite Member is a medium-grained, pink quartz-feldspar-biotite gneiss with rare hornblende. The Hornblende Member is pink quartz-feldspar-hornblende-biotite gneiss with some hornblende megacrysts. Both are moderately to strongly lineated and weakly foliated and both members contain megacrysts of pink microcline and/or oligoclase which play an important role in the development of kinematic indicators. Minor rock types include lenses of feldspathic quartzite, gray gneissic units similar to the Poplar Mountain Gneiss and rare amphibolite lenses. One quartzite, the Pelham Quartzite (Figure 1.3), is extensive enough to have been mapped as a separate member (Zen and others, 1983). Geochemical work has documented compositional variations that are consistent with the protolith having been a rhyolitic tuff (Hodgkins, 1985).

Stratigraphically overlying the Dry Hill Gneiss is the Poplar Mountain Gneiss. Based on similarities between minor lithologies, previous workers (Robinson 1967; Ashenden, 1973; Onasch, 1973) have suggested that the two units are related, so that the Poplar Mountain Gneiss is also assigned to the latest Proterozoic. Two separately mapped members, a gneiss and a quartzite, make up the bulk of this unit.

The quartzite member of the Poplar Mountain Gneiss, known more simply as the Poplar Mountain Quartzite, is found at the contact between the Poplar Mountain Gneiss and the Dry Hill Gneiss. The Poplar Mountain Quartzite is a mineralogically variable unit which contains at least 60% quartz and up to 40% other phases including one or more of the following: feldspar, muscovite or actinolite, and biotite. The color of the quartzite can be gray, brown, or green depending on the impurities present. The quartzite contains local schistose and amphibolitic layers, calc-silicate and hornblende-rich nodules, and attenuated and disaggregated feldspar pegmatites.

The Gneiss Member of the Poplar Mountain Gneiss is a medium- to dark-gray, medium-grained, quartz-microcline-plagioclase-biotite gneiss commonly with muscovite. The unit is generally weakly layered with a moderate to strong lineation and a weak foliation. Feldspar megacrysts similar to those in the Dry Hill Gneiss are common, except that the microcline megacrysts in the Poplar Mountain Gneiss are white while those in the Dry Hill Gneiss are pink.

The Poplar Mountain Gneiss contains several distinctive mappable minor rock types. Onasch (1973) described a light-gray, buff-weathering felsic gneiss, typically with hornblende and containing megacrysts of pink potassium feldspar. It is informally known as the Jerusalem Hill Gneiss (Onasch, 1973; Laird, 1974). Associated with this gneiss is a lenticular zone of interlayered quartzite and gneiss (Onasch, 1973), and a biotite schist unit has also been described (Onasch, 1973; Laird, 1974).

In the southern part of the Pelham dome, the stratigraphic position of the Poplar Mountain Gneiss appears to be occupied by the Mount Mineral Formation

(Figure 1.4). On this basis, and the fact that both units commonly have a basal actinolite quartzite, Robinson (1979) previously correlated the unit with the Poplar Mountain Gneiss. The Mount Mineral Formation is more aluminous and less feldspathic than the Poplar Mountain Gneiss and is commonly a kyanite or sillimanite schist (Roll, 1987). Zen and others (1983) have suggested that the lithological differences are the result of a primary facies change. The Mount Mineral Formation has only minor outcrop in the study area and was not sampled. Recent geochronologic work has shown that the quartzite at the top of this unit is Silurian in age (Robinson and Tucker, 1991), a gneiss in the middle is Ordovician (P. Robinson, personal communication, 1992), and therefore the interpretation of this unit has become problematic.

The youngest of the core gneisses, the Late Ordovician Fourmile Gneiss, occurs above the Poplar Mountain Gneiss (Ashenden, 1973; Zen and others, 1983). The unit is a gray, fine- to medium-grained, hornblende-plagioclase gneiss with biotite and/or epidote, or a gray, fine- to medium-grained, biotite-quartz-feldspar gneiss. Lineation and foliation are moderately to strongly developed and some outcrops are compositionally layered. The unit is one of several similar Late Ordovician plagioclase gneisses (Monson, Swanzey, Pauchaug, Glastonbury gneisses) found in the Bronson Hill Anticlinorium that were originally assigned to the Oliverian plutonic series (Billings, 1937). In the southern part of the dome the Fourmile Gneiss contains a mappable quartzite member (Figure 1.4)(Zen and others, 1983).

The "core gneisses" of the Pelham dome are overlain by a sequence of "cover rocks" that are commonly inverted or shortened by deformation. In the southern part

of the dome the oldest cover unit present is the Ordovician Ammonoosuc Volcanics (Figure 1.4). However, this unit is not present in the northern part of the dome, so its complex internal stratigraphy (Schumacher, 1988) will not be discussed here. The oldest cover unit in the study area is the Ordovician Partridge Formation (Robinson, 1963) (Figure 1.4). The Partridge Formation is a rusty-weathering, quartz-biotite-muscovite schist commonly with garnet, rarely with staurolite, and in one sample from this study, kyanite. The unit also contains thin layers of amphibolite, ultramafic rock, quartzite, and felsic gneiss.

The Silurian in this area consists only of the Clough Quartzite. The Clough Quartzite is a well bedded, gray to buff quartzite with variable amounts of mica, feldspar and other accessory minerals. Some layers are conglomeratic, containing quartz pebbles with very large axial ratios (Robinson, 1963). The Clough Quartzite tends to be thin in the Bronson Hill anticlinorium and occurs discontinuously along the boundary between the Ordovician and Devonian units. This is probably due to the combined effect of non-deposition, pre-Devonian erosion, and tectonism.

The Lower Devonian Littleton Formation is typically a graphitic staurolite-garnet-muscovite-biotite schist. It is coarse grained; porphyroblasts of garnet and staurolite can exceed 2 cm. in size. Although kyanite has not been described before from the Littleton Formation in this area, a few small grains have now been seen in thin sections from one sample. The schist has a strong mineral lineation and a micaceous foliation and it varies in thickness (Robinson, 1963).

The Lower Devonian Erving Formation is composed of two dominant types of rock. Amphibolite layers are composed of a dark-green to black plagioclase-

hornblende amphibolite \pm epidote locally with smaller white calc-silicate layers. The amphiboles in these rocks typically have a strong parallel orientation. The "granulite" layers are granular quartz-feldspar rock with some garnet, mica, and other accessories. Finely interlayered in the granular rock are thin schistose layers of highly variable composition. It was in one of these schistose layers that Robinson (1963) first observed kyanite-staurolite-garnet-biotite assemblages in this area. Most of these layers contain porphyroblasts of garnet, staurolite, and locally kyanite which have proven important for determining timing relationships between deformation and metamorphism as discussed below (Reed, 1990). Calc-silicate and cotecule layers also occur in the granular rock (Robinson, 1963).

Recent geochronological work (Tucker and Robinson, 1990) has shown that the stratigraphy described above is not a simple depositional sequence. Dates ranging from 455 to 442 million years have been obtained from zircons in the Monson, Pauchaug, Fourmile, and Swanzey gneisses. Dates of 453 ± 2 Ma and $449 + 3/-2$ Ma have been obtained from "overlying" Ammonoosuc Volcanics and Partridge Formation. Robinson's (1981) suggestion that the Ordovician cover units were deposited on the eroded remnant of early Ordovician felsic volcanics is therefore unlikely. An alternative interpretation (Zartman and Naylor, 1984; Leo, 1985) is that the Ordovician plagioclase gneisses are intrusive into the cover units. However, a purely intrusive relationship fails to account for either the presence of a basal quartzite at the contact between the Ammonoosuc Volcanics and the Monson Gneiss (Robinson, 1981; Schumacher, 1988), the presence of a quartzite member within the Fourmile Gneiss (Zen and others, 1983), or the fact that some of the basement appears to be

older than the cover (Robinson and Tucker, 1991). No intrusive relationships have been seen between the Fourmile Gneiss and the Poplar Mountain Gneiss or any of the overlying units.

A third alternative to explain the overlap of radiometric dates is that the apparent stratigraphy is tectonic in origin. Deformation may have played more of a role in creating the total stratigraphic package than previously thought. Recent workers (Robinson and others, 1989; Tucker and Robinson, 1990; Robinson and Tucker, 1991) have suggested that detachment faults produced during the Taconian or Acadian orogenies may have been responsible for assembling the stratigraphy. One detachment fault may have brought the Ammonoosuc Volcanics and the Partridge Formation into contact with the Ordovician plagioclase gneisses. Another may have brought the Ordovician plagioclase gneisses into contact with the Proterozoic rocks. While it is generally assumed that the stratigraphic succession described here was assembled prior to the early Acadian, the possibility that the cover rocks were thrust onto the plagioclase gneisses during the middle Acadian has not been ruled out.

Structural Geology

The general structure of the Pelham dome has long been known (Emerson, 1898), but continued study has produced a changing view of the deformational history (Balk, 1956a, 1956b; Robinson, 1963, 1967; Ashenden, 1973; Onasch, 1973; Laird, 1974; Robinson, 1979; Michener, 1983; Reed and Williams, 1989). A series of three Acadian deformational stages have been suggested for the region (Robinson, 1979;

Robinson and Hall, 1980) (Figure 1.5). The earliest, the nappe stage, involves the development of large west-verging fold nappes with amplitudes up to 40 kilometers. These fold nappes were cut by a series of west-directed thrust-nappes (Thompson and others, 1987; Robinson and others, 1991). There are four stacked levels of nappes, and the cover rocks of the Pelham dome appear to be in or below the lowest of these (Thompson and others, 1968).

The second stage of Acadian deformation, known as the backfold stage (Robinson and others, 1989), is characterized by upright to overturned folds with west-dipping axial surfaces that deform the earlier-formed fold and thrust nappes. This stage was accompanied by the emplacement of tonalitic to granitic igneous intrusions, the development of mylonites with top-to-the-east sense of shear, and an east- or west-trending mineral lineation (Field, 1975; Tucker, 1977; Robinson, 1979; Peterson, 1984; Berry, 1989; Robinson and others, 1989; Peterson and others, 1990; Peterson and Thomson, 1991). Robinson and others (1989) and Peterson and others (1990) have suggested that large-scale uplift of the plagioclase gneisses in the Bronson Hill anticlinorium may have taken place during this stage.

The final stage of Acadian deformation was the dome-stage. This stage was characterized by the development of an en-echelon series of gneiss domes. The formation of the Bronson Hill gneiss domes has been ascribed to density-driven gravitational upwarping of the gneissic core rocks (Eskola, 1949; Thompson and others, 1968). Recent work (Reed and Williams, 1989; Reed, 1990; Peterson and others, 1990) has documented a large component of penetrative ductile shearing

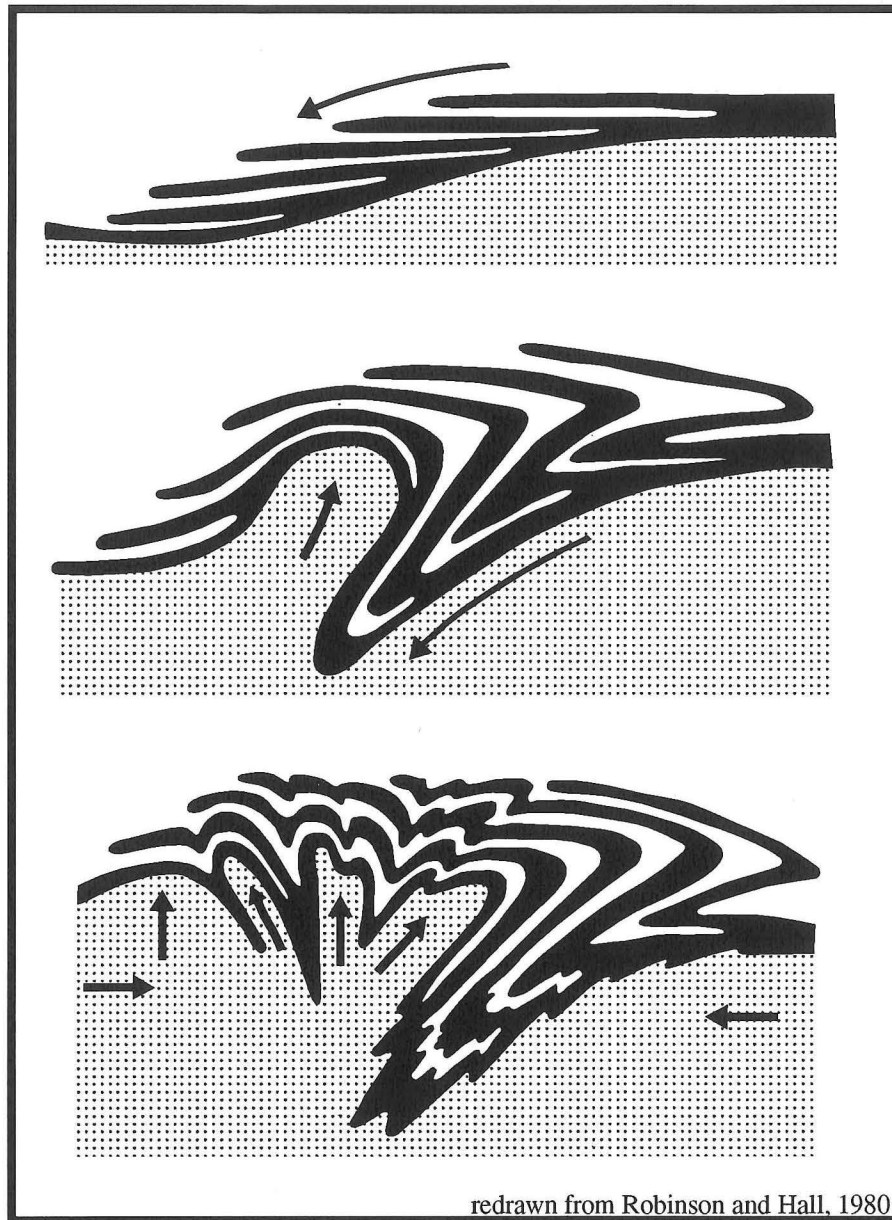


Figure 1.5. Cartoon of the sequence of major deformations in the Bronson Hill anticlinorium and Merrimack belt, central Massachusetts and adjacent New Hampshire.

Top: Early Acadian nappes overfolded from east to west, both fold nappes and thrust nappes are formed.

Middle: Backfolding of early nappe axial surfaces with overfolding from west to east, accompanied by west-dipping late-stage mylonitization.

Bottom: Gneiss-dome stage involving tight to isoclinal folding of earlier axial surfaces and the formation of gneiss domes.

associated with this stage. Robinson and Tucker (1991) now suggest that part of the doming may have occurred in the late Paleozoic and not in the Acadian orogeny.

These three stages of deformation provide a useful regional framework, but the local structural history is commonly much more complicated. Onasch (1973) identified 5 phases of ductile deformation in the north-central portion of the Pelham dome: early recumbent folding with folding from west to east, the main phase of gneiss dome formation, late asymmetric folding, late shears of reversed sense, and late extension with flattening. Correlation of these phases with the regional stages is not completely clear. The earliest structural features clearly documented in the dome are the east-directed recumbent folds (Robinson, 1963; Ashenden, 1973) which have recently been ascribed to the regional backfold stage (Robinson and others, 1989). In the core rocks, this deformation involves isoclinal folding of the younger Poplar Mountain Gneiss around the older Dry Hill Gneiss (Ashenden, 1973), recognized by stratigraphic repetition. This repetition has lead to the common practice of referring to the "upper" and "lower" Poplar Mountain Gneiss. Several east-southeast directed recumbent folds of the contact between the Fourmile Gneiss and the cover sequence, as well as folds in the cover (Robinson, 1963), are now attributed to the backfold stage (Robinson and others, 1989). Microfabric evidence for this phase, such as relict foliations or lineations, has not been clearly identified in the Pelham dome, although some small folds in the well bedded Poplar Mountain and Clough Quartzites may be related (Robinson, 1963; Onasch, 1973).

The main phase of gneiss dome formation is represented by the strong north-south lineation, the broad foliation arch, and by tight folds in the Poplar Mountain

quartzite that are reformed by later stage folds (Onasch, 1973). The subhorizontal top-to-the-south shearing has been tentatively assigned to this phase. Previous workers have described some structures which were either then or are now believed to be shear-related. Onasch (1973) described "late asymmetric folding", and suggested it followed the main phase of gneiss dome formation because these folds deform the dome-stage lineation. Ashenden (1973) suggested that asymmetric folding occurred during a top-to-the-south shearing event. Onasch (1973) also considered the possibility that the dominant N-S mineral lineation is related to this phase. He showed that the lineation is parallel to the transport direction of the folds, but he concluded that the lineation was probably formed during the earlier "main phase of gneiss dome formation".

Onasch's (1973) two minor late deformational phases do not correlate well with regional phases. The first of these phases is described as small shear zones which give a sense opposite (top-to-the-north) to the asymmetric folding and the common microfabric kinematic indicators. The other minor phase described is a late stage extension and flattening indicated by "chocolate-tablet" boudinage.

The Mesozoic Connecticut Valley border fault lies along the western edge of the Pelham dome. This fault and Mesozoic brittle faults related to it and the overall brittle extensional regime in the Mesozoic have, in some localities, offset structural features produced during the ductile deformational phases.

Tectonics

The tectonic history of central New England has many controversial aspects. It is believed that the pre-Cambrian gneisses were formed in the early phases of a Proterozoic continental rifting event (Hodgkins, 1985), although the nature and identity of the continents involved is debatable. These pre-Cambrian gneisses were probably the base onto which an island arc was built above an east-dipping subduction zone during the Ordovician. The Taconian orogeny is generally believed to be the result of the collision of this Ordovician island arc with Laurentia. However, the age of the rocks that are thought to form this arc are slightly younger than the date of emplacement of the major thrust sheets (Tucker and Robinson, 1990), so this orogenic event probably has further complications that have not yet been incorporated into the tectonic history.

There are several theories about the formation of the Merrimack trough and the cause of the subsequent Acadian orogeny (c.f. Osberg and others, 1989). One of the more prominent theories is that a continental margin formed to the east of the Ordovician island arc at the end of the Taconian orogeny (Osberg and others, 1989). The Siluro-Devonian rocks of the Merrimack trough are sediments that were deposited along this continental margin (Hatcher, 1989). Subduction resumed in the Devonian with subduction zones forming on both sides of the ocean (Bradley, 1983). Two volcanic arcs were formed, which eventually collided, deforming the sediments and the volcanic arcs. The second prominent theory is that the Ordovician arc underwent a period of post-collision extension, perhaps back-arc related. The Siluro-Devonian

sediments were deposited on this thinned crust. The sediments were deformed when the stress regime changed from one of tension to one of compression, perhaps due to the resumption of subduction (Osberg and others, 1989; Hatcher, 1989). In either scenario the western part of the Ordovician island arc was covered by a layer of Silurian and Devonian sediments (Connecticut Valley Sequence) prior to the Acadian orogeny.

Most of the deformation and metamorphism in the Bronson Hill anticlinorium is considered to be Acadian in age (Robinson and Hall, 1980; Osberg and others, 1989). Recent geochronologic work in and around the Pelham dome has raised questions about this interpretation. Many, but not all, radiometric ages for hornblende closure, titanite recrystallization, and other mineral crystallization or recrystallization are late Paleozoic rather than Acadian (Tucker and others, 1988; Gromet, 1989, 1990; Tucker and Robinson, 1990). These writers believe this is a record of both a thermal and deformational event that severely overprinted older features in the Pelham dome area.

Location of Study

Deformational fabrics have been studied in the northern part of the Pelham dome including all parts of the dome in the Miller's Falls, Northfield, and Greenfield quadrangles (Figure 1.3) of north-central Massachusetts. This area comprises roughly the northern third of the Pelham dome. Several previous detailed mapping, stratigraphic, and structural studies were undertaken in this region (Robinson, 1963;

Ashenden, 1973; Onasch, 1973; Laird, 1974; Michener, 1983) and thus it is an excellent area for a microfabric study.

Methods of Study

Oriented rock samples have been collected from the study area. Sample station locations were selected based on three criteria 1) obtaining widespread coverage of the field area, 2) sampling as many different rock types as was feasible and 3) sampling outcrops with distinctive or unusual structural features. Macroscopic or non-collectible shear-related structural features present in these outcrops were documented and described.

Oriented petrographic thin-sections have been made for examination under a polarizing microscope. The predominant orientation for petrographic thin-sections is parallel to the lineation and perpendicular to foliation (X-Z plane of strain). Some additional thin-sections have been cut either perpendicular to the lineation (Y-Z plane of strain) or parallel to foliation (X-Y plane) of strain. These additional sections have proved helpful in documenting relict fabrics. Multiple thin sections have been constructed from some samples to document more thoroughly all of the fabric elements.

CHAPTER 2

MICROFABRICS AND KINEMATIC INDICATORS

Descriptions of Microfabrics

A wide variety of microfabrics are found within the northern part of the Pelham dome. A shear-related foliation with an accompanying mineral lineation dominates the rock, with a number of types of kinematic indicators also being present. These microfabrics have been studied in detail in an attempt to clarify the structural history of the area.

Foliation

The dominant fabric in rocks from the northern part of the Pelham dome is a strong foliation. In gneissic rocks, the foliation is defined by biotite and elongate quartz and feldspar. In pelitic rocks, both muscovite and biotite define the foliation. The foliation is generally parallel to the compositional layering in the rocks. Regionally, foliation trends define an oval shape which helps define the dome structure. The foliation dip varies from horizontal to subhorizontal along the axis of the dome to more steeply dipping along the sides.

The dominant foliation is not always strictly planar. Locally, the foliation is folded by asymmetric micro- and macro-folds which will be discussed later. The

foliation is also commonly curved around rigid objects such as porphyroblasts and porphyroclasts. In some lineation-parallel thin sections, a second foliation is present at an angle to the first. These secondary foliations are generally interpreted as S-surfaces from S-C fabrics, a type of kinematic indicator. Perpendicular to the lineation, the development of foliation varies greatly. Some specimens have a strong foliation, while others show more anastomosing or contorted foliations in this orientation. Several show small upright microfolds of the shear foliation.

Previous workers (Ashenden, 1973; Onasch, 1973; Laird, 1974) have suggested that the current shape of the dominant foliation was produced during the dome stage of deformation. This foliation is not the first to form in the rocks; earlier foliations are locally preserved as intra-folial folds, or as inclusion fabrics within porphyroblastic minerals (to be discussed in Chapter 3). Based on textures seen in the rock, the dominant foliation is interpreted to have formed by the progressive recrystallization and reorientation of earlier foliations (Bell and Rubenach, 1984) during a ductile deformation event involving a significant component of simple shear.

Lineation

A well developed mineral lineation lies within the dominant foliation in most of the rocks from the northern part of the Pelham dome. The trend of the lineation is approximately north-south with generally shallow plunges to the north or south (Figure 2.1). The lineation has been interpreted as a stretching lineation, associated with

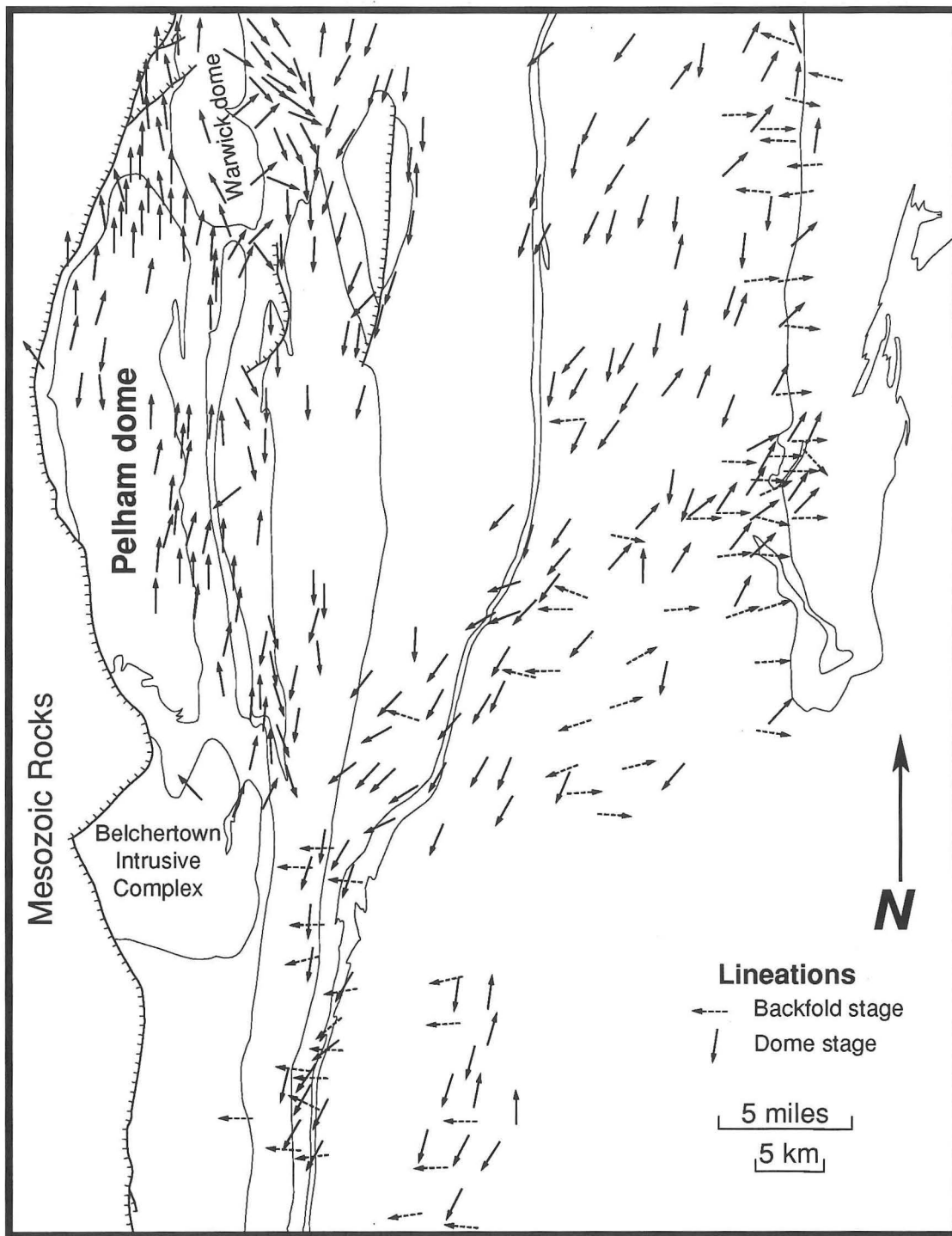


Figure 2.1. Regional map showing representative orientation and distribution of backfold- and dome-stage lineations across central Massachusetts. Data compiled from Robinson (1963), Pike (1968), Ashenden (1973), Onasch (1973), Field (1975), Tucker (1977), Michener (1983), Peterson (1984, 1992), Berry (1989), Springston (1990), and unpublished field data of Robinson and students. From Peterson and Robinson (1993).

transport parallel to the orogen (Onasch, 1973; Reed and Williams, 1989, Peterson and others, 1990).

The lineation is generally defined by the alignment of elongate minerals. In gneissic rocks, the lineation is defined by quartz rods and ribbons, stringers of mica, elongate recrystallized tails on porphyroclastic minerals, and rare elongate amphibole crystals. In pelitic rocks, the lineation is defined by elongate staurolite and rare kyanite, quartz rods and ribbons, stringers of mica, and elongate pressure shadows on porphyroblastic minerals. Amphibolites show the best lineations with elongate hornblendes defining the fabric.

Most rocks display a well developed foliation and a lineation making them L-S tectonites (Flinn, 1965). However, as discussed previously, in some cases the foliation is not so well developed in lineation-perpendicular cuts. Many of the rocks tend more toward being L-tectonites rather than toward being S-tectonites. The presence of microfolds in lineation-perpendicular thin sections suggests a component of shortening perpendicular to the lineation during shearing.

Kinematic Indicators

A variety of kinematic indicators are present in the rocks of the northern part of the Pelham dome. These occur with different intensities and different abundances in different types of rock. The presence of these kinematic indicators was used as a guide to investigate the orientation, character, and areal extent of shear strain in the Pelham dome area.

Porphyroclast/Porphyroblast Systems

The most common types of kinematic indicators are those involving curving fabrics and asymmetric recrystallization around rigid or semi-rigid crystals (Figure 2.2). These are divided into two types; relationships around recrystallizing porphyroclasts (Simpson and Schmid, 1983; Passchier and Simpson, 1986), which develop asymmetric "tails" or "wings" (Figure 2.2a-b), and those around non-recrystallizing porphyroblasts (Simpson and Schmid, 1983; Hanmer and Passchier, 1991, pgs. 56-58), which can develop asymmetric "strain shadows" (Figure 2.2c). These two cases are end-member situations of which real systems including those in the Pelham dome, are commonly combinations. In either case, it is the asymmetry of the recrystallized tails or strain shadows that allows the sense of shear to be determined (Figure 2.2).

Asymmetric Recrystallized Tails. Passchier and Simpson (1986) have described two different geometries of recrystallized tails in porphyroclast systems. In σ -type systems, the recrystallized tails or wings are wedge-shaped and emanate from the top of the grain (Figure 2.2a). In δ -type systems, the recrystallized tails are curved and begin at the bottom of the grain, cross the center line of the grain, and then curve out along the foliation (Figure 2.2b). The vast majority of winged porphyroblasts that have been seen in the Pelham dome, are σ -type systems.

Asymmetric porphyroclast systems are more common in the Proterozoic basement gneisses than in the other rocks of the dome. Large feldspar megacrysts

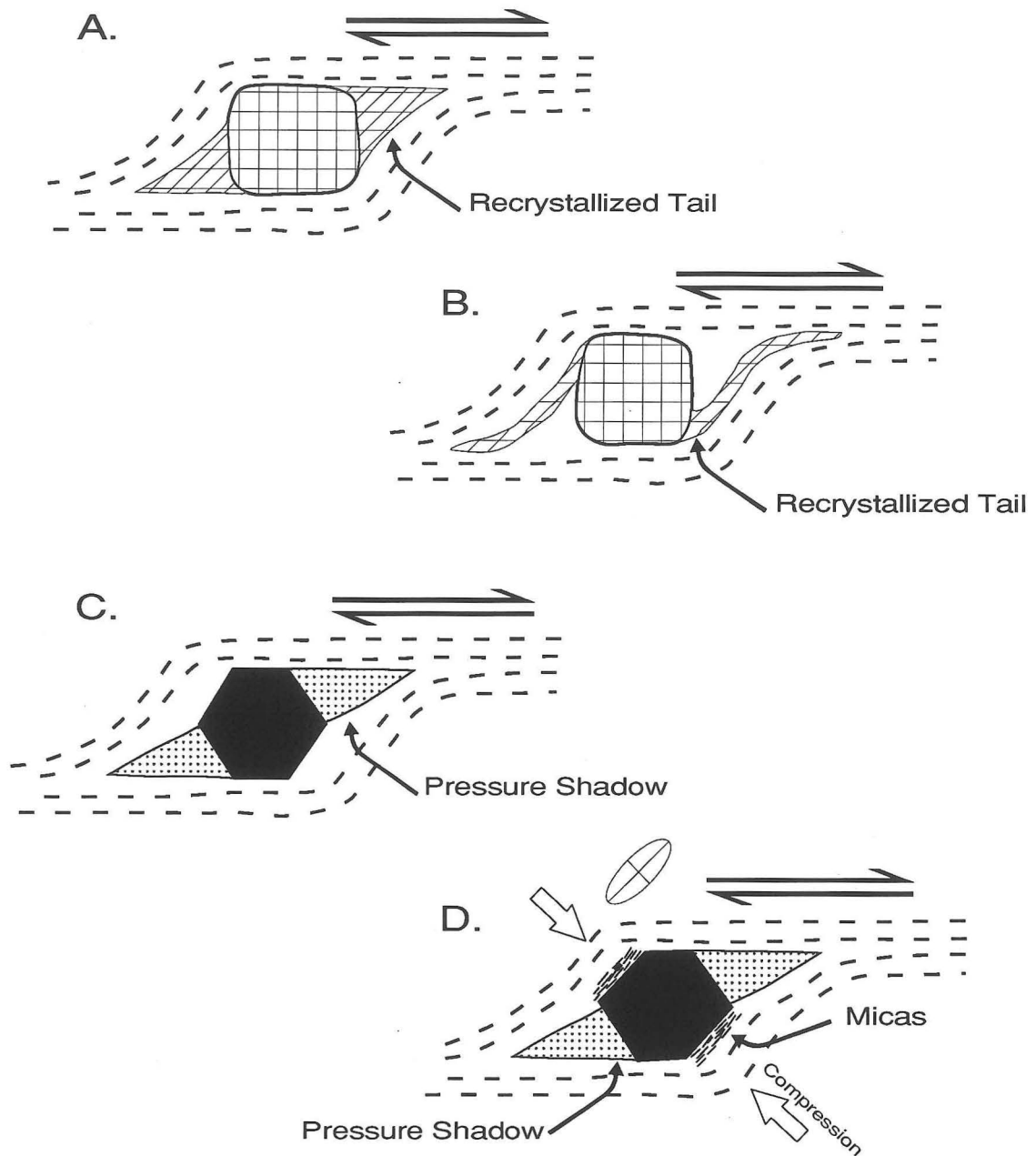


Figure 2.2. Kinematic indicators seen in the northern part of the Pelham dome that involve asymmetries around porphyroclasts or porphyroblasts. Pressure shadows are shown in a dotted pattern, recrystallized tails are shown as a sheared line pattern. A. Sigma-type asymmetric porphyroclast system. B. Delta-type asymmetric porphyroclast system. C. Asymmetric strain shadows around a porphyroblast. D. Quarter structure around a porphyroblast with concentration of micas on the porphyroblast perpendicular to the principal shortening direction.

present in these rocks act as material heterogeneities around which asymmetries can develop during shear (Figure 2.3). In addition to the recrystallized tails, the foliation is commonly asymmetrically warped around the megacrysts (Figure 2.3a) in a manner similar to the foliation geometry of S-C fabrics (Lister and Snoke, 1984).

The amount of recrystallization into the tails varies widely from megacryst to megacryst and may be a function of the amount of strain and the amount of feldspar in the rock. In many cases, the tails are combinations of recrystallized feldspar and quartz. Recrystallized tails are developed around objects continuously varying in size from porphyroclasts visible in standard size thin sections to very large megacrysts to multi-grain pods of feldspathic pegmatite.

The orientation of the recrystallized tails is such that the asymmetric tails on the southern edge of the feldspar megacrysts end above the median line of the feldspar; the asymmetric tails on the northern edge end below the median line (Figure 2.3). Such an asymmetry is interpreted as indicating top-to-the-south sense of shear (Figure 2.2). The clearest kinematic indicators in the gneisses are developed around these megacrysts.

Asymmetric Pressure or Strain Shadows. In the pelitic cover rocks of the Pelham dome, the most common kinematic indicators are asymmetric strain shadows developed around porphyroblasts. Asymmetric strain shadows, commonly called asymmetric pressure shadows (Hanmer and Passchier, 1991), are similar in appearance and interpretation to σ -type asymmetric porphyroclast tails (Figure 2.2c). Large crystals that are not undergoing significant amounts of deformation or recrystallization

Figure 2.3. Asymmetric recrystallized tails from the northern part of the Pelham dome.

a. Photomicrograph of asymmetric recrystallized tails on a plagioclase feldspar porphyroclast indicating top-to-the-south sense of shear. Sample is NMI-1 from the Dry Hill Gneiss, north is to the right and top is up. Taken in plane-polarized light, field of view is 13 mm. across.

b. Photomicrograph of asymmetric recrystallized tails on a feldspar porphyroclast in a micaceous rock indicating top-to-the-south sense of shear. Sample is JHR3C from the Poplar Mtn. Quartzite, north is to the left and top is up. Taken in plane-polarized light, field of view is 13 mm. across.

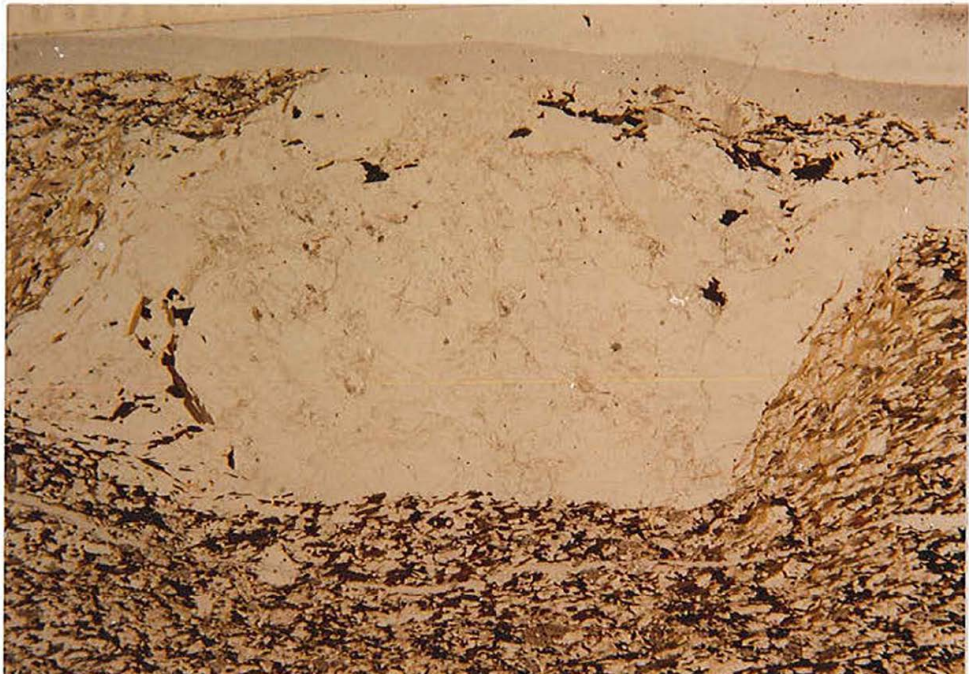
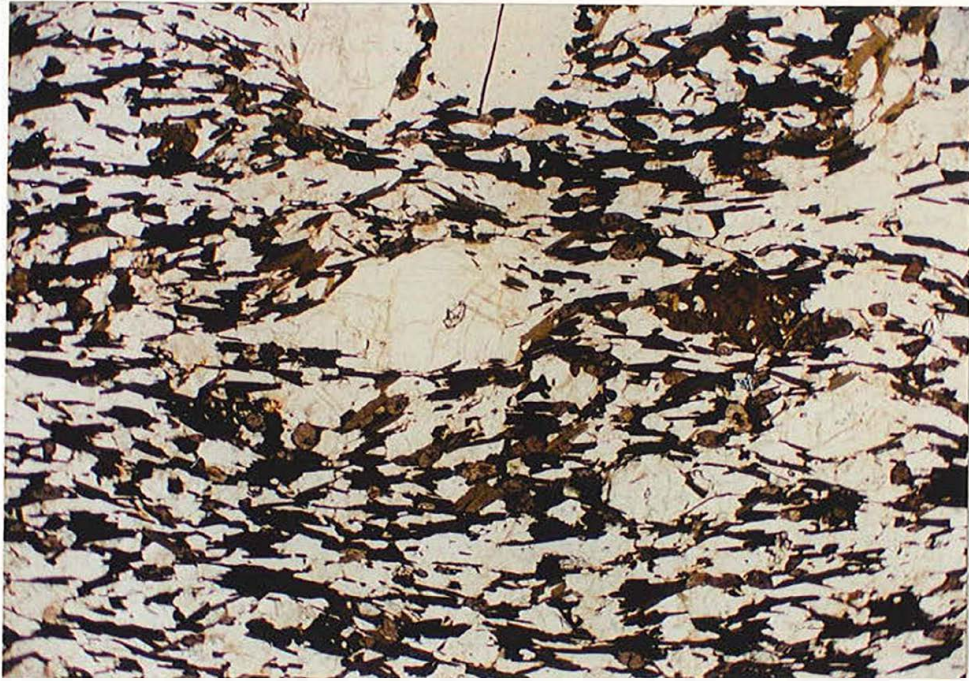


Figure 2.3 continued. Asymmetric recrystallized tails from the northern part of the Pelham dome.

c. Photograph of asymmetric recrystallized tails on a feldspar megacryst showing top-to-the-south sense of shear. Slab is from sample SM1 from a pegmatite-rich exposure of the Fourmile Gneiss, a lineation-parallel section, north is to the left and top is up. Scale is shown in centimeters.

d. Photograph of asymmetric recrystallized tails on a feldspar porphyroclast showing top-to-the-south sense of shear. Sample is NM1 from the Dry Hill Gneiss, outcrop face trends approximately N-S and lineation-parallel, north is to the left and top is up.



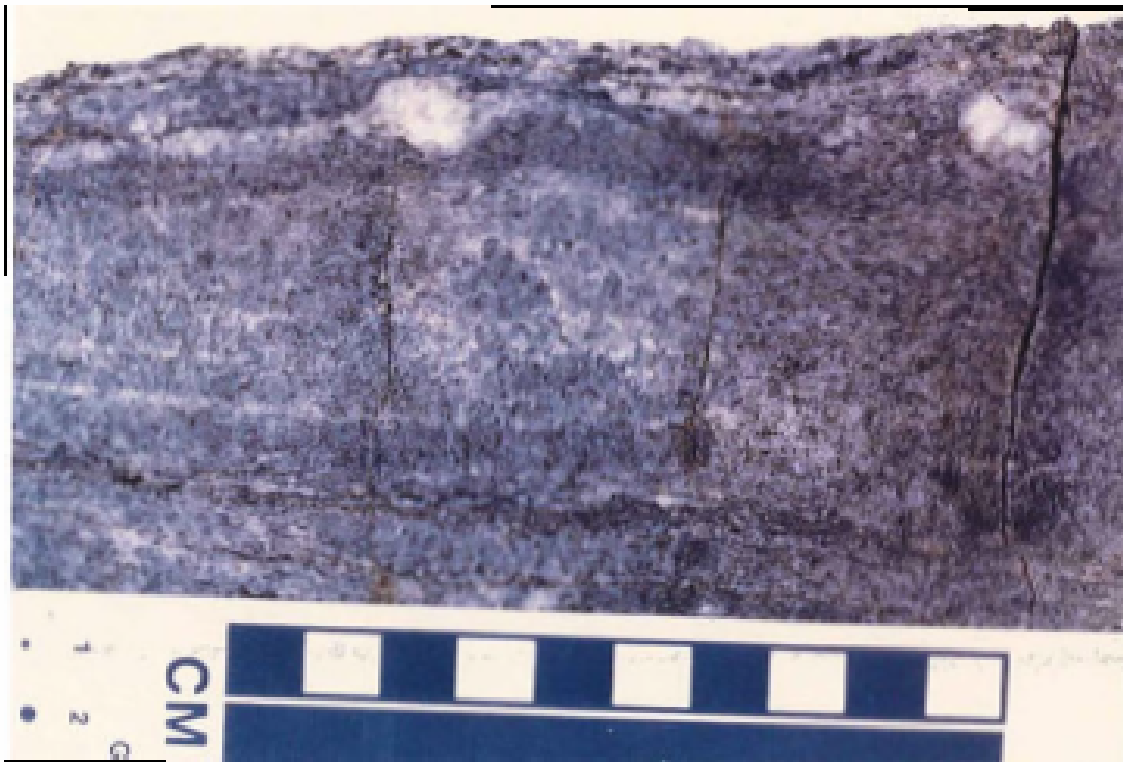


Figure 2.3 continued. Asymmetric recrystallized tails from the northern part of the Pelham dome.

e. Photograph of large asymmetric recrystallized tails on a feldspar megacryst showing top-to-the-south sense of shear. Sample is JHR3-3 from the Poplar Mountain Quartzite. Slab is cut parallel to the lineation and north is to the left and top is up. Scale is in centimeters.

take up much of the stress that is being exerted on a volume of rock. This causes the matrix around the porphyroblast to be shielded from some of the stress. Material is recrystallized into this low stress and low strain region. In simple shear environments, the low strain regions are asymmetrical, so the strain shadows are asymmetrally developed. The asymmetry of porphyroblast strain shadows is regarded as being less reliable for determining sense of shear than asymmetry of recrystallized tails on porphyroclasts (Simpson and Schmid, 1983; Hanmer and Passchier, 1991). Rotation of the porphyroblasts and interference between porphyroblasts can produce ambiguous or even inaccurate appearing results (Hanmer and Passchier, 1991, pgs. 56-58). Nevertheless, if approached with caution, most asymmetric porphyroblasts can be used for determining kinematics.

Most of the garnet and staurolite, and some of the kyanite in the pelitic units of the northern part of the Pelham dome, show asymmetric strain shadows (Figure 2.4). Asymmetric strain shadows are also present around some hornblendes from the core gneisses or from cover amphibolites (Figure 2.4c). The most common mineral present in strain shadows is recrystallized quartz, although micas and other minerals are present as well. The foliation asymmetries, generally defined by micas, around these grains reflect the asymmetry of the strain shadows (Figure 2.4).

In the northern part of the Pelham dome, the strain shadow developed on the southern end of the grain is generally at the top of the grain, while the strain shadow on the northern end is at the bottom (Figure 2.4). This sort of asymmetry suggests top-to-the-south sense of shear (Figure 2.2).

Figure 2.4. Asymmetric strain (pressure) shadows occurring on porphyroblasts from the northern part of the Pelham dome.

a. Photomicrograph of asymmetric strain shadows on a garnet porphyroblast indicating top-to-the-south sense of shear. Note faint sigmoidal inclusion fabric in garnet. Sample is LL2A from the Devonian Littleton Formation, north is to the left and top is up. Taken in cross-polarized light, field of view is 5 mm. across.

b. Photomicrograph of poorly-developed asymmetric strain shadows on a hornblende (center of picture) indicating top-to-the-south sense of shear. Sample is GSR2 from the amphibolite member of the Devonian Erving Formation, north is to the left and top is up. Taken in plane polarized light, field of view is 13 mm. across.

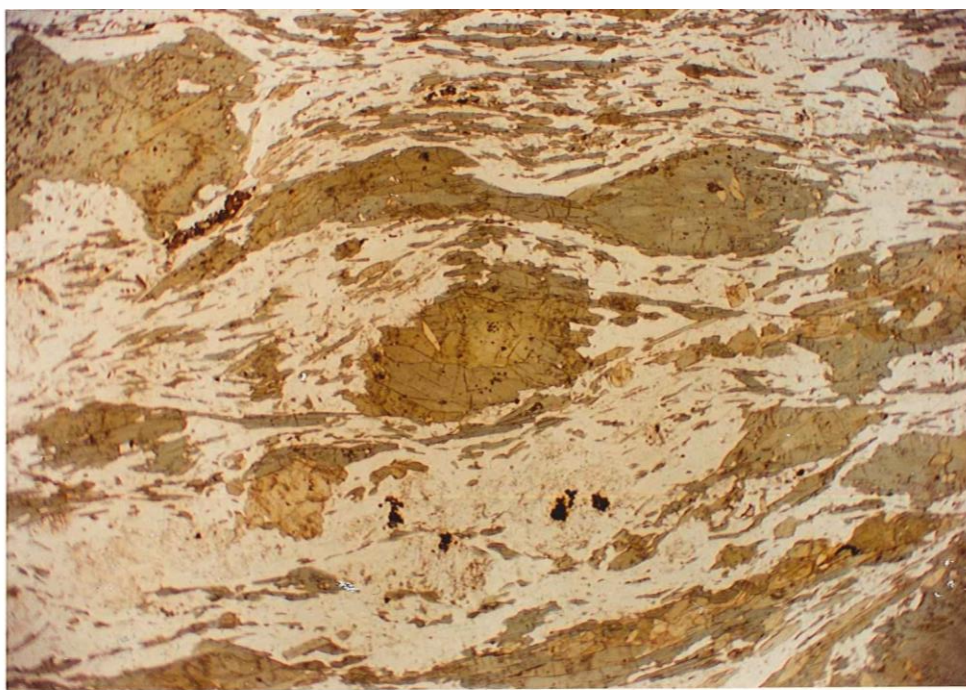
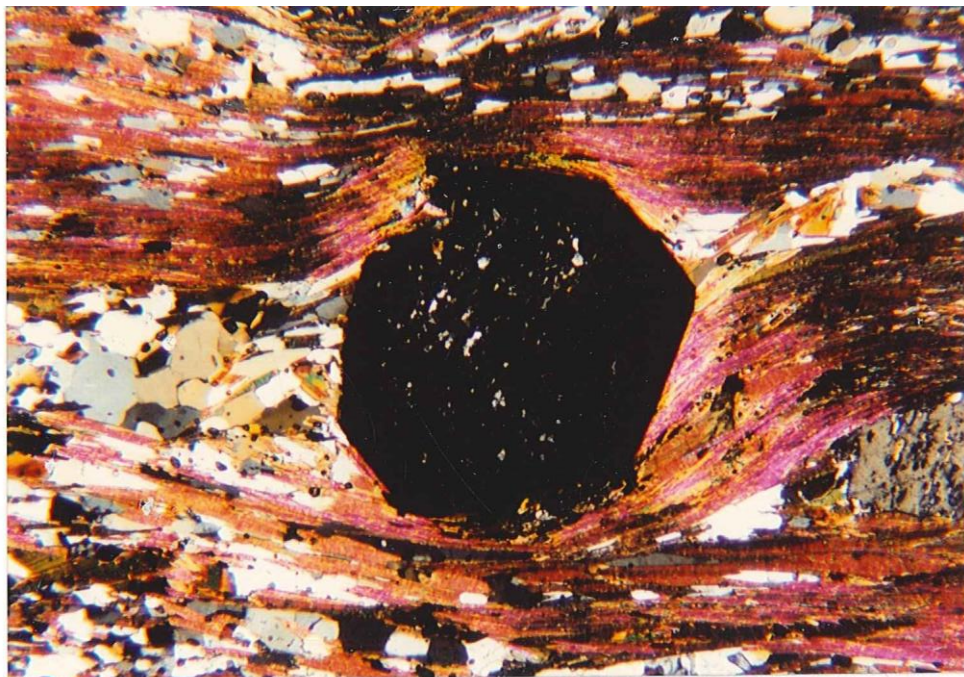




Figure 2.4 continued. Asymmetric strain (pressure) shadows occurring on porphyroblasts from the northern part of the Pelham dome.

c. Photomicrograph of asymmetric strain shadows on a staurolite indicating top-to-the-south sense of shear. Sample is DR2E from a pelitic layer in the Devonian Erving Formation, north is to the left and top is up. Taken in plane polarized light, field of view is 13 mm. across.

Quarter Structures

Kinematic indicators known as a "quarter structures" (Hanmer and Passchier, 1991) involve the different deformation conditions at the different corners or quarters of a rigid inclusion during shear (Figure 2.2d). There is more than one type of quarter structure, but a common one is that thick concentrations of foliated micas occur on the corners of a porphyroblast that are adjacent to the principal shortening direction of the strain ellipse (Figure 2.2d). This is interpreted to result from the preferential dissolution of quartz relative to micaceous material.

Quarter structures are common on garnets and staurolites from the pelitic cover units of the Pelham dome (Figure 2.5). Muscovite is more common than biotite in these structures. Quarter structures also occur on other porphyroblasts present in non-pelitic core and cover rocks but are less well developed.

In the northern part of the Pelham dome, the characteristic asymmetries are concentrations of mica on the upper north and lower south ends of the porphyroblasts or porphyroclasts. This asymmetry suggests top-to-the-south sense of shear. The asymmetries seen commonly re-enforce top-to-the-south senses of shear derived from asymmetric strain shadows or asymmetric recrystallized tails on the same crystals.

S-C Fabrics

An S-C fabric (Lister and Snoke, 1984) is a kinematic indicator that is based on the different orientations of two planar fabrics that can develop in a rock during

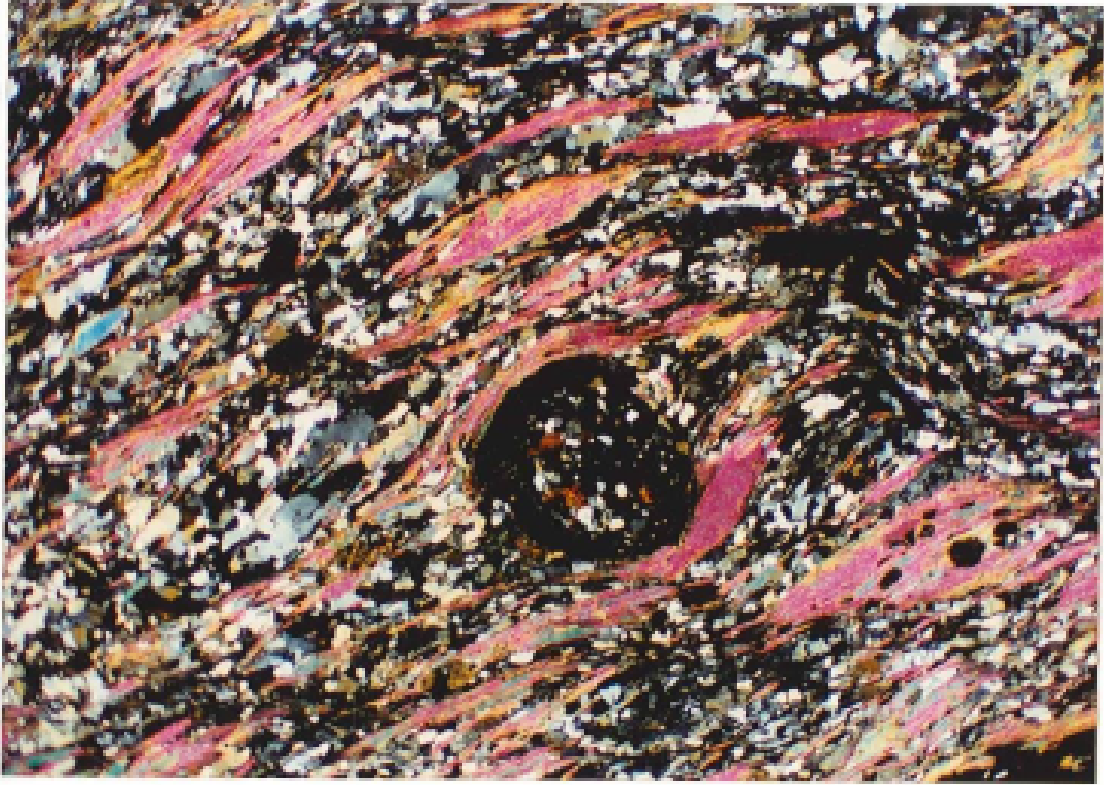


Figure 2.5. Photomicrograph of a quarter structure developed on a garnet indicating top-to-the-south sense of shear. Micas are concentrated on corners of the garnet perpendicular to the principal shortening direction. Note the asymmetric pressure shadows which indicate the same sense of shear. Sample is MR2B from the Ordovician Partridge Formation, north is to the left and top is up. Taken in cross-polarized light, field of view is 13 mm. across.

shearing (Figure 2.6a). The S-surface (*schistosity* or cleavage) is developed perpendicular to the maximum shortening direction of the strain ellipse. The C-surface (*cisaillement* or shear) is developed parallel to the shear plane. The acute angle between these two fabrics (Figure 2.6a) is interpreted to indicate the direction of shear (Lister and Snoke, 1984). Despite some problems in differentiating between S-C fabrics and two separately-formed fabrics that intersect at an acute angle, this has come to be one of the more widely used kinematic indicators.

The development of S-C fabrics in the core rocks of the Pelham dome is limited because the rocks commonly contain little mica. In some gneisses, the second foliation is weakly developed or absent, but in most cases a kinematic interpretation can be made. The fabrics interpreted as S-surfaces are commonly defined by some of the biotites. The fabrics interpreted as C-surfaces are defined by elongation of quartz and the orientation of other biotites. C-surfaces are better developed than S-surfaces and the development of S-surfaces increases in areas adjacent to porphyroclasts (Figure 2.7a). There is no evidence to suggest that the interpreted S and C surfaces did not develop synchronously.

S-C fabrics are commonly absent in the pelitic rocks. In some cases, there are two foliations present in the schists. S-surfaces are generally defined by biotite and/or muscovite. C-surfaces are defined by the same minerals and the elongation of some quartz grains (Figure 2.7b). C-surfaces are generally slightly more prominent than S-surfaces. The micas that define the S-surfaces can be clearly seen to bend into the C-surfaces and vice-versa, suggesting that the fabrics formed synchronously.

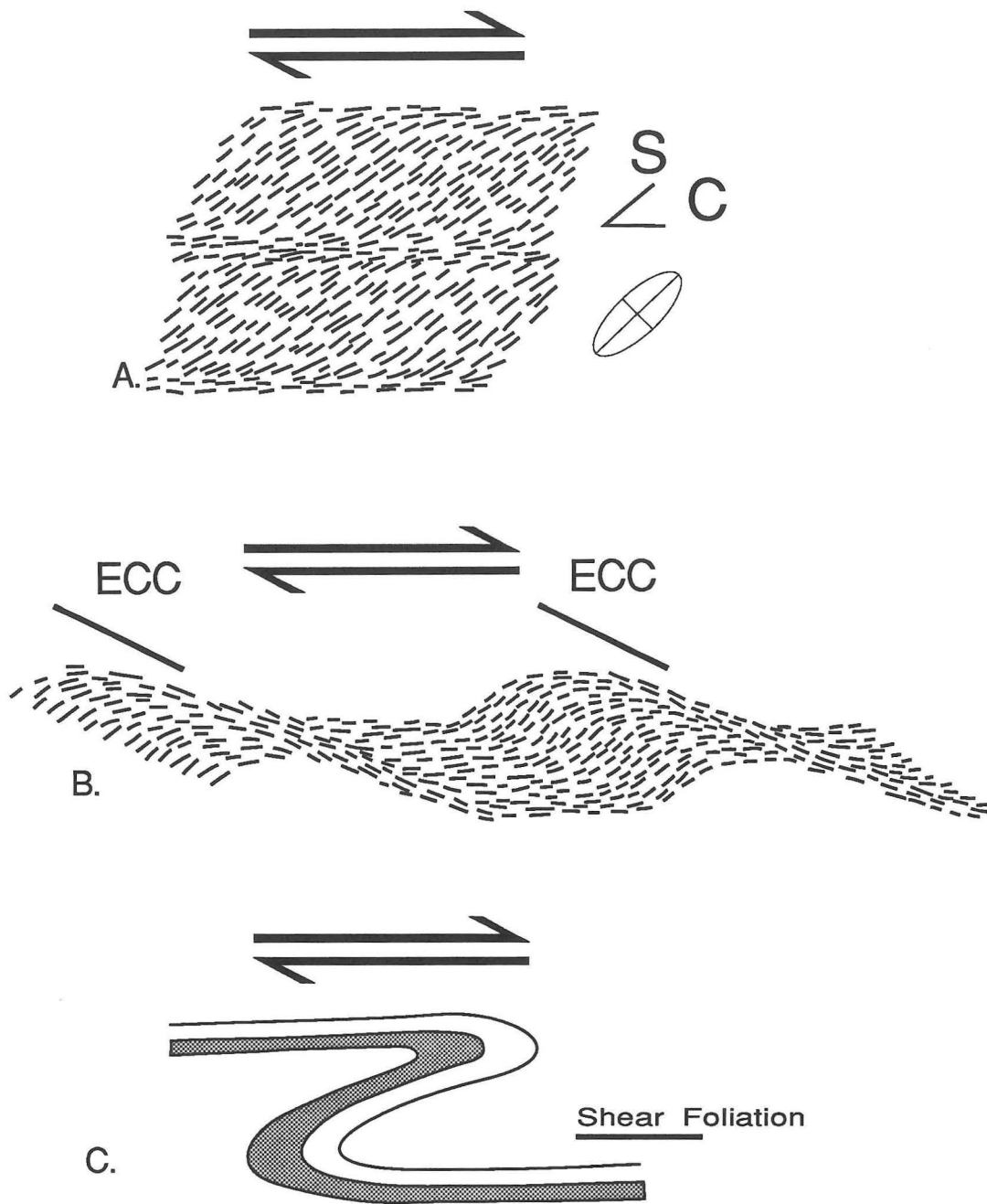
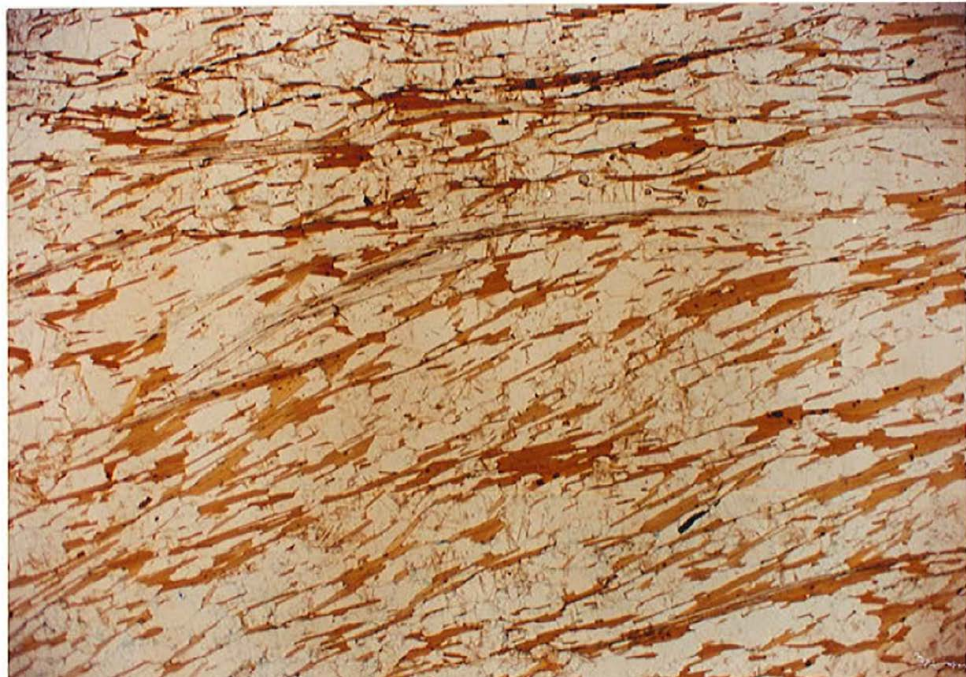
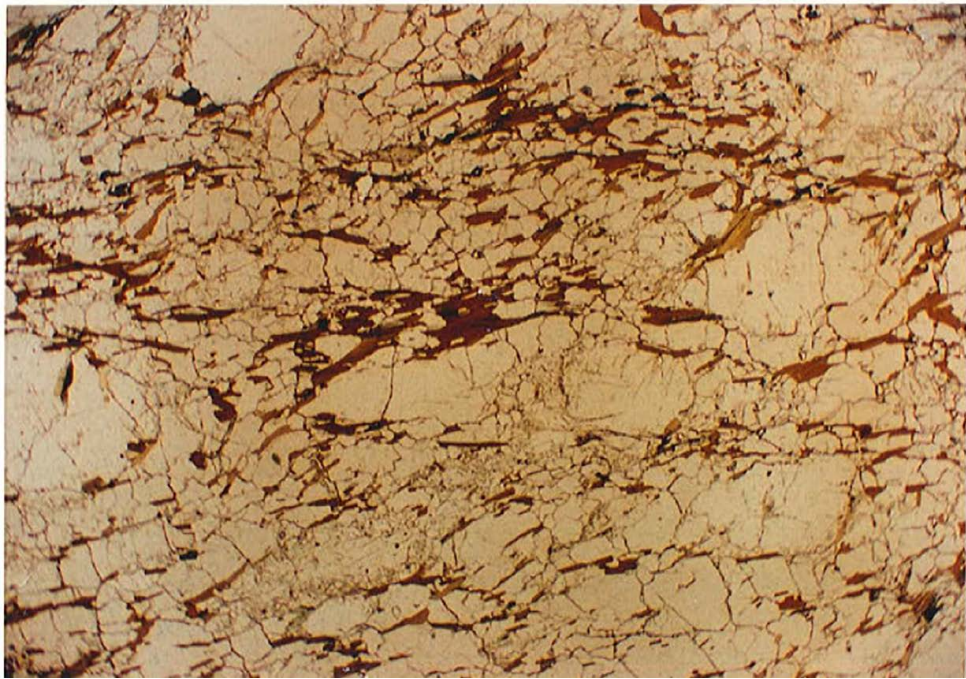


Figure 2.6. Kinematic indicators seen in the northern part of the Pelham dome that involve asymmetries of foliations and/or layering. A. Typical S-C fabric with dextral sense of shear, strain ellipse is shown. B. Extensional crenulation cleavages (ECC's) or asymmetrical shear bands with dextral sense of shear. C. Asymmetrical fold geometry indicating dextral sense of shear.

Figure 2.7. S-C fabrics from the northern part of the Pelham dome.

a. Photomicrograph of an S-C fabric in a gneissic rock. C-surface is horizontal and S-surface is diagonal from upper left to lower right, this indicates top-to-the-south sense of shear. Sample is ART2X from the Poplar Mountain Gneiss, north is to the left and top is up. Taken in plane-polarized light, field of view is 13 mm. across.

b. Photomicrograph of an S-C fabric in a pelitic rock. C-surface is horizontal and S-surface is diagonal from upper right to lower left, this indicates top-to-the-south sense of shear. Sample is L2B2 from the Devonian Littleton Formation, North is to the left and top is up. Taken in plane-polarized light, field of view is 13 mm. across.



In schists and gneisses from the northern part of the Pelham dome, the S-surface commonly dips at a shallow to moderate angle to the north with a roughly east-west strike. The C-surface is the dominant shear-related foliation which helps define the dome geometry. This orientation of the S-C fabric indicates a consistent top-to-the-south sense of shear.

Foliation or Mica Fish

Foliation or mica fish (Lister and Snoke, 1984; Hanmer, 1986) are similar in some ways to S-C fabrics and asymmetric porphyroclast tails. The mineral, most commonly mica, forming the "fish" is commonly aligned parallel to the S-surface. Asymmetrical tails of recrystallized material are commonly strung out from the grain along the C-surface with asymmetries similar to those seen around porphyroclasts.

Mica fish have been observed in some pelitic rocks within the Pelham dome, but are not common. The fish that have been seen are typically large muscovites oriented parallel to S-surfaces with weak tails that curve into the dominant foliation (Figure 2.8). The micas defining the fish typically dip to the north. Recrystallized material is strung out from the upper south and lower north ends of the mica grains. This geometry of the structure indicates top-to-the-south sense of shear (Figure 2.8)

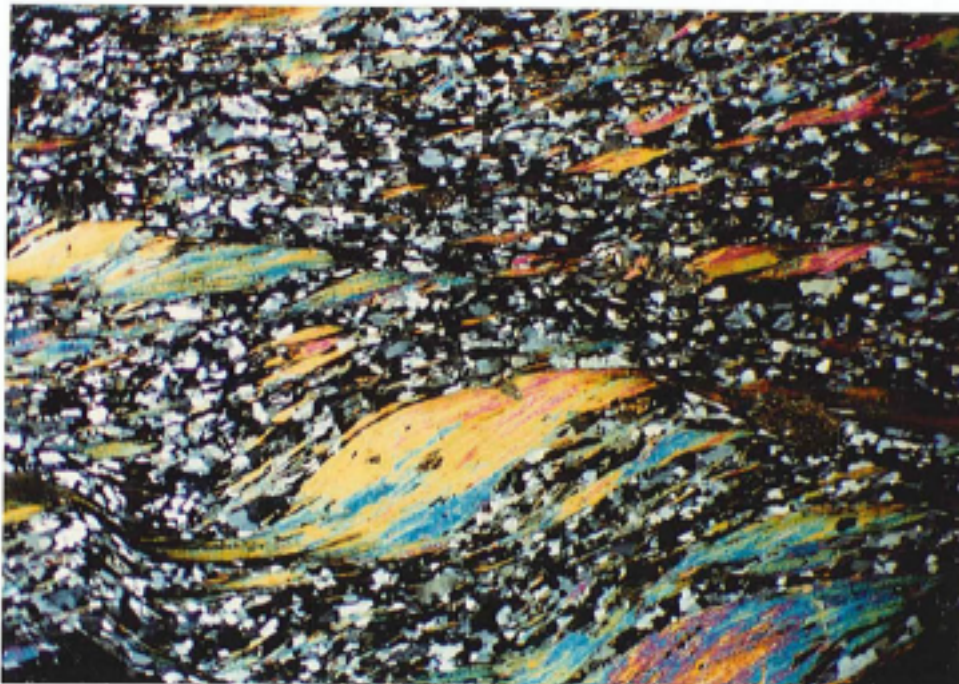


Figure 2.8. Photomicrograph of a mica fish indicating top-to-the-south sense of shear. Sample is MR2B from the Ordovician Partridge Formation, north is to the left and top is up. Taken in cross-polarized light, field of view is 13 mm. across.

Micro-scale Asymmetric Folds

The asymmetry of minor folds (Figure 2.6c) in a sheared rock can be used as a kinematic indicator (Hanmer and Passchier, 1991, pgs. 64-67). The direction of movement is indicated by the vergence or the overturning direction of the fold. There are two ways that asymmetric folds can form during shear. New asymmetric folds can result from heterogeneities in the flow, or pre-existing folds can be rotated and elongated by the shearing. Newly formed folds are better kinematic indicators because heterogeneous strain and earlier asymmetry can cause problems with the reorientation of pre-existing folds (see Hanmer and Passchier, 1991).

In pelitic rock samples from the northern part of the Pelham dome, microfolds are common in lineation-parallel thin sections or hand-sample cuts. In most cases, these folds are intra-folial and not enough of the fold is preserved to allow an interpretation if the fold was symmetrical or not. The trace of the axial planes of these intra-folial folds is generally parallel to the foliation. There are, however, some symmetric microfolds with the trace of the axial plane perpendicular to the fold axis, but these seem to be preserved in areas isolated from shear.

In rare instances, enough of the fold is present to tell the fold vergence (Figure 2.9a). The microfolds commonly fold the shear fabric into tight to isoclinal shapes, indicating folding took place after the initiation of shearing. Fold shapes are predominantly rounded, commonly with crenulation-like morphologies. A continuous size range from microfolds (Figure 2.9a) to macrofolds (Figure 2.9b) to large outcrop-scale folds (Figure 2.9c) is present.

Figure 2.9. Asymmetric micro- and macro-folds from the northern part of the Pelham dome. In all cases, the fold axis is roughly perpendicular to the plane of the picture

a. Photomicrograph of an asymmetric fold in a pelitic rock indicating top-to-the-south sense of shear. Sample is LLR4 from a schistose layer in the Devonian Erving Formation, north is to the left and top is up. Taken in plane-polarized light, field of view is 13 mm. across.

b. Asymmetric fold in the Jerusalem **Hill** member of the Poplar Mountain Gneiss indicating top-to-the-south sense of shear. Note asymmetric recrystallized tails on porphyroblast indicate same direction. North is to the left and the outcrop trends approximately N-S and roughly parallel to the lineation.

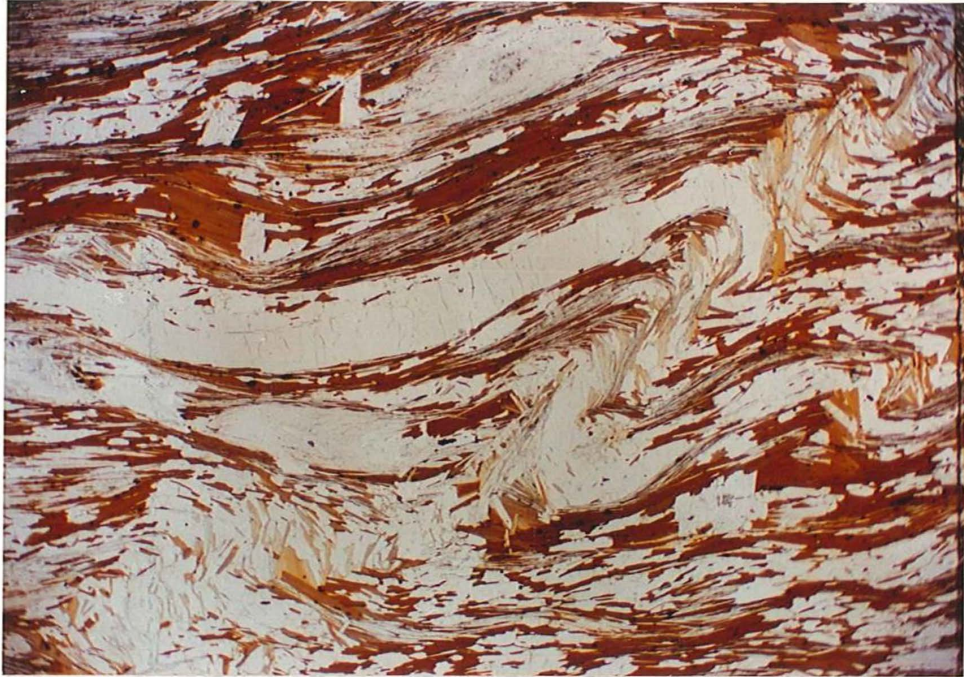




Figure 2.9 continued. Asymmetric micro- and macro-folds from the northern part of the Pelham dome.

c. Asymmetric fold in quartzitic layers of the Dry Hill Gneiss. Location is a on the western slope of Ames Hill in the southeastern part of the study area. North is to the left, outcrop trends approximately N-S and roughly parallel to the lineation.

In the northern part of the Pelham dome, the asymmetric microfolds seen typically have a consistent southerly vergence. This asymmetry indicates top-to-the south sense of shear. No folds have been seen with the opposite asymmetry.

Extensional Crenulation Cleavages

Extensional crenulation cleavages (Platt and Vissers, 1980) or asymmetrical shear bands (White and others, 1980) are asymmetric structural features in which a secondary foliation occurs at an angle to the shear plane (Figure 2.6b). The asymmetry is opposite to that seen in S-C fabrics and care must be taken not to confuse these two structures. Extensional crenulation cleavages (ECC's) can form in two orthogonal orientations, with one ECC showing movement synthetic to the bulk shear and the other showing antithetic motion. The synthetic ECC, which intersects the shear-related foliation at a low angle (Figure 2.6b), is the more common of the two types (Hanmer and Passchier, 1991, pgs. 30-32.)

Extensional crenulation cleavages are not common in the rocks of the northern part of the Pelham dome. The shear bands that are present occur in pelitic schists from the cover rocks. The ECC's are generally not well developed and only moderately reorient the micaceous primary foliation (Figure 2.10). The shear bands intersect the primary foliation at a low angle and the apparent sense of movement is synthetic to the bulk shear (Figure 2.10).

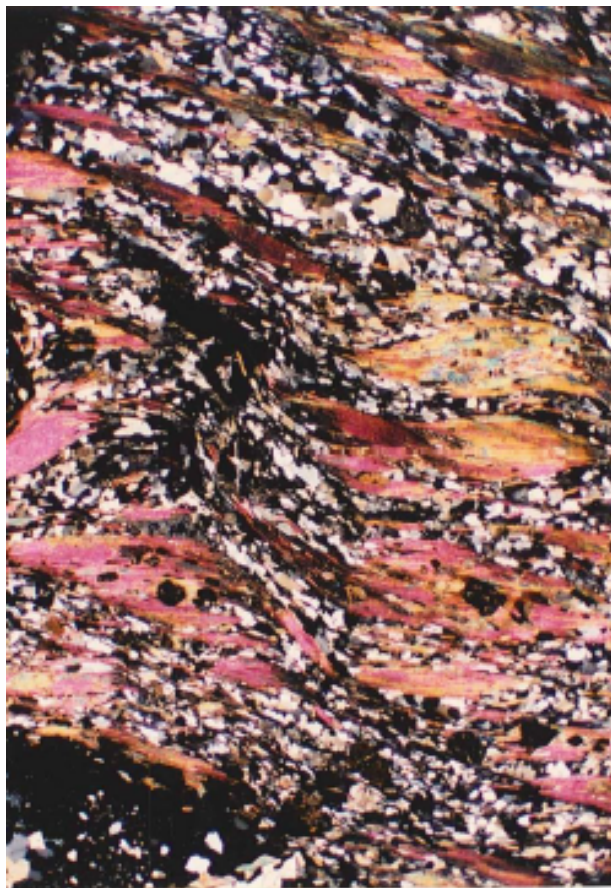


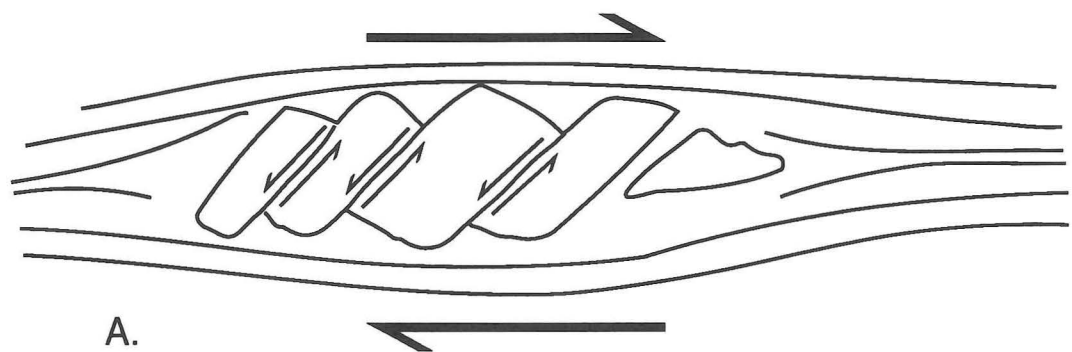
Figure 2.10. Photomicrograph of a poorly-developed extensional crenulation cleavage or shear band in a pelitic rock indicating top-to-the-south sense of shear. ECC cuts across figure diagonally from upper left to lower right. Sample is MR2B from the Ordovician Partridge Formation, north is to the left and top is up. Taken in cross-polarized light with the 1/4 wave plate inserted, field of view is 13 mm. from top to bottom.

When present, the extensional crenulation cleavages have shallow dips to the south relative to the dominant foliation in the rocks. This orientation is interpreted to indicate top-to-the-south sense of shear.

Broken Grains or Asymmetric Pull-aparts

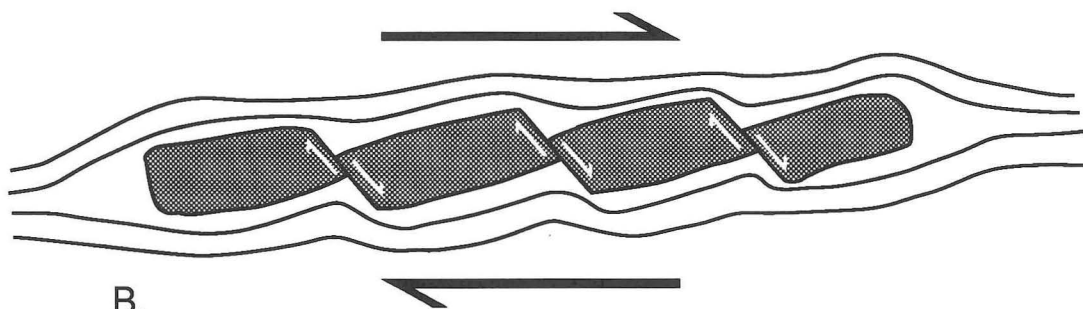
In a rock undergoing shear, there is commonly a ductility contrast between materials being deformed. This difference in ductility can lead to the development of structures which can be used to determine a sense of shear. If the difference in ductility causes one material to deform brittly and if the less-ductile material is a porphyroblast or porphyroclast, the object can be called a "broken grain" or a pull-apart structure (Hanmer, 1986). Alternatively, the less-ductile object rotates but does not deform. When two adjacent objects rotate and interfere with each other, a domino or tiling structure is formed (Hanmer and Passchier, 1991, pg. 59). Breaking apart of a grain generally leads to the development of a domino structure as the rocks undergo further shear. Broken grains can be ambiguous as kinematic indicators. Simpson and Schmid (1983) and Hanmer (1986) have noted two different ways in which brittle grains tend to break and possibly rotate during shearing (Figure 2.11). These methods can give opposite senses of shear for grains that appear very similar. Thus, determination of sense of shear from broken grains can be extremely difficult.

While the majority of deformation occurring in the northern part of the Pelham dome is ductile, it is not atypical to see feldspar grains undergoing a degree of brittle deformation. A few grains of both types (Figure 2.11) occur in rocks from the



A.

(Redrawn from Simpson and Schmid, 1983)



B.

Figure 2.11. Sense of shear determination from asymmetrical pull-aparts or broken grains. A. Type I (Hanmer, 1986) pull-aparts. B. Type II (Hanmer, 1986) pull-aparts.

Pelham dome (Figure 2.12), but the sense of shear is generally ambiguous. Where present they are commonly accompanied by other structural features in the rock which clearly indicate top-to-the-south sense of shear.

Non-Kinematic Microfabrics

Crystallographic Preferred Orientation

Quartzites and quartz-rich rocks from both basement and cover units show varying degrees of preferred orientation of quartz c-axes. When viewed under the microscope with cross-polarized light and the gypsum plate inserted, weak to strong preferred orientations can be seen (Figure 2.13). The degree of preferred orientation does not vary coherently with location but seems to be a function of the rock type and the degree of recrystallization. Extinction bands in quartz are generally sub-parallel to c-axes. This indicates that slip has been perpendicular to the c-axes and that the predominant slip system acting is basal slip. The preferred orientation seems to be the result of reorientation of quartz c-axes during this basal slip (Etchecopar, 1977).

Deformation, Recovery, and Recrystallization Features in Minerals

Different minerals vary widely in their deformational behavior, depending on conditions of pressure and temperature, the presence of fluid, and the strain rate.

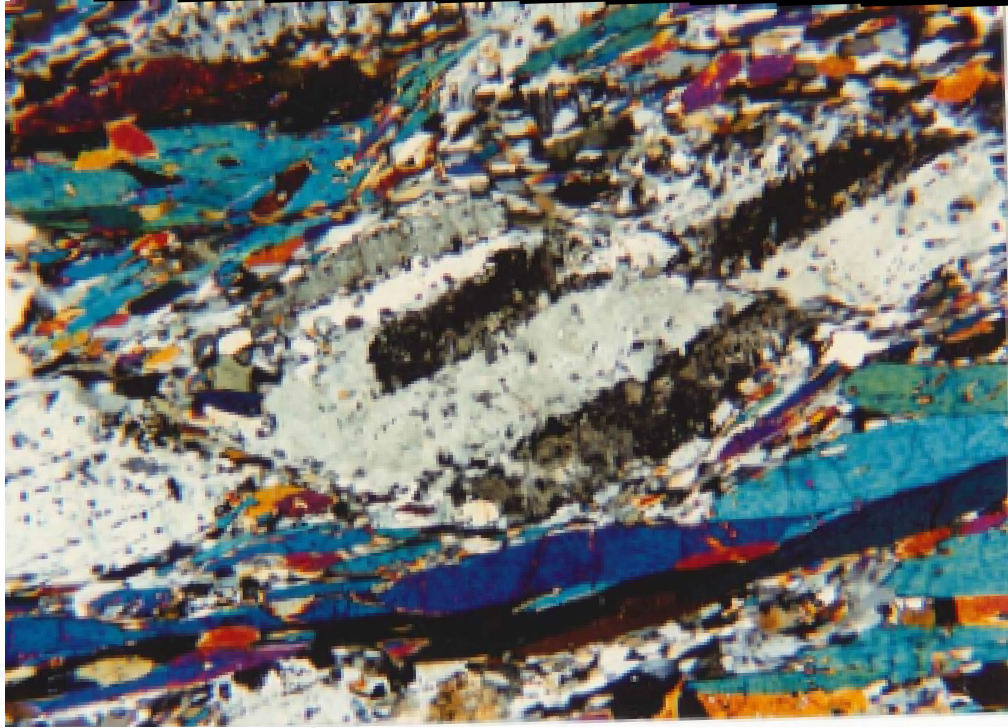


Figure 2.12. Photomicrograph showing a broken plagioclase grain. Asymmetry is similar to that shown in Figure 2.11b, and indicates top-to-the-south sense of shear. Calculated stretch from this broken grain is approximately 36 %. Sample is GSR2 from the amphibolite member of the Devonian Erving Formation, north is to the left and top is up. Taken in cross-polarized light, field of view is 5 mm. across.

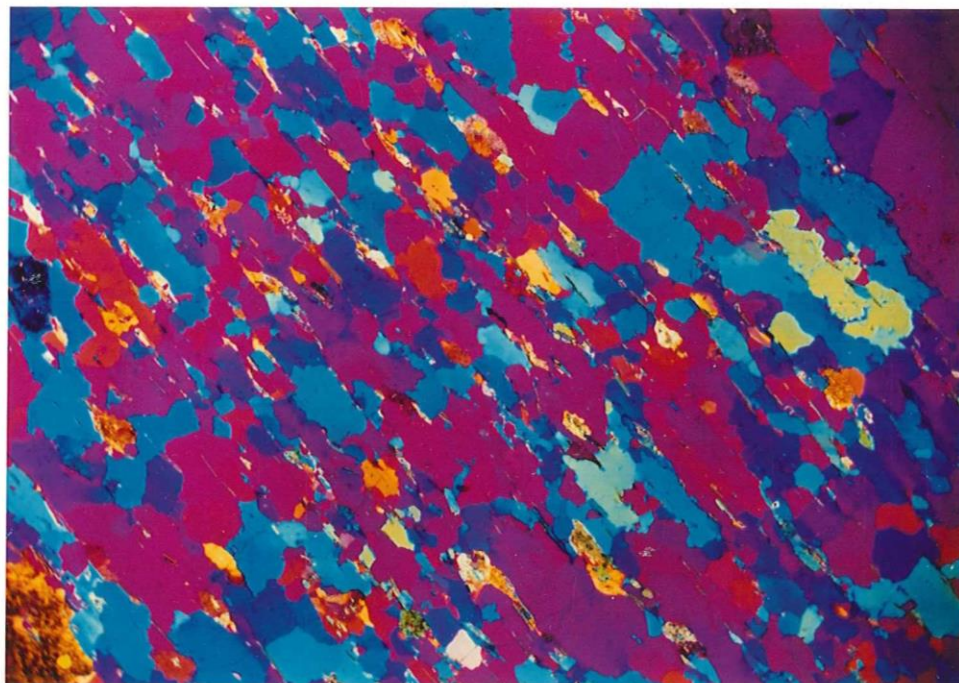


Figure 2.13. Photomicrograph showing preferred orientation of quartz c-axes. Foliation cuts across figure diagonally from upper left to lower right, slow ray of gypsum plate is perpendicular to the direction of elongation/foliation. Sample is JH5-2 from the Poplar Mountain Quartzite. Taken in cross-polarized light with the gypsum plate inserted, field of view is 13 mm. across.

Pressure and temperature in the Pelham dome during the dominant deformation are believed to have been about 580°C and 5.5 kilobars (Roll, 1987). The presence of numerous hydrous minerals, such as micas and amphiboles, suggests the presence of a fluid phase. Many minerals present in the Pelham dome, including garnet, hornblende, staurolite, and kyanite show few or no characteristics of ductile deformation, recovery, or recrystallization. These appear to have undergone little or no plastic strain during deformation. The bulk of strain seems to have been taken up by deformation of quartz, feldspar, and the micas. The behavior of quartz and feldspar is deserving of further mention.

Quartz Features. At the temperatures and pressures at which shear was taking place, quartz was undergoing ductile deformation. The degree of development of undulatory extinction in the rocks of the Pelham dome is diverse. Many rocks show recrystallized fabrics with little or no undulatory extinction. Other samples show well developed continuous to discontinuous undulatory extinction and subgrains, and in some cases these are overprinted on a well developed recrystallization fabric. The primary slip system seems to have been basal slip with prism slip also occurring as indicated by the development of subgrains. At the present time, there does not appear to be a geographic pattern to the occurrence of these features.

There are two main types of dynamic recrystallization that occur in quartz; rotational recrystallization and grain boundary migration (Poirier and Guillope, 1979). Evidence for both has been seen in quartz from sampled rocks. Equant grains with slightly different orientations appear to have formed through subgrain enhancement

(Poirier and Nicolas, 1975; Poirier, 1985, p. 169). This indicates the presence of rotational recrystallization. Rotational recrystallization was apparently the dominant recrystallization mechanism in gneisses and schists. Quartz grains in quartzites and quartz veins show serrate edges and nucleation of smaller new grains along grain boundaries, suggesting that grain boundary migration was more common in quartzites and quartz veins.

In quartzites and deformed quartz veins there are large irregularly-shaped, strain-free grains that contain foliated micas. These grains are probably the result of primary recrystallization, a predominantly static process driven by differences in stored strain energy between adjacent grains (Urai and others, 1985). Low-strain grains are more stable and grow at the expense of highly-strained grains after the cessation of deformation. No evidence was found to suggest that normal grain growth (static annealing), the other common static recrystallization process (Urai and others, 1985), has effected quartz grains after deformation. This suggests that the rocks were not heated to higher temperatures after deformation.

Feldspar Features. Feldspar crystals of various sizes and compositions occur in the vast majority of rocks sampled in the northern part of the Pelham dome. It is therefore not surprising that the feldspars show a wide variety of deformation microstructures.

Feldspars are believed to undergo relatively little dynamic recrystallization under the lower amphibolite facies conditions in which deformation was taking place (Tullis, 1983). Many feldspars show brittle features of some sort. Most brittle

deformation involves feldspars pulled apart along cleavages, commonly followed by dispersal of the fragments. It is also common to see bending of polysynthetic twins in plagioclase that may be the result of non-visible microcracking or microtwinning (Tullis, 1983).

Brittle deformation played an important part in the development of feldspar megacrysts in the Proterozoic gneisses. Large feldspar pegmatites have undergone boudinage to smaller feldspar aggregates which were in turn pulled apart to single feldspar crystals. At this point grain-size reduction continued by breaking of feldspar crystals along cleavages. The mechanism is predominantly a brittle process, but is accompanied by some dynamic recrystallization of the feldspar. This recrystallization commonly leads to two disaggregated feldspars connected by tails of recrystallized feldspar material. The tails connect the bottom of one megacryst to the top of the other megacryst (Figure 2.3c). These recrystallized tails cut across foliation and can complicate the interpretation of kinematics.

A common ductile deformation feature seen in feldspars of the northern part of the Pelham dome is twinning. Plagioclase feldspars can deform by twinning (Tullis, 1983). Many plagioclase feldspars in the core gneisses show extensive polysynthetic twinning which may be related to deformation. Deformation twinning of feldspars and its implications will be discussed more fully in a later section.

Feldspars in rocks from the northern part of the Pelham dome show evidence for dynamic recrystallization. The degree of dynamic recrystallization of feldspars varies widely. In general, the more quartz and micas that are present in a rock the less recrystallization is seen in feldspars. This is probably the result of strain

partitioning into the more ductile quartz and micas. The primary mode of recrystallization that has been observed in feldspars from the Pelham dome is grain boundary migration with new grains forming at the edges of old grains. However, there are instances in which the presence of new grains and subgrains along twin planes indicates that migration of twin planes also occurred (Figure 2.12). Some feldspars have developed indistinct core and mantle structures from grain boundary recrystallization.

Post-Shearing Microfabrics

Several types of deformation structures and microstructures appear to post-date the dominant shear fabric in the Pelham dome. The deformation is brittle or dominantly brittle in nature and brittle structural features cut across the shear fabric without obscuring it. Brittle deformation accompanied by retrograde metamorphism and locally small amounts of ductile deformation is expressed as small microfaults (Figure 2.14). Most of these are normal faults, but reverse and strike-slip faults have been seen as well. The fault surfaces commonly have well developed slickensides. These faults are probably related to Mesozoic extension, and so, it is not surprising that they are most common on the west side of the study area near the Connecticut Valley border fault.

The one area where late deformation and retrograde metamorphism has obscured the shear fabric is less than 200 meters from the border fault in the southwest corner of the study area. The sample (PL3, Plate 1) is a schist from the Ordovician

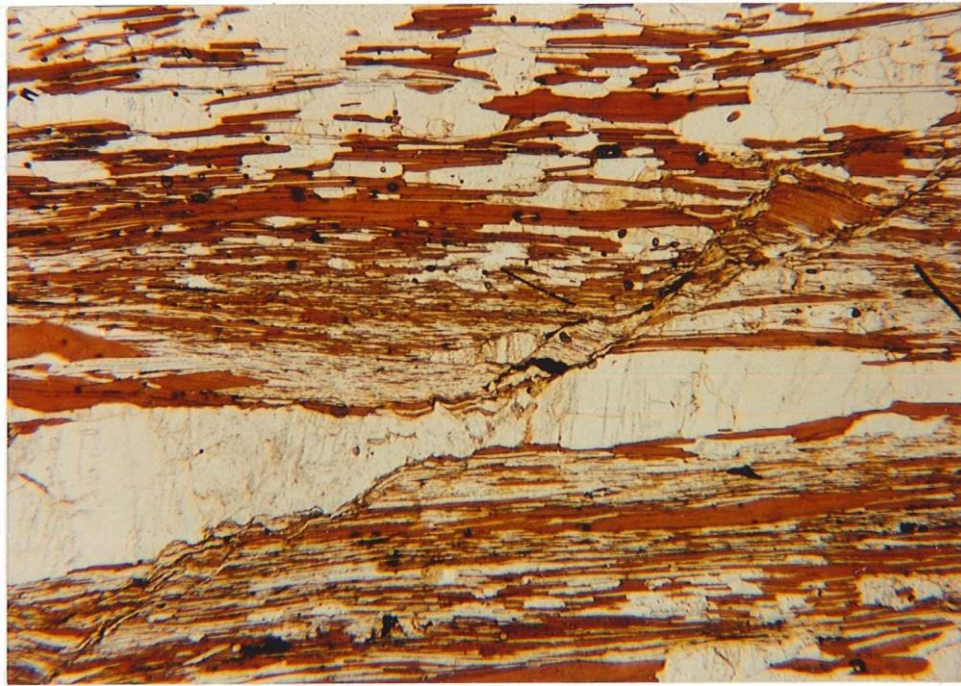


Figure 2.14. Photomicrograph showing brittle deformation cross-cutting shear-related fabrics. Microfault with normal movement cuts across figure from upper right to lower left. Note slight bending that occurs adjacent to the microfault. Sample is DR4C from a pelitic layer in the Devonian Erving Formation, north is to the left and top is up. Taken in plane-polarized light, field of view is 13 mm. across.

Partridge Formation which shows extensive retrograde metamorphism. Small closed vugs and veins within the rock contain crystals of quartz and cloudy albite, some of which are euhedral. The mineralization seen is very much like albitization observed in the Jurassic Mount Toby Formation adjacent to the study area (J. Taylor, personal communication, 1990). Some of the euhedral quartz shows undulatory extinction. Folding and other deformation in this sample may be related to movement along the Connecticut Valley border fault.

Kinematic Indicators in Outcrop

While the primary focus of this study was microfabrics, there are a number of larger structural features that contribute to the kinematic analysis of the northern part of the Pelham dome. In fact, outcrop-scale asymmetric folds first lead Onasch (1973) and Ashenden (1973) to suggest large amounts of south-directed shearing in the Pelham dome. In some cases, these structural features are part of a continuous range in scale from similarly formed microfabrics. The larger features commonly were important in determining the presence of shear in areas where microfabric kinematic indicators were not observed.

Asymmetric Folds

Asymmetric folds with a wide-range of sizes and geometries occur in the northern part of the Pelham dome (Ashenden, 1973; Onasch, 1973; Laird, 1974).

There is a continuous gradation of fold size from microscopic (Figure 2.9c) to mesoscopic (Figure 2.9b) to outcrop scale (Figure 2.c). Larger folds appear most commonly in the Poplar Mountain Quartzite. Care should be taken in determining sense of shear from asymmetric folds (Hanmer and Passchier, 1991, pgs. 64-67). Careful examination has shown that the asymmetry of the folds in the Pelham dome is consistent with top-to-the-south shear.

The relative timing relationship between folding and shearing is difficult to interpret. In one instance, a fold and a porphyroclast with large asymmetric recrystallized tails occur in close proximity (Figure 2.9b). Some material that may have been part of the recrystallized tail nearer the fold has been folded. However, an unfolded, younger recrystallized tail has also formed on the porphyroclast. Smaller porphyroclasts along the short limb of the fold do not give clear asymmetries while those present along the long limbs do have clear asymmetries which are consistent with top-to-the-south shearing. The probable truncation of the recrystallized tail suggests that shearing preceded folding. The non-folded recrystallized tail currently present suggests that shearing occurred after folding. The lack of asymmetry for the porphyroclasts on the short limbs suggests that they were changed in shape after being folded. The most likely explanation for these disparate relationships is that shearing and folding were related parts of a continuous process. Disseminated bulk shearing occurred before, during, and after folding, both types of deformation being in response to the same strain field.

For determining kinematics, sheath folds are a special case of asymmetric folds in which the hinge line of the fold is curved. The geometry of well developed sheath

folds can be used to determine the direction and sense of shear (Hanmer and Passchier, 1991, pgs. 64-67). Previous workers in the Pelham dome have either noted the presence of sheath folds (Robinson, 1979) or have shown illustration of folds (Ashenden, 1973; Onasch, 1973) that have sheath geometries. These folds are all characterized by a subhorizontal orientation with the nose of the anticlinal fold to the south and have an asymmetry which indicates top-to-the-south sense of shear.

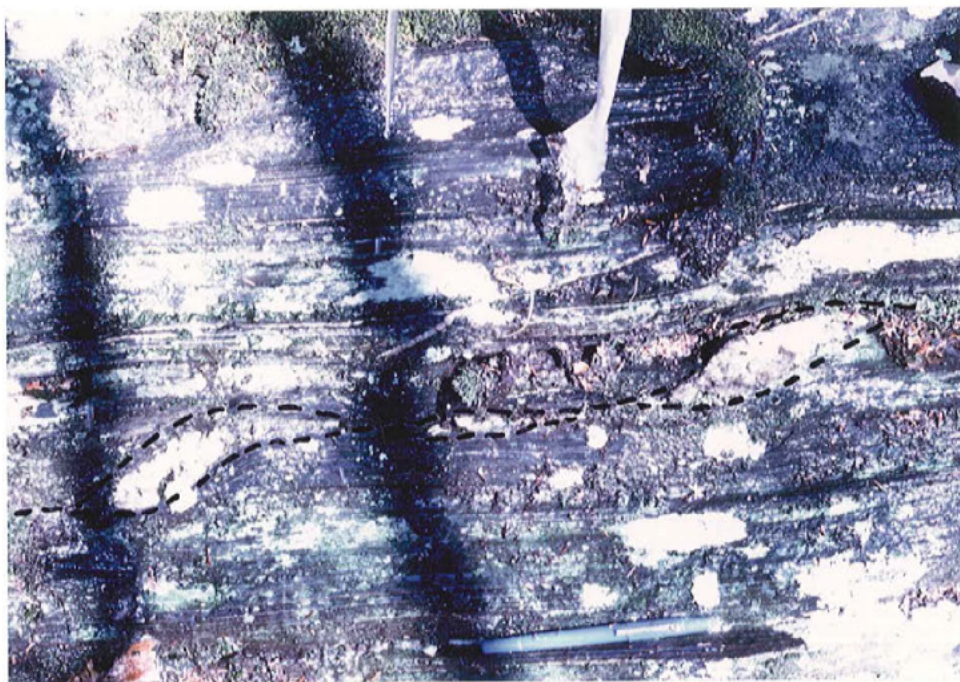
Asymmetrically-boudinaged Pegmatites

Discordant or concordant pegmatites are present in numerous places in the Pelham dome and most of them have been asymmetrically boudinaged (Figure 2.15). In the Erving amphibolite, a north-dipping feldspar pegmatite that cut across foliation and layering has been boudinaged into small pods (Figure 2.15a). The pods have asymmetric tails extending parallel to foliation and indicating the plane along which the pegmatite has been extended (Figure 2.15a). The individual boudins have morphologies similar to those of the "general winged inclusion" of Hanmer and Passchier (1991). Judging shear sense from boudins can be difficult (Hanmer, 1986; Goldstein, 1988) but this example is relatively simple and indicates top-to-the-south sense of shear. The elongation direction of deformed pegmatites in the basement rocks is generally subparallel to the layering. However, when these pegmatites boudinaged, many developed asymmetric tails or wings similar to those seen on smaller feldspar porphyroclasts (Figure 2.15b). The asymmetry of these structures indicates top-to-

Figure 2.15. Asymmetrically-boudinaged pegmatites from the northern part of the Pelham dome.

a. An asymmetrically-boudinaged feldspar pegmatite from the amphibolite member of the Erving Formation. Location is NR1. Note that boudins have been deformed at ends and have morphologies similar to foliation fish. Extension calculated from this extended pegmatite is approximately 1.32. North is to the left, outcrop trends approximately N-S and roughly parallel to the lineation. Dashed lines have been added to highlight location of boudins

b. An asymmetrically-boudinaged feldspar pegmatite from a quartzitic layer within the Dry Hill gneiss. Location is a road cut on the western slope of Ames Hill in the southeastern part of the study area. Dashed lines added to mark boundaries of boudins. North is to the left, outcrop trends approximately N-S and roughly parallel to the lineation.



the-south sense of shear. There is a continuous gradation in size of large feldspathic boudins down to thin-section-scale feldspar megacrysts with similar asymmetries.

Analysis of Shear Fabrics

Extent of Shearing in the Pelham Dome

As previously mentioned, one of the goals of this study was to identify the extent of shearing, as marked by shear-related fabrics, in the northern part of the Pelham dome (Reed and Williams, 1989). Samples were taken in widespread parts of the study area in order to facilitate this. In addition, some reconnaissance work has been done outside the study area to help delineate the extent of shearing.

Top-to-the-south, sub-horizontal shearing pervades the entire study area. From the lowest exposed levels of the core gneisses to the uppermost units in the cover, south-verging kinematic indicators are present. Microfabric kinematic indicators are difficult to see in some of the units, particularly finer-grained parts of the Fourmile Gneiss, the Clough Quartzite, and the amphibolite member of the Erving Formation. However, it is always evident that these units have undergone significant ductile shear, even if the sense of shear is not evident. In some of these cases, where microfabric kinematic indicators are not present, larger kinematic indicators such as asymmetrically-boudinaged pegmatites (Figure 2.15) and asymmetric folds (Figure 2.9) confirm the interpreted shearing.

It is not merely the kinematic indicators present in the northern part of the Pelham dome that are the product of top-to-the-south shearing. Virtually all fabrics, including the lineation and the foliation, were produced or extensively modified during an intense ductile shear event. For the most part, earlier fabrics are preserved only as inclusions in porphyroblasts. Matrix grains show strong recrystallized fabrics developed during shearing. Feldspar pegmatites have been broken and feldspar megacrysts dispersed throughout the gneisses.

Because intense shear-related fabrics occur throughout the northern part of the dome, the next step is to consider whether shear has occurred throughout the entire Pelham dome. The shallow, north-south trending mineral lineation that is associated with the shearing in the northern part of the Pelham dome is also present in the rest of the dome (Figure 2.1). Earlier workers in the southern part of the Pelham dome (Tracy and others, 1976; Roll, 1987), noted pods of relict high grade metamorphism surrounded by sheared and hydrated rocks, though a sense of shear was not noted. Late asymmetric folds with asymmetries consistent with top-to-the-south shearing are present in the southern part of the dome (Michener, 1983; Robinson, personal communication, 1989). Reconnaissance work by the author in the central part of the dome (Ryans Hill, Leverett), and by V. DelloRusso (personal communication, 1989) in the southern part of the dome, has revealed top-to-the-south kinematic indicators associated with the north-south stretching lineation. Therefore, it is probable that the entire Pelham dome has been involved in this top-to-the-south shearing event.

Possible Extent of Shearing in the Bronson Hill Anticlinorium

The extent of top-to-the-south shearing outside of the Pelham dome is more problematic. In the Pelham dome, the shear-related microfabrics are associated with a strongly-developed, north-south trending, shallowly-plunging, mineral lineation. An examination of a lineation map for a large part of central Massachusetts (Figure 2.1) shows that lineations with similar orientations are present throughout much of the Bronson Hill anticlinorium. An important question is whether a shearing event correlative with that observed in the Pelham dome is associated with this lineation throughout the Bronson Hill anticlinorium.

South of the Pelham dome, Ashwal (1974) described mylonites in the Belchertown intrusive complex (Figure 1.1) although a sense of shear was not determined. The Belchertown intrusive complex was intruded at 380 Ma (Ashwal and others, 1979) and post-dates Acadian backfold structures (Robinson, 1979). It seems possible that these mylonites are related to this same shearing event. Ashwal (1974) described pods of rocks in the interior of the complex with igneous textures surrounded by narrow hydrated and sheared zones of rock with a foliation and lineation. The lineations shown for these sheared rocks (Ashwal, 1974) are on average steeper and trend more to the east than those in Pelham dome, but include many orientations similar to those seen in the Pelham dome. The pods described are remarkably similar to those Bell and Hammond (1984) have suggested are characteristic of partitioning of strain and hydration in sheared rocks. The lineation

and elongation direction of the pods described by Ashwal (1974) are consistent with transport of material in a north-south direction.

Guthrie (1972) measured data on lineations in the northern part of the Belchertown intrusive complex and the surrounding country rocks (Figure 2.16). A strong north-south lineation is present in the country rocks near the intrusion (Figure 2.16c). A narrow band of pelitic rock occurs as a septum in the intrusion. The contact metamorphic grade of this pelitic septum increases towards the center of the intrusion (Robinson, 1983). Minerals from this septum are also characterized by a roughly north-south lineation (Figure 2.16c) which seems to imply shearing during metamorphism. Intrusive rocks from near the contact show more of a north-south lineation than rocks further inside the complex (Figure 2.16a-b). Given the close proximity of the Pelham dome and the Belchertown complex (Figure 1.1), it seems probable that the lineation and shear zones are related to the same event seen in the Pelham dome, although more study is needed.

East of the Pelham dome in the Bronson Hill anticlinorium, M.L. Williams (personal communication, 1990) has seen north-south shearing with dextral sense in steeply-dipping, high grade rocks on the eastern shores of the Quabbin Reservoir. Work along the boundary between the Bronson Hill anticlinorium and the Merrimack belt (Peterson, 1989, 1992; Peterson and Robinson, 1993) has documented two lineation orientations in rocks that dip steeply to the west. One lineation orientation is north-south and shallowly plunging and the other is east-west and steeply plunging. Both are defined by elongate sillimanite. Textural relations suggest that the east-west-oriented lineation is older. Associated with the shallow north-south lineation is a

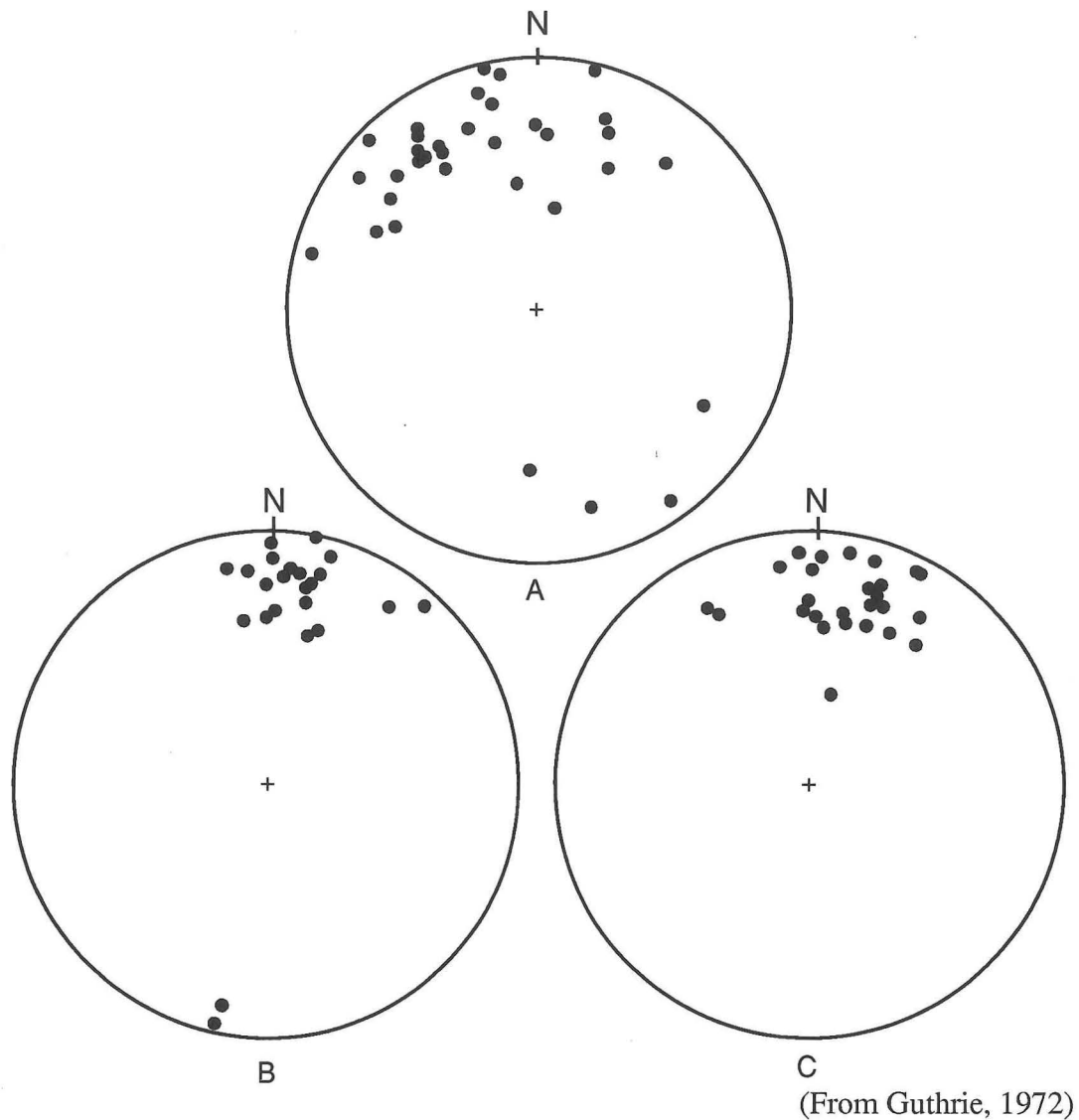


Figure 2.16. Equal-area stereographic plots of mineral lineations from the Belchertown Intrusive Complex and the country rock surrounding it. a. 34 lineations measured in the rock of the complex itself, excluding rocks from the schistose border zone. b. 23 lineations from the schistose border zone of the Belchertown Intrusive Complex. c. 26 lineations from a septum of Partridge Schist included in the intrusive rocks and from the country rock surrounding the intrusive complex. Note the similarity between B and C.

dextral shear (Peterson, 1989, 1992). It is possible that this dextral shear is related to the shearing seen near the Quabbin reservoir and in the Pelham dome. However, recent isotope geochronology (Robinson and Tucker, 1991) suggests that the deformation seen by Peterson (1989, 1992) is probably of a different age than that seen in the Pelham dome. Problems of timing will be discussed more in Chapter 5.

One area in the Bronson Hill anticlinorium, in which the dominant mineral lineation is not roughly north-south, is the northern part of the Warwick dome (Robinson, 1963; Figure 2.1). Some previous microfabric work has been done in this area (DelloRusso and Robinson, 1989). The shear senses seen in this area vary considerably and not all of them fit well with those seen in the Pelham dome. However, some of the samples for this study (site LL2, Plate 1) are east of the axis of the Northfield syncline and should be considered cover rocks for the Warwick dome. The units here are overturned, but these samples still show kinematic indicators indicating that the physical, not stratigraphic, top of the rocks has moved south relative to the physically lower part of the rock. This disparity is troublesome. It may be that the parts of the Warwick dome without a north-south lineation are related to some other tectonic event. More study is needed in the Warwick dome to tie together these different kinematic elements.

While further work is needed, there is a wide area where orogen-parallel shearing may have occurred. It seems possible that the shearing event pervades the areas of the Bronson Hill anticlinorium where the north-south lineation is present.

Quantification of Shear Strain

All of the rocks in the study area have strong top-to-the-south shear fabrics although it is less obvious what the magnitude of this shear is. The rocks have seen enough shear to develop kinematic indicators but probably not enough shear and grain-size reduction to be called mylonites in the classical sense. Strain is relatively evenly distributed within units of homogeneous composition. Strain heterogeneities that are present are clearly associated with changes in rock type.

Quantification of strain in the Pelham dome is difficult because, with the exception of local occurrences of pebbles within the Clough Quartzite, the most commonly analyzed strain markers (ooids, reduction spots, fossils, etc.) are not present in the Pelham dome. However, some less precise techniques can be applied.

Throughout most of the northern part of the Pelham dome strain is relatively homogeneous on an outcrop scale. The rocks typically do not show discrete shear zones or any other evidence of large strain gradients. However, in one outcrop (SR1, Plate 1) a pegmatite that cuts through the Dry Hill Gneiss is offset at a localized high strain zone. This "shear zone" is in fact a lithologically different layer in the gneiss. This sheared layer is richer in biotite which probably is the reason strain was localized into it. The difference in orientation of the pegmatite inside and outside of the biotite-rich sheared layer can be used to determine the angular shear of the zone. The orientations of the various features have been manipulated on a stereographic net (Figure 2.17) to derive the answer. If the XZ plane of shear is considered to be a

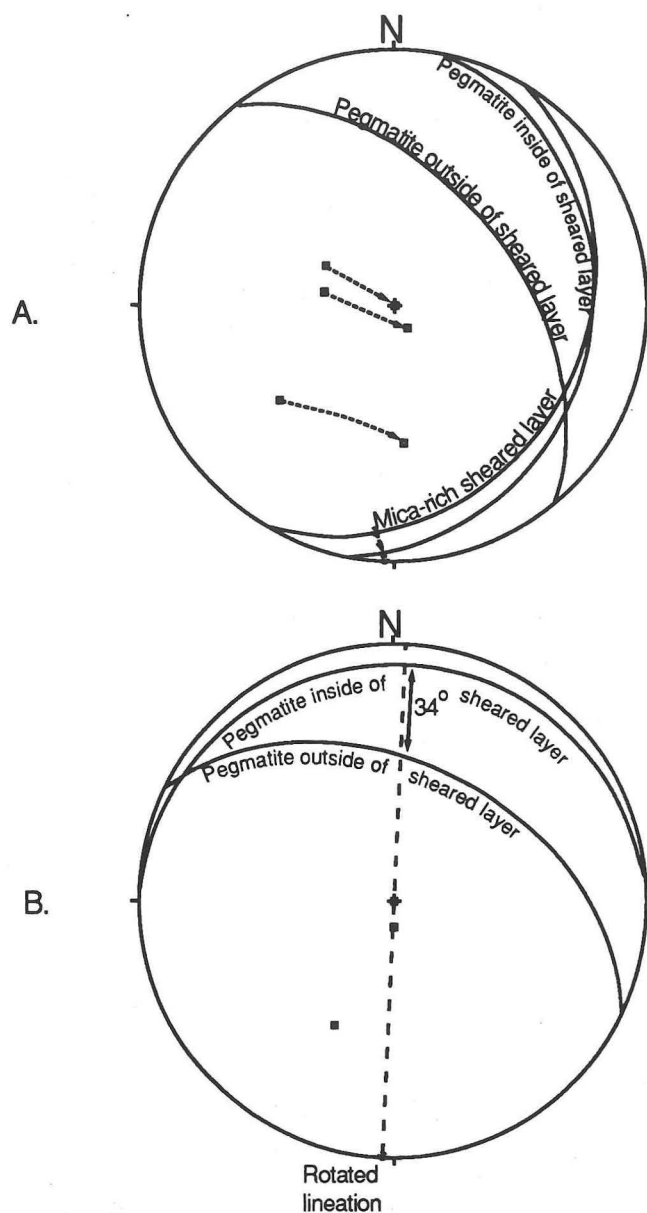


Figure 2.17. Angular shear of a deformed pegmatite from the Dry Hill Formation. A. Equal area stereographic plot showing orientation of the pegmatite, inside and outside of the sheared layer, the sheared layer, and the stretching lineation. Also shown are the poles to the planes if the poles are rotated so that the sheared layer is horizontal. B. Stereographic plot rotated so that the sheared layer is horizontal. Plot shows the rotated orientation of the pegmatite, both inside and outside of the sheared layer. The dotted line marks the X-Z plane of shearing, a plane perpendicular to the sheared layer and parallel to the stretching direction. The angular shear of the pegmatite in this plane is 34 degrees.

plane parallel to the lineation and perpendicular to the biotite-rich sheared layer, the pegmatite has been rotated 34° to the south in the XZ plane of shear.

Problems with strain partitioning make it unclear whether this 34° angular shear can be considered representative of the bulk strain. The rocks below the biotite-rich layer are also sheared, but to a lesser extent. Therefore, the angular shear must be viewed as a minimum for the biotite-rich layer. However, because this is a clear case of partitioning of strain into a weaker layer, it can not be assumed that strains in other parts of the dome are as high. A further problem is the pegmatite itself. Unlike many pegmatites seen in the core gneisses, it has not been dismembered by shearing, although it has been somewhat deformed. This suggests that the pegmatite may not have been present throughout the entire shearing event. These are valid considerations, but it is reasonable to use the calculated angular shear as a low estimate of strain.

If this 34° angular shear is taken as a valid minimum shear then an offset for the stratigraphic thickness of sheared rocks can be worked out. An approximate thickness of 2 kilometers for the units known to be sheared was derived from published cross-sections (Zen and others, 1983). Using this thickness, the top of the uppermost sheared unit present would have been offset a minimum of 1.35 kilometers to the south relative to the lowest gneiss exposed.

Extensions due to shear can be calculated from objects pulled apart during shearing (extension is equal to final length minus the original length, the difference divided by the initial length). Several samples display feldspar grains that have been broken and dispersed by shear (Figure 2.12). Reconstruction of the original length of

the grain in the stretching direction versus the current length in that direction gives an estimate of the extension. This extension represents a minimum value because matrix strain has been partitioned to some extent around the feldspars. Calculated extensions vary significantly. Values of 0.08, 0.25, 0.36, 0.57, and 0.85 were obtained. It is unfortunate that more broken feldspars with obvious offsets were not present. A similar reconstruction carried out on the boudinaged pegmatite discussed earlier (Figure 2.15a), shows an of extension of 1.32 or 132% lengthening.

These extensions can be converted into minimum angular shears. The angular shear necessary to produce an extension of 0.85 along the maximum extension direction is 40.36° . Therefore, the largest feldspar-grain extension suggests a minimum south-directed transport over 2 kilometers of section of 1.7 kilometers. The minimum angular shear necessary to produce the extension of 1.32 calculated from the dismembered pegmatite is 52.43° . Over the 2 kilometers of section present, this translates to a minimum south-directed transport of 2.6 kilometers.

Just to the north of the study area in the Silurian Clough Quartzite, Robinson (1963) measured strained quartz pebbles that were elongate in a north-south direction. Although the orientation data necessary for an R/Phi analysis are not present, the average axial ratio for these pebbles is 28.4:4.8:1 (Robinson, 1963, Table 27). The trend and plunge of the principal stretching direction is N23°W and the principal shortening direction is perpendicular to foliation. While it would be foolish to assume that these pebbles have only undergone one deformation, the regional tectonic model suggests that the principal stretching direction of the previous deformations would probably have been other than north-south. Previous deformations must not have been

too severe because pebbles that were too flattened or elongated would have folded if reformed. Based on the orientation of the principal stretching direction and the proximity to the study area, it is possible that these pebbles have undergone the same deformation that the Pelham dome experienced. Thus, the elongation of quartzites in the Pelham dome was probably on the same order of magnitude.

Relative Magnitude of Shear Strain

Several factors limit the use of textural criteria for constraining the magnitude of shear strain. It is difficult to apply these criteria to different rock types, because they have different characteristic responses to shear. In addition, while shear has been interpreted as being relatively homogenous within individual units, partitioning of strain between different rock types is almost inevitable.

After examination of the situation and the samples available it was necessary to set certain limitations on which units would be compared. The nature of the outcrop within the study area makes it easier to check for shear variation vertically rather than horizontally. It is necessary to have two rocks of very similar compositions in order to compare textures. No true pelitic rocks were sampled within the core gneisses so comparisons between core rocks and any of the pelitic cover units are not possible. One rock type, common in both the core and the cover, is an impure quartzite. Therefore, a textural comparison was made between a quartzitic unit in the core and a quartzite from the Silurian Clough Quartzite. Other than this, the samples collected

are not suitable for comparing shear intensity between rocks in the core and rocks in the cover.

There is an excellent opportunity to check for vertical changes in shear intensity within the Proterozoic gneisses. Large-scale pre-shear folding of the Proterozoic gneisses has made the Poplar Mountain Gneiss both the structural lowest and the structural highest of the Proterozoic gneiss exposure. Comparisons of similar compositions of gneiss from the upper and lower occurrences provide the best opportunity for seeing vertical changes in shear intensity.

Textural Criteria for Shear Development

Several textural criteria have been derived to aid in determining variations in shear strain intensity. These criteria will be briefly reviewed, before their application is discussed.

Feldspar Textures. A major textural criterion of shear strain intensity is the condition of the feldspar megacrysts in the Proterozoic gneisses. Several distinct features are developed in feldspar megacrysts with increased deformation. However, care must be taken because feldspar deformation is influenced by changes in mineral abundances which affect the degree of strain partitioning. For example, increased quartz and mica in a gneiss allow partitioning of strain around feldspars; more feldspar in a rock means less partitioning and more deformed-appearing feldspars.

The size and shape of feldspar megacrysts are a possible criterion. With increasing strain the feldspars are expected to become increasingly rounded by recrystallization of the corners, at least if the feldspars are recrystallizing. This process is somewhat limited by the tendency of the feldspars to break along cleavage planes and form smaller but less rounded megacrysts. The size of the megacrysts thus also may be a criterion, keeping in mind that the original sizes may have varied and strain partitioning might allow different clasts to be affected to differing degrees.

It is not unreasonable to assume that there are limitations in the amount of strain that can be partitioned around feldspars in a deforming gneiss. With increasing amounts of shear strain it could become more difficult for strain to be partitioned around feldspar megacrysts. Thus, with increased strain the megacrysts themselves should have increased stored strain energy. A direct result of this would be an increased chance of recrystallization of the feldspars by grain boundary migration. Increased recrystallization could lead to larger recrystallized tails on the feldspar megacrysts. So, increased strain could be recognized by increased amounts of recrystallization or increased size of recrystallized tails.

There is a wide variation in the amount of microcline twinning present in potassium feldspar megacrysts from the Proterozoic gneisses. In some samples, only small grains that appear to have recrystallized off the megacrysts have microcline twinning. Microclines do not twin due to deformation because of the internal order of Al atoms (Tullis, 1983; Smith and Brown, 1988). However, Smith and Brown (1988) note that deformation can cause microcline twinning already present in feldspar to coarsen. Many microclines in the gneisses show well developed tartan twinning at the

outside margins and no visible twinning in the center (Figure 2.18). This is probably the result of deformation being localized in the margins and coarsening the submicroscopic microcline twinning previously present in the megacrysts. The intensity of microcline twinning may therefore be related to the degree of deformation and/or deformation-induced recrystallization.

Plagioclase feldspars can form twins due to deformation (Tullis, 1983). Therefore, the degree of twinning in plagioclase megacrysts can be used as a criterion for deciding how much the grains have been strained.

Simpson and Wintsch (1989) have proposed that myrmekite develops as a result of deformation, specifically deviatoric stress. Vernon (1991) has questioned this interpretation, but it nevertheless seems that some relationship exists between the development of myrmekite in the Proterozoic gneisses and deformational processes. Megacrysts in the Pelham dome show significant development of myrmekite, and the myrmekite appears principally on the edges of megacrysts and not in their centers. This pattern of occurrence supports a deformational formation method because deformation tends to be concentrated on the edges of the megacrysts. The amount of myrmekite present in a gneiss might be a clue to the amount of deformation that the rock has experienced. Once again this would be sensitive to the amount of feldspar in the rock.

Preferred Orientation of Quartz C-Axes. When quartz is undergoing slip by dislocation glide, the c-axes of the deforming quartz crystals tend to rotate toward the principal stress directions (Etchecopar, 1977). This study did not include an attempt

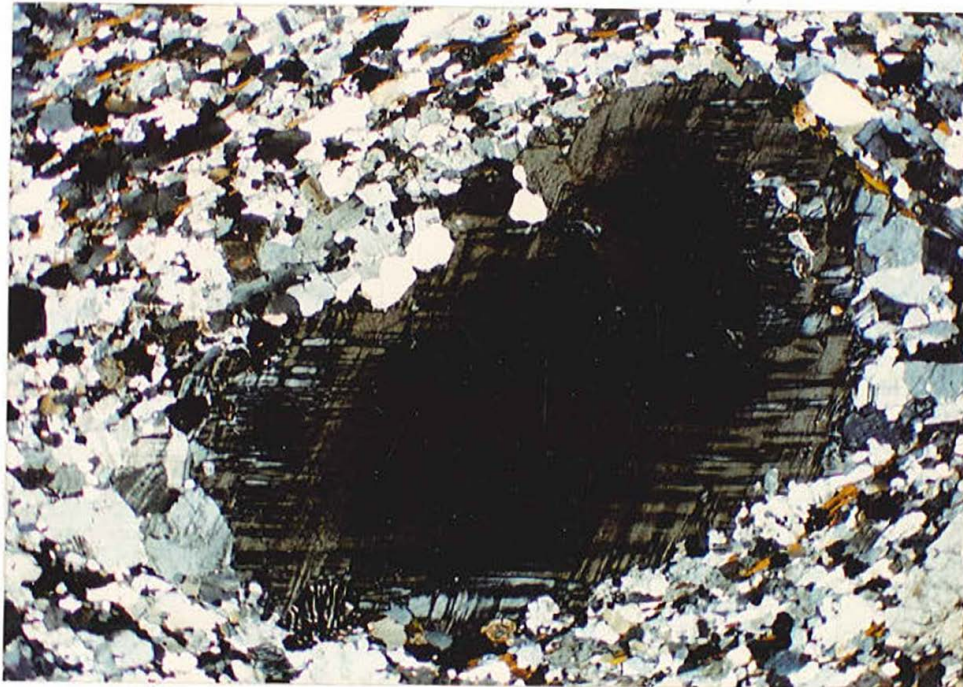


Figure 2 .18. Photomicrograph showing zoned development of tartan twinning in a microcline porphyroblast. Twinning is coarser near the edges, fades out toward the center of the crystal. Note myrmekite in lower left corner of porphyroblast. Foliation cuts from upper right to lower left of photograph. Sample is HQ from the Dry Hill Gneiss. Taken in cross-polarized light, field of view is 13 mm. across.

to do comprehensive c-axes studies with a universal stage. However, the degree of preferred orientation can be visually estimated by inserting the gypsum plate while examining thin sections in cross-polarized light. Increased preferred orientation may result from increased strain magnitude.

Foliation Development. Increased magnitude of shear should lead to increased intensity of foliation within the rock. Elongation of quartz and development of pressure shadows and recrystallized tails also lead to a more intense planar fabric. The major deflection of foliation in many mylonites is the warping of foliation around porphyroclasts. Grain-size reduction decreases the size of these grains which decreases the deflection of foliation.

Recrystallized Grain Size. Both of the major dynamic recrystallization processes, grain-boundary migration and rotational recrystallization, tend to decrease the grain size of a deforming rock. So the more a rock is recrystallized the smaller its grain size should be. This criterion is extremely dependent on the pre-deformation size of the grains that are being recrystallized.

Shear Intensity in the Poplar Mountain Gneiss

When choosing samples for comparative strain analysis, care was taken to choose samples with approximately the same mineral modes because all of the textural

criteria are sensitive to small changes in composition. Two pairs of thin sections were chosen as satisfying the compositional conditions discussed.

The first pair was sample NM4 (Plate 1) from the upper Poplar Mountain Gneiss and sample ART2-X (Plate 1) is from the structurally lowest outcrop found within the core of the Pelham dome. Both samples are relatively rich in biotite and poor in potassium feldspar for samples of the Poplar Mountain Gneiss. The microcline from the sample of the upper Poplar Mountain Gneiss seems to be more recrystallized and broken and has developed more myrmekite. Recrystallized tails around porphyroclasts are larger in the upper sample and fewer porphyroclasts are present. From visual estimation, the preferred orientation of quartz appears stronger in the upper sample. These observations suggest that the upper sample has been more sheared. However, plagioclase megacrysts from the lower sample have more internal polysynthetic twinning which suggests that these plagioclases have been more strained. In contrast to this, plagioclase megacrysts from the upper sample show more recrystallization around the grain edges. The evidence for the upper sample being more sheared is not completely conclusive, but this conclusion seems more likely than the inverse.

A second pair of samples from the Poplar Mountain Gneiss were also examined. The sample from the upper gneiss is 63A (Plate 1) and the sample from the lower gneiss is RRC1 (Plate 1). These samples are lithologically different from the previously compared samples in that they contain much less biotite and much more microcline so that they deformed in a distinctly different manner. The sample from the upper gneiss has microcline megacrysts with more twinning and slightly more

myrmekite. In general, feldspar megacrysts in 63A show more marginal recrystallization and more brittle deformation structures. Sample 63A also contains fewer megacrysts and more matrix, and seems to have a slight preferred orientation of quartz c-axes that sample RRC1 does not have. The sample from the lower gneiss does have a slightly smaller matrix grain size, but as previously noted there is much less matrix present. Taking into account all of the above observations it seems likely that the sample from the upper gneiss (63A) has undergone a greater magnitude of shearing.

In both of these cases, it seems that the amount of strain may be decreasing with depth in the dome. The major problem with this has to do with the possibility that the rocks were heterogeneously strained prior to the initiation of shearing. The upper gneiss is considerably thinner than the lower gneiss and if this thinning is tectonic it would influence the observations.

Shear Intensity in Quartzites

It was more difficult to find pairs of quartzite samples of similar compositions. Quartzites from the Silurian Clough Quartzite, the Proterozoic Poplar Mountain Quartzite, and isolated layers within the Proterozoic Dry Hill Gneiss are all impure, with varying amounts of secondary constituents. A pair of muscovite-biotite quartzites, one from a layer within the Dry Hill Gneiss (DHR1, Plate 1), and one from the Clough Quartzite (MW2, Plate 1) were chosen. The samples are very similar in composition with the exception that MW2 contains a small amount of garnet. Both

samples show ample evidence of deformation and have weak S-C fabrics indicating top-to-the-south sense of shear. The foliation within MW2 appears more planar and better developed. DHR1 has smaller grain size, more undulatory extinction, and a slightly stronger preferred orientation of quartz c-axes.

Difficulty arises with making comparisons between the fabrics because both have undergone primary recrystallization after the cessation of shear. In primary recrystallization, low-strain grains grow by grain-boundary migration at the expense of high-strain grains. In the samples studied, the result of this is large strain-free grains of irregular shape that contain within them micas parallel to the shear foliation. The selective growth of some grains at the expense of others during primary recrystallization has obscured the deformation fabrics to a large extent. Based on the number of large strain-free grains of irregular shape, more primary recrystallization seems to have occurred in MW2.

The textural differences in these two quartzites are rather small. Quartzites from the cover and the core appear extremely similar, having undergone the same deformation processes to apparently similar extents. It does not seem possible to determine a difference between the amount of strain shown by the quartzite samples.

Perhaps an important factor to consider when comparing the strain of quartzites from the core and the cover is the partitioning of strain. In most cases in the cover rocks, including the one examined here, the quartzites are surrounded by easily deformable pelitic rocks, so strain should have been partitioned around the quartzites. In the core rocks, the quartzites are surrounded by stronger feldspathic gneisses, so strain would be expected to partition into the quartzites.

Shear and Previously Documented Deformational Phases

One of the goals of this study was to correlate deformation fabrics seen in the northern part of the Pelham dome with phases of deformation described by previous workers. Onasch (1973) interpreted two stages of ductile deformation as following the development of asymmetric south-verging folds and south-directed shear. These two phases are "late shears of reversed sense" and "late-flattening and extension". In this study, a different interpretation has been made. These "late" fabrics have been reinterpreted as being part of the dominant top-to-the-south shearing.

Onasch (1973) gives two lines of evidence for this phase involving "late shears of reversed sense". The first includes supposedly rotated augen and boudins present in the core rocks (Figure 2.19). Many such bodies were seen in the course of this study, and all have geometries consistent with top-to-the-south shearing. In fact, the line drawing shown in Onasch (1973) bears a strong resemblance to the "general winged inclusions" of Hanmer and Passchier (1991, pgs. 40-44). The asymmetry present can be interpreted as indicating top-to-the-south sense of shear rather than rotation in the opposite direction (Figure 2.19).

The second line of evidence for "late shears of reverse sense" are discrete north-dipping shear zones that cut across layering (Onasch, 1973). These shears were described as normally occurring in the Poplar Mountain Quartzite. Several attempts were made to locate these shear zones. Late in the study, one such shear was found in the Poplar Mountain Quartzite (Figure 2.20) and a similar structure was observed in the Jerusalem Hill Member of the Poplar Mountain Gneiss. In both cases, as well as

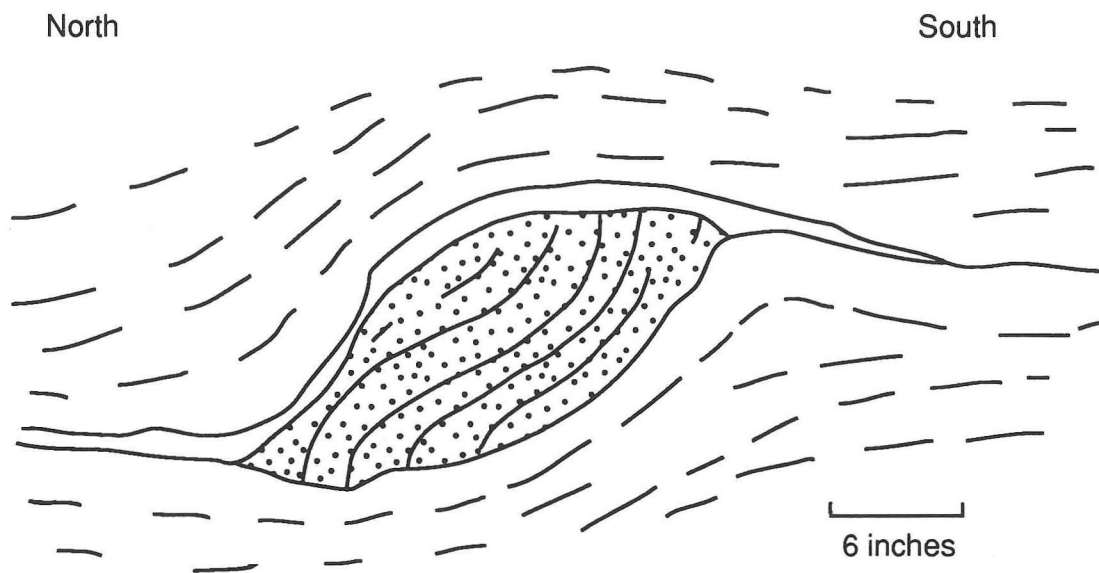


Figure 2.19. Sketch from Onasch (1973) showing supposedly rotated amphibolite lens in the Biotite Member of the Dry Hill Gneiss. Note the asymmetry of the structure and its resemblance to a foliation fish or a porphyroclast with recrystallized tails. Correct interpretation should be top-to-the-south shearing.



Figure 2.20. Shear of reverse sense from the Poplar Mountain Quartzite. Note that shear is cutting the short limb of an asymmetric fold indicating the opposite sense of shearing and that the reverse shear curves into the layering above and below the fold. North is to the left, and the length of the area in the photograph is approximately 1.25 m.

the figure in Onasch (1973), the shear zones are associated with south-verging asymmetric macrofolds. The shear zones seem to have formed along the short limbs of these folds and die out quickly above and below the folds (Figure 2.20).

In this study, these features are interpreted as resulting from interaction between shearing and folding and not as occurring after shearing. As the folds developed during shearing the lower limbs were rotated until they were roughly perpendicular to the maximum principal shortening direction (Figure 2.21). Folding had already thinned and weakened the rocks along the lower limb of the fold. There are well-documented cases of bodies within shear zones undergoing antithetic shears along planes in this orientation (Figure 2.11). It is probable that the fold had tightened to the point of no longer accommodating shear strain. The folding caused local thickening, and it is inferred that the folded layers began to behave as a rigid object. This area was then pulled apart with shear occurring along the pre-existing weakness (Figure 2.21). This interpretation explains why the shear zones are confined to the folded layers and another phase of deformation after shearing is not needed.

Interpretation of the "late flattening and extension" (Onasch, 1973) was more problematic. Boudins seen in this study were commonly asymmetric, were very ductile in appearance, and were apparently associated with shearing (Figure 2.15). Onasch (1973) correlates the boudinage and extension with closely-spaced brittle fractures that occur in the quartzite. He bases the timing of boudinage on the fact that the fractures overprint other structures. It seems possible that the ductile boudinage is actually related to shearing and that the brittle fractures are due to a later reactivation of an older anisotropy.

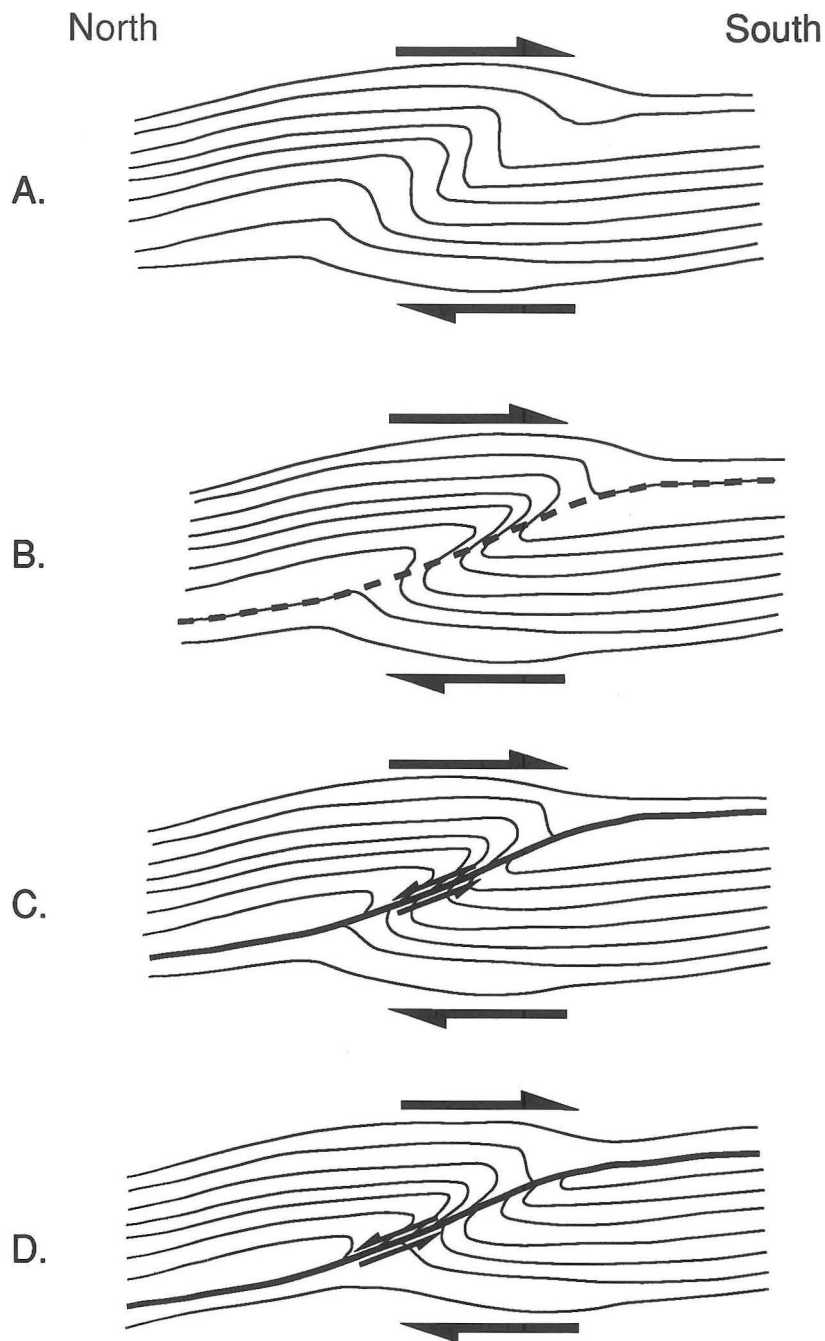


Figure 2.21. Development of reverse sense shears in the northern part of the Pelham dome. A. A fold begins to form in response to top-to-the-south shearing. B. The fold tightens to a point where it can no longer accommodate shearing. Note that the short limb of the fold has been thinned. The dashed line marks the incipient fault plane. C. The fault has formed along the weakened short limb and the fold is being extended with an antithetic sense of shear. D. With further fault movement the thickness of the folded area is reduced.

CHAPTER 3

RELATIVE TIMING OF METAMORPHISM AND DEFORMATION

Introduction

Evidence from inclusion fabrics, deformation textures, and the relationship of metamorphic minerals with existing foliations can be used to constrain the relative timing of deformation and metamorphic events. A large amount of such evidence has been collected from the northern part of the Pelham dome, primarily from the cover rocks. This information has been integrated with a large body of previous work on metamorphism in the area (c.f. Robinson and others, 1986), to produce new insights into the metamorphic history.

Metamorphic Events in the Pelham Dome Area

The Pelham dome area contains evidence of at least four distinct metamorphic events (Figure 1.4): an early (Acadian?) granulite-facies metamorphism, contact metamorphism related to the Belchertown intrusive complex, a regional metamorphism to the lower amphibolite facies, and at least 1 localized late retrograde metamorphism (Robinson, 1983). The most prominent of these is a regional metamorphism to the kyanite zone of the lower amphibolite facies (Robinson, 1983; Zen and others, 1983).

Estimated conditions of this metamorphism are 580°C and 5.5 kilobars (Tracy and others, 1976).

Peak assemblages associated with this regional metamorphism vary with the bulk composition of the pelitic units. Some schistose layers within the granulitic rocks of the Devonian Erving Formation contain either biotite-garnet-staurolite-kyanite assemblages or biotite-staurolite-kyanite assemblages (Figure 3.1). With a few recently discovered exceptions, the pelitic rocks of the Devonian Littleton and Ordovician Partridge Formations in the northern part of the Pelham dome contain no kyanite but do contain abundant staurolite, garnet and biotite (Figure 3.1). Less aluminous layers contain no staurolite and locally no garnet. Mafic units commonly contain the assemblage hornblende-plagioclase (andesine to labradorite)-titanite \pm epidote, also indicating the lower amphibolite facies (Laird and Albee, 1981). Until recently, this metamorphism was thought to be Acadian, but recent work suggests that it was probably Pennsylvanian (Gromet and Robinson, 1990; Robinson and Tucker, 1991).

Enclaves with sillimanite-potassium feldspar-garnet-biotite assemblages have been found in rocks assigned to the Mount Mineral Formation (Figure 1.4), south of the study area (Tracy and others, 1976; Roll, 1987). These enclaves contain relict assemblages, which are preserved inside sheared rocks with lower amphibolite grade assemblages (Roll, 1987). The relict metamorphism is not clearly evident in the northern part of the Pelham dome, but textural relations in a small mafic pod suggest retrograde reaction of what may have been this assemblage. Until recently, the timing of this high grade metamorphism was uncertain, but new geochronologic evidence

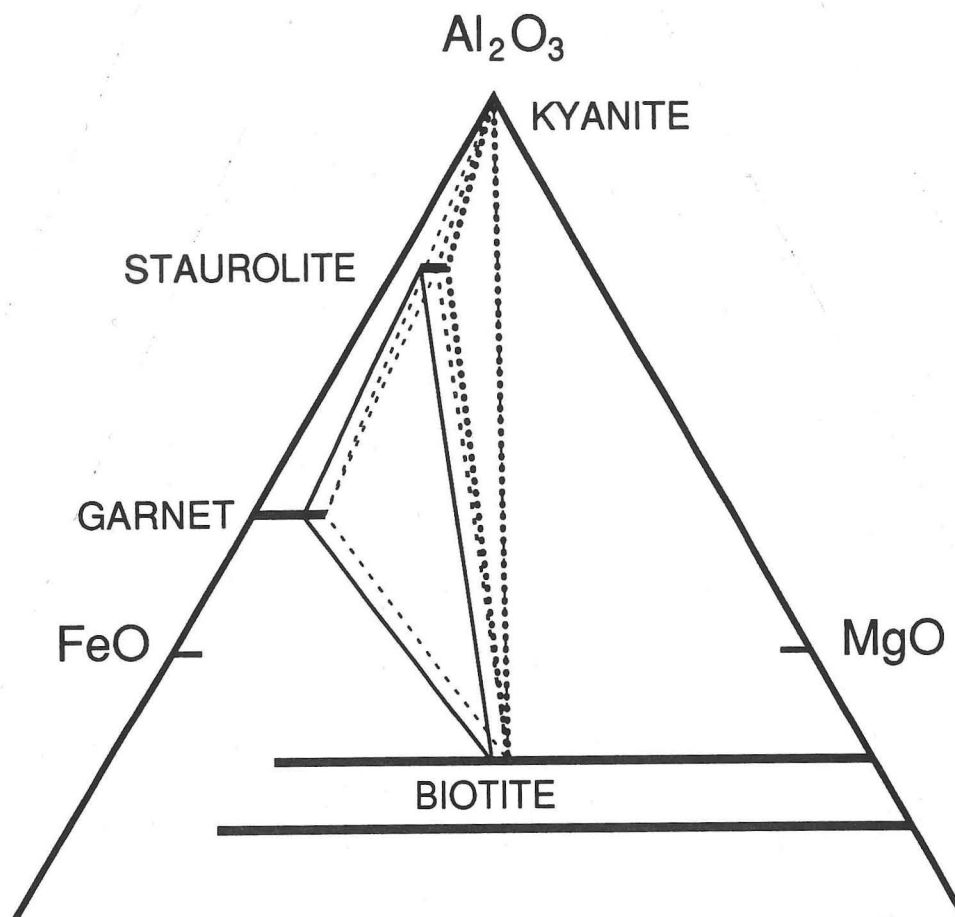


Figure 3.1. AFM diagram showing phase relations of pelitic units in the northern part of the Pelham dome. Dotted lines represent phase relations in certain thin pelitic units in the Erving Formation (staurolite-kyanite-biotite). Dashed lines are other pelitic units in the Erving Formation which show four-phase stability (garnet-staurolite-biotite-kyanite). Solid lines are phase relations for most pelitic units within the Littleton and Partridge Formations (garnet-staurolite-biotite). Fe/Mg ratios of garnet and biotite are from Tracy and others (1976), staurolite Fe/Mg ratios shown are arbitrary.

suggests an Acadian age (Robinson and Tucker, 1991). It remains unclear why remnants of this metamorphism have not been seen in the cover units of the northern part of the Pelham dome.

The New Salem retrograde zone (Figure 1.4) of Robinson (1963) and Hollocher (1981) lies southeast of the study area. Rocks in this area have undergone retrograde metamorphism to as low as the chlorite zone of the greenschist facies (Hollocher, 1981). Hollocher (1981) has suggested that these rocks were formed by a localization of metamorphic fluid adjacent to the Prescott Intrusive Complex (Figure 1.1). Some localized retrograde metamorphism in the northern part of the Pelham dome may be associated with this event. Robinson and Tucker (1991) have suggested that the New Salem and Quabbin Hill retrograde metamorphic zones (Figure 1.2) lie near the boundary between Acadian and the newly suggested Pennsylvanian deformation in the Bronson Hill anticlinorium.

Narrow layers of alteration are common along post-metamorphic, brittle faults in the Pelham dome area (Robinson, 1963; Ashwal, 1974). Some samples from the study area show effects that may be related to this alteration.

The remaining metamorphic event seen in the Pelham dome area affects only the extreme southern end of the Pelham dome. This event was contact metamorphism associated with the Belchertown Intrusive Complex (Guthrie, 1972; Ashwal, 1974; Robinson, 1983). Contact metamorphism elevated the regional lower amphibolite grade to as high as the sillimanite-muscovite-K-feldspar zone of the upper amphibolite facies (Figure 1.2). A sill of hornblende monzodiorite, thought on lithological evidence to be related to the Belchertown intrusive complex (Hodgkins, 1985), is

found within the study area at the contact between the Poplar Mountain Gneiss and the Fourmile Gneiss on Northfield Mountain. No appreciable contact metamorphism is associated with this sill. Radiometric dating of this sill has yielded an age of 370 Ma (G.W. Leo and R.E. Zartman, unpublished data) similar to an age of 380 ± 5 Ma for the intrusive complex as a whole (Ashwal and others, 1979). While contact metamorphism does not affect rocks within the study area, its effects in the southern part of the dome may give important clues in the determination of timing of the main shearing event (see below).

Fabric/Porphyroblast Relations

There are a number of textural relationships between the porphyroblasts and the fabrics present which provide important clues about the relative timing of metamorphism and deformation. The normal reference for timing relationships is the dominant foliation present in the rock. In the Pelham dome, this foliation is believed to be related to a major top-to-the-south shearing. One important textural relationship is whether this dominant foliation is truncated by porphyroblast growth or whether the foliation is deflected by the porphyroblasts. Another important textural relationship is whether the porphyroblasts have strain (pressure) shadows and whether these appear to be related to the dominant foliation. The most interesting and informative relationships in the northern part of the Pelham dome are those between the porphyroblasts and fabrics preserved within them as inclusion trails. Interpretation of these inclusion trails is quite complex and merits a brief review.

Formation of Inclusion Trails in Porphyroblasts

The geometry of inclusion trails in porphyroblasts relative to external fabrics is an important tool in determining timing (Figure 3.2). If different kinds of porphyroblastic minerals grew at different times and consequently have different inclusion fabrics, they can be used to determine the timing of deformation versus metamorphism.

Inclusion fabrics can be divided into two general types. The first involves internal fabrics that are coherent with the external fabric (Figure 3.2). The interpretation of these porphyroblasts is typically simple; the porphyroblast grew after the fabric formed.

The second kind of internal fabrics are those where the internal fabric is not concordant with the external fabric (Figure 3.2). Porphyroblasts with these types of inclusions are either pre- or syn-kinematic with respect to the last fabric formed. The interpretation of these fabrics is more difficult and controversial. Two interpretations are possible; 1) reorientation of the porphyroblast during or after growth or 2) the overgrowing of earlier fabric or fabrics. The subject is complex and will be discussed below for the case of curved or crenulated inclusion trails that are non-concordant to the exterior fabric.

Formation of Curved Inclusion Trails. The interpretation of some inclusion geometries is relatively straightforward, but the timing relationships of spiral-shaped inclusion trails are less clear. Early work on curved and spiral inclusion trails in

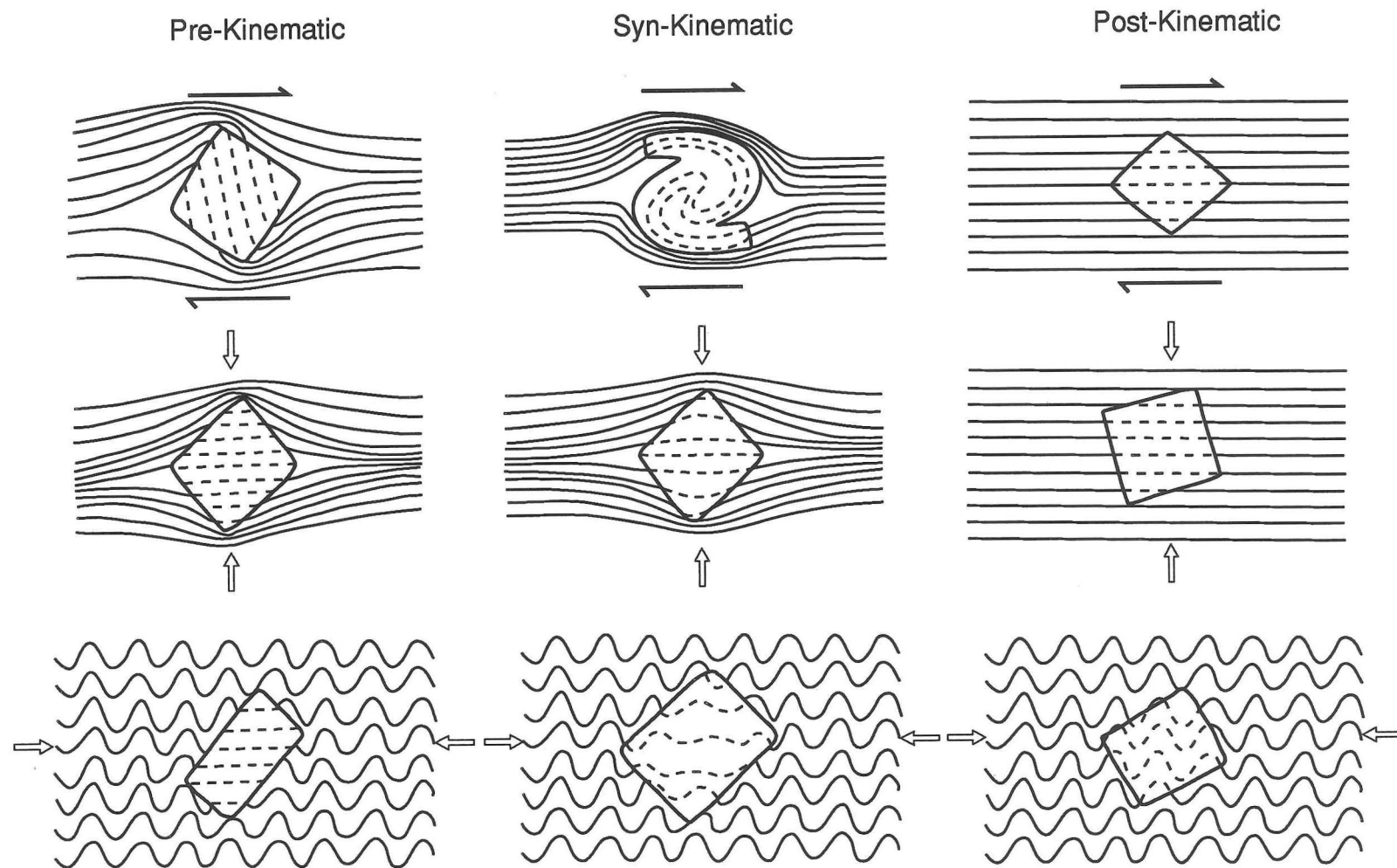


Figure 3. 2. Classic diagnostic forms for porphyroblast inclusion patterns with regard to time and deformation. Redrawn from Zwart (1962).

porphyroblasts suggested that such complex inclusion patterns, at least in garnets, were the result of rotation during growth of the garnet relative to the matrix (Spry, 1969; Rosenfeld, 1968, 1970; Schoenveld, 1977). This type of garnet has come to be called a "rotated" or "snowball" garnet in reference to its supposed manner of growth. This method of formation was inferred not only for porphyroblasts with complex helicoidal inclusion patterns but also for those with less complex sigmoidal inclusion patterns (Bell, 1985). In some instances, porphyroblasts with straight fabrics, not parallel to the external fabric, were also interpreted as forming through rotation rather than overgrowth of an earlier fabric. Differences in complexity were ascribed to differences in amount and/or speed of rotation. However, other researchers (Ramsay, 1962; Bell, 1985; Vernon, 1988, 1989; Bell and Johnson, 1989, 1990) have suggested that in many circumstances, porphyroblasts do not rotate during growth. Evidence for the non-rotation of metamorphic porphyroblasts during growth has been summarized by Vernon (1988), Bell and others (1986) and Bell and Johnson (1989, 1990).

Of the many reasons given for formation of curved inclusion trails without rotation, the most compelling reason is consistency in orientation of inclusion fabrics between porphyroblasts. In a single sample, typically in an outcrop, and even across large folds (Steinhardt, 1989; Johnson, 1990), all inclusion fabrics from porphyroblasts formed synchronously have a similar orientation. In order to produce such consistent orientations, each porphyroblast would have to have rotated exactly the same amount as its neighbors. Taking into account the general heterogeneity of deformation, this consistency in orientation seems a more likely result of the garnets overgrowing a crenulation than of all the porphyroblasts rotating the same amount.

Furthermore, it has been suggested (Bell, 1985; Vernon, 1987) that rotating porphyroblasts should be associated with adjacent microfolds of the matrix, similar to folds of asymmetric tails seen in delta-type asymmetric porphyroblast systems (Passchier and Simpson, 1986). These folds are not seen in most rocks containing supposedly "rotated" porphyroblasts.

Bell and Johnson (1989) also note "fabric truncations" in the interiors of supposedly rotated garnets. In addition to fabrics being cut-off at these truncations there are also changes in chemical composition of the garnet across these truncations. These physical and chemical truncations are not in positions that would arise from growth during rotation (Bell and Johnson, 1989).

"Rotated" garnets have been used as kinematic indicators (Rosenfeld 1970; Trouw, 1973). However, there are instances in which the shear sense obtained from rotation is opposite to that given by other kinematic indicators present for the shear zone (Trouw, 1973; Bell and Johnson, 1990). This inconsistency either requires two directions of movement in the shear zone or adds further support to the suggestion that curved inclusion trails are not necessarily the result of rotation of porphyroblasts during growth.

An alternative method for the development of complex inclusion geometries has been proposed (Bell, 1985; Bell and Johnson, 1989). It is suggested that curved inclusion trails result from minerals overgrowing crenulated or multiply-crenulated foliations. These crenulated microfabrics are developed in the transposition of one foliation to the next (Bell and others, 1986)(Figure 3.3).

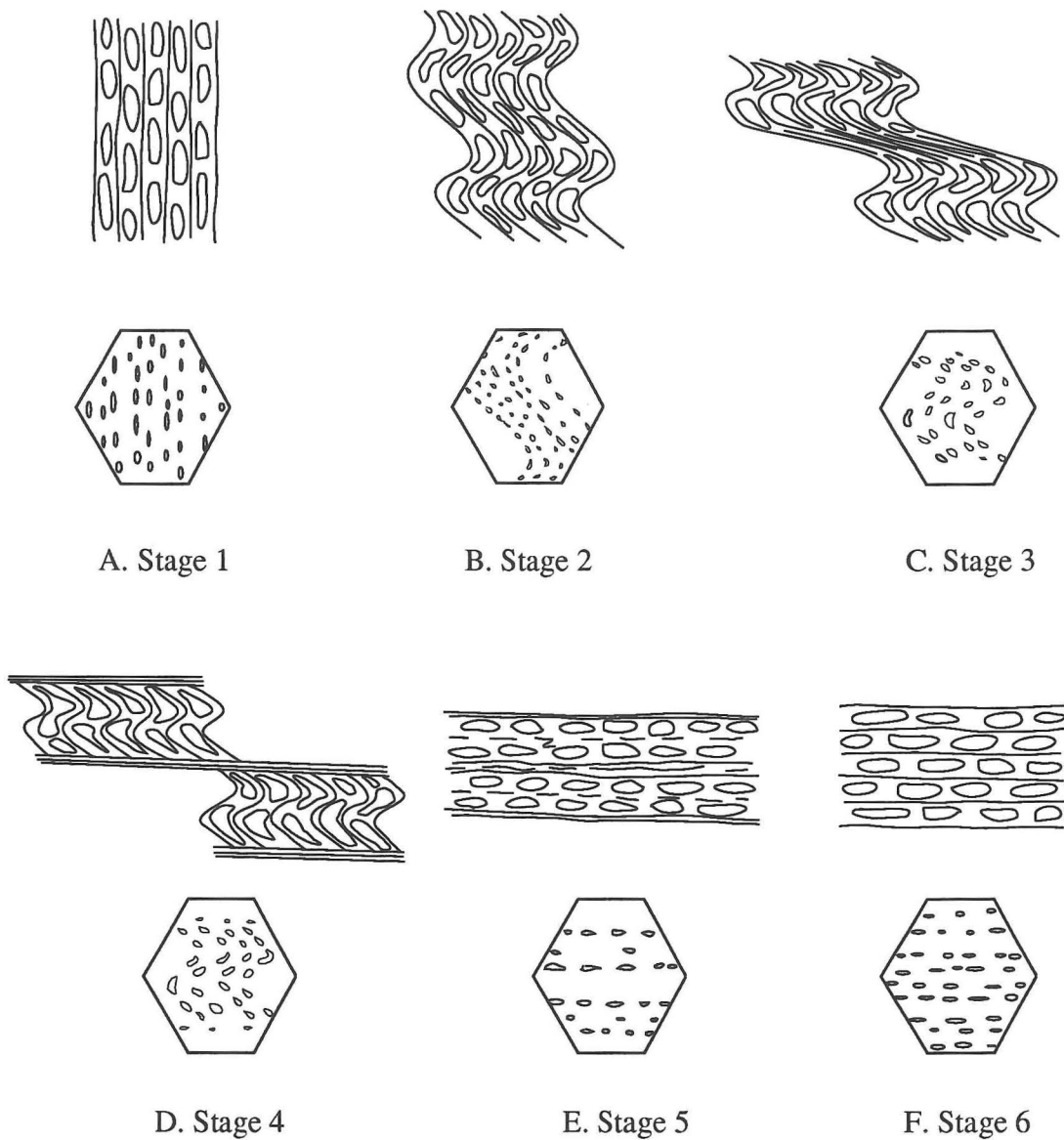


Figure 3.3. The six steps of progressive foliation development through tightening of a differentiated crenulation cleavage. Upper drawing of each pair shows shape of the crenulation at each stage. Lower drawing shows how a garnet that overgrew the foliation at that stage and preserved quartz inclusions might look. Note the difficulty in telling apart Stages 3 and 4 without micaceous inclusions. Modified from Bell (1986).

Simple sigmoidal fabrics with apparent rotations of less than 90° can result from the overgrowth of a single crenulation (Figure 3.3). Bell and Johnson (1989) have proposed a more complex explanation for the helicoidal inclusion patterns which have the fabric truncations discussed above. These fabrics are suggested (Bell and Johnson, 1989) to result from multiple overgrowths of variously oriented external fabrics (Figure 3.4).

While the helicoidal inclusion patterns remain a source of intense controversy, an increasing body of data suggests that most sigmoidal fabrics are formed by overgrowth and not rotation (Vernon, 1989). It remains possible that some of the more spectacular examples of helicoidal garnets may have rotated during growth (i.e. Figure 1, Plate 2, Rosenfeld, 1968); but the inclusion fabrics seen in the present study have proven to be better interpreted as forming through the overgrowth of pre-existing fabrics.

Fabric/Porphyroblast Relations in the Pelham Dome

Inclusion patterns in porphyroblasts and the relationship of these phases to the existing foliation can be used to determine relative timing of mineral growth. In this study, the dominant foliation to which the timing of porphyroblast growth is being compared formed as the result of shearing. The foliation is generally defined by alignment of micaceous phases and elongation of other minerals. Different mineral species from the cover rocks of the Pelham dome show different inclusion geometries and different timing of growth relative to deformation.

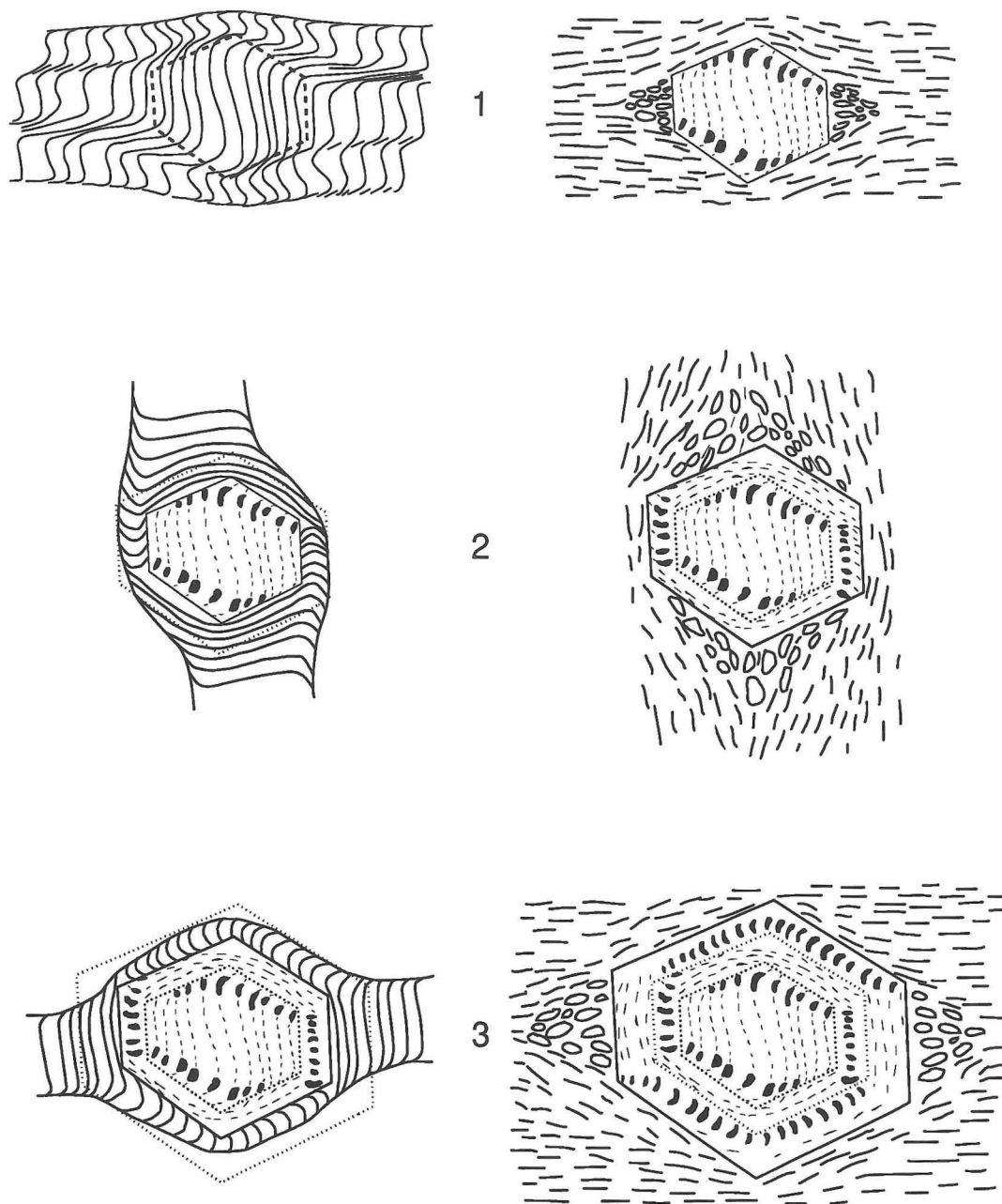


Figure 3.4. Model showing the progressive development of spiral-shaped (helicoidal) inclusion trails in a garnet porphyroblast. Drawings on the left show strain around the porphyroblast during deformation, drawings on the right show how the porphyroblast appears after overgrowing the results of the deformation. Quartz is preferentially preserved in crenulation hinges and strain shadows. Quartz inclusions are shown in black to highlight development of the spirals. Based on Bell and Johnson (1989).

Fabric/Porphyroblast Relations of Garnets

Garnets have the most diverse inclusion geometries of any porphyroblasts in the northern part of the Pelham dome. They show different types of curving inclusion patterns (Figures 3.5, 3.6), including simple sigmoidal trails (Figure 3.5). In lineation-parallel thin sections, the axial-plane traces of some of these folded patterns intersect the dominant foliation at a high angle with steep apparent dips to the north or south. A few garnets show curved fabrics with the trace of the axial plane parallel to the trace of the external foliation. The degree of curvature of the sigmoids varies from open to tight. No curved patterns have been seen in lineation-perpendicular sections, but this could be merely a function of the limited number of sections made in this orientation.

These sigmoidal trails have a number of characteristics. In general, the trails are defined by parallel ovoid quartz inclusions (Figure 3.5). These quartz inclusions are aligned with one another, but in some cases seem to be separated into distinct linear belts. In some garnets, there are opaque and mica inclusions as well. It is not uncommon for the sigmoidal trails to be truncated along sharp lines within the garnet crystal (Figure 3.5) and an inclusion-free rim to be present.

Several garnets with helicoidal trails (Figure 3.6) have also been seen in the northern part of the Pelham dome. The central crenulation of these complex helicoidal patterns is typically fairly tight, with the trace of the axial plane always at a high angle to the dominant foliation. The inclusion trails continue to spiral outward from the central simple sigmoid-shaped inclusions giving the garnet a "rotated" appearance

Figure 3.5. Photomicrograph of a garnet with sigmoidal crenulated inclusion pattern. The trace of the axial plane is oblique to the external foliation. Taken in plane-polarized light, field of view is 3.3 mm. across. Sample is DR2C from the Erving Formation, a lineation-parallel section, north is to the left and the top is up.

Figure 3.6. Photomicrograph of two garnets with helicoidal inclusion fabrics. The trace of the axial plane of the inner crenulations is at a high angle to the external fabric. Taken in cross-polarized light, field of view is 8.5 mm. across. Sample is DR1 from the Littleton Formation, a lineation-parallel section, north is to the left and the top is up.



(Figure 3.4). The inclusions consist primarily of quartz, but unlike inclusions in simple sigmoidal trails, the quartz inclusions are likely to be curved in shape (Figure 3.6). The truncations suggested by Bell and Johnson (1989) are seen in some cases.

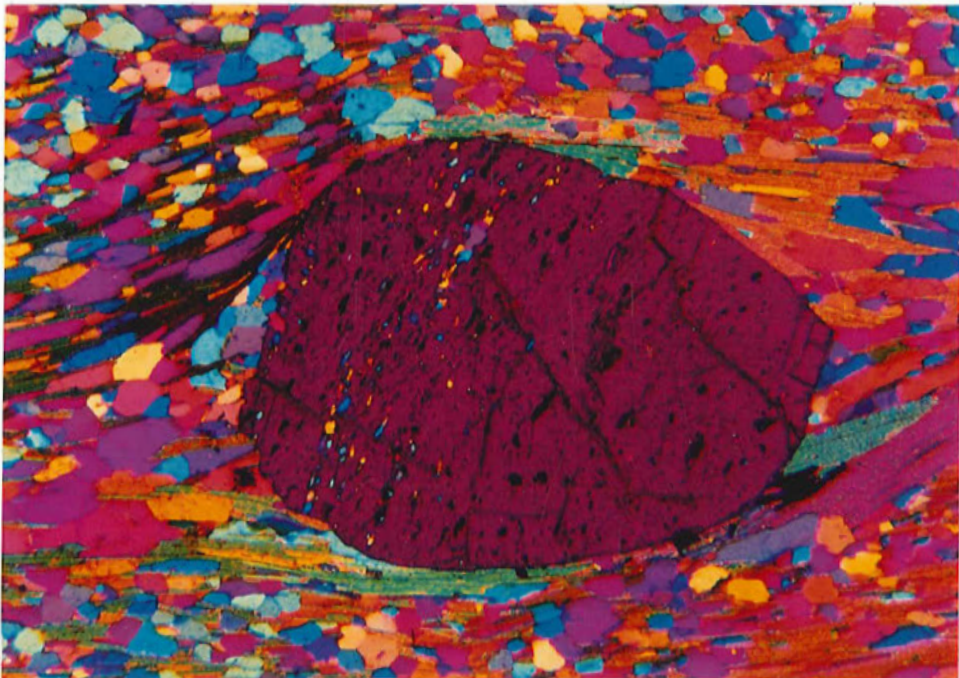
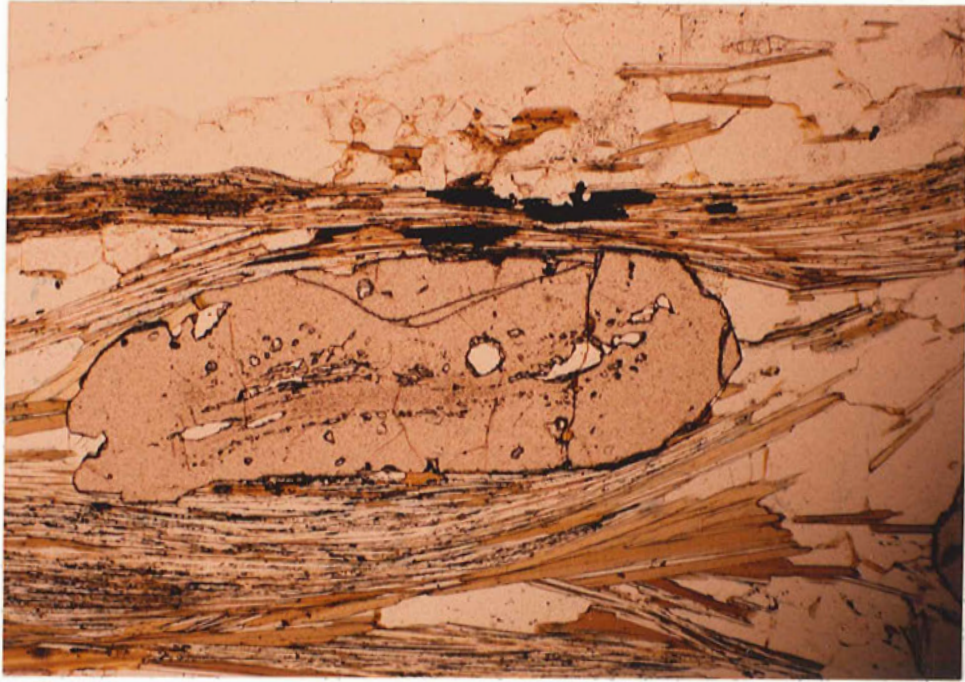
These curved patterns could be either the result of overgrowth of crenulated fabrics or rotation of the garnet during growth. Because the orientation of these fabrics seems to fall into two distinct groups, and for reasons described earlier, these fabrics are being interpreted as having formed by the overgrowth of earlier fabrics, and not by rotation during growth.

Straight fabrics (the two-dimensional trace of planar fabrics) in garnets include straight inclusion trails parallel to the exterior foliation (Figure 3.7a), and straight inclusion trails which are oblique to the exterior foliation (Figure 3.7b) which will hereafter be referred to as oblique straight fabrics. In lineation-parallel thin sections, oblique straight fabrics typically intersect the dominant foliation at a high angle with steep apparent dips to the north or south (Figure 3.7). This orientation is very similar to that of the axial-plane traces of crenulations described above. In lineation-perpendicular sections, straight fabrics both parallel and oblique to the external fabric were seen. The inclusions that define these straight trails in garnets are very similar in composition and size to those seen in sigmoidal inclusion trails in garnets. The predominant mineral is quartz, generally with an elongate oval shape (Figure 3.7). There seems to be a higher occurrence of micas and opaque inclusions in straight fabrics than in curved fabrics (Figure 3.7b). Some garnets have straight fabrics which run from one edge to the other without interruption (Figure 3.7b), other garnets have inclusion-poor rims (Figure 3.7a).

Figure 3.7. Garnets with straight inclusion patterns from the northern part of the Pelham dome.

a. Photomicrograph of a garnet with asymmetric strain shadows showing slightly anastomosing straight inclusion pattern parallel to the external foliation. Taken in cross-polarized light with the $\frac{1}{4}$ -wave plate inserted, field of view is 3.3 mm. across. Sample is L3 from the Littleton Formation, a lineation-parallel section, north is to the left and the top is up.

b. Photomicrograph of a garnet with asymmetric strain shadows showing a straight inclusion pattern oblique to the external foliation. Taken in cross polarized light with the gypsum plate inserted, field of view is 5 mm. across. Sample is DR4 from the Erving Formation, a lineation-parallel section, north is to the left and the top is up.



These straight inclusion fabrics seem to have two consistent sets of orientations. There is no reason to assume that these straight fabrics did not form as the result of overgrowth of the current foliation and a previous high-angle fabric rather than rotation.

In most thin sections, garnets have pressure/strain shadows and the matrix foliation wraps around the garnets reflecting the asymmetry of the strain shadows (Figures 3.5-3.7). The strain shadows present are generally elongate parallel to the dominant foliation, indicating that they formed during the same deformational phase as the foliation. Rarely, the foliation in a thin-section will remain planar in the vicinity of a garnet (Figure 3.8) with no strain shadows being present.

Fabric/Porphyroblast Relations of Staurolites

Staurolites contain most of the inclusion fabric geometries seen in garnets. Many staurolites contain simple sigmoidal patterns (Figure 3.9a), but none contain the helicoidal patterns. The sigmoidal patterns are typically gently curved, not tightly curved like those present in some garnets. Curved fabrics which look like one half of a crenulation were also observed (Figure 3.9b). These apparent partial crenulations are truncated at sharp boundaries which can either be the edge of the crystal or an inclusion-free rim of the crystal. In most staurolites, the trace of the axial plane of these curved fabrics is parallel to the external subhorizontal foliation (Figure 3.9).

Straight fabrics are common with some being concordant (Figures 3.10a, 3.10b) and some discordant (Figure 3.10c) with the external foliation. Discordant



Figure 3.8. Photomicrograph of a garnet that truncates the dominant foliation. Taken in plane-polarized light, field of view is 5 mm. across. Sample is DR2E from the Erving Formation, a lineation-parallel section, north is to the left and the top is up.

Figure 3.9. Staurolites with sigmoidal inclusion fabrics from the northern part of the Pelham dome.

a. Photomicrograph showing a single crystal of staurolite with a sigmoidal inclusion pattern. The trace of the axial plane is parallel to the external foliation. Taken with plane-polarized light, field of view is 10 mm. high. Sample is LL1A from the Littleton Formation, lineation-parallel section, north is to the left and the top is up.

b. Photomicrograph of staurolites showing partial crenulations as inclusion patterns. Taken in plane-polarized light, field of view is 5 mm. across. Sample is DR1 from the Littleton Formation, a lineation-parallel section, north is to the left, and the top is up.

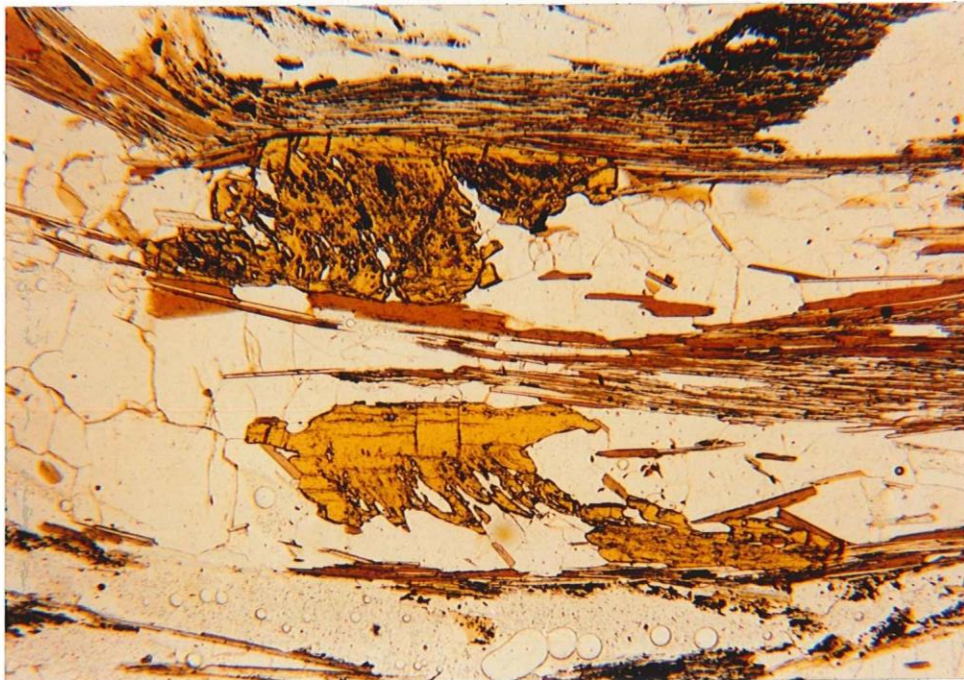
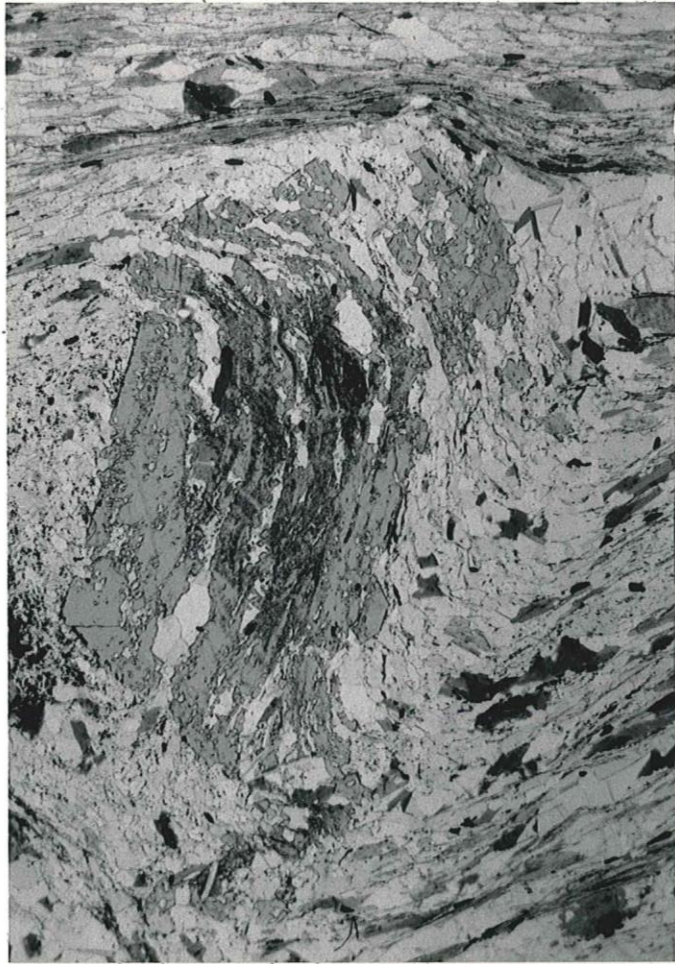


Figure 3.10. Staurolites with straight inclusion trails from the northern part of the Pelham dome.

a. Photomicrograph of a staurolite with straight inclusion fabric parallel to the external foliation and no strain shadows. Taken in plane-polarized light, field of view is 5 mm. across. Sample is L2 from the Littleton Formation, a lineation-parallel section, north is to the left and the top is up.

b. Photomicrograph of a staurolite with asymmetric strain shadows and a straight inclusion fabric sub-parallel to the external foliation. Taken with plane-polarized light, field of view is 5 mm. across. Sample is DR1 from the Littleton Formation, a lineation-parallel section, north is to the left and the top is up.

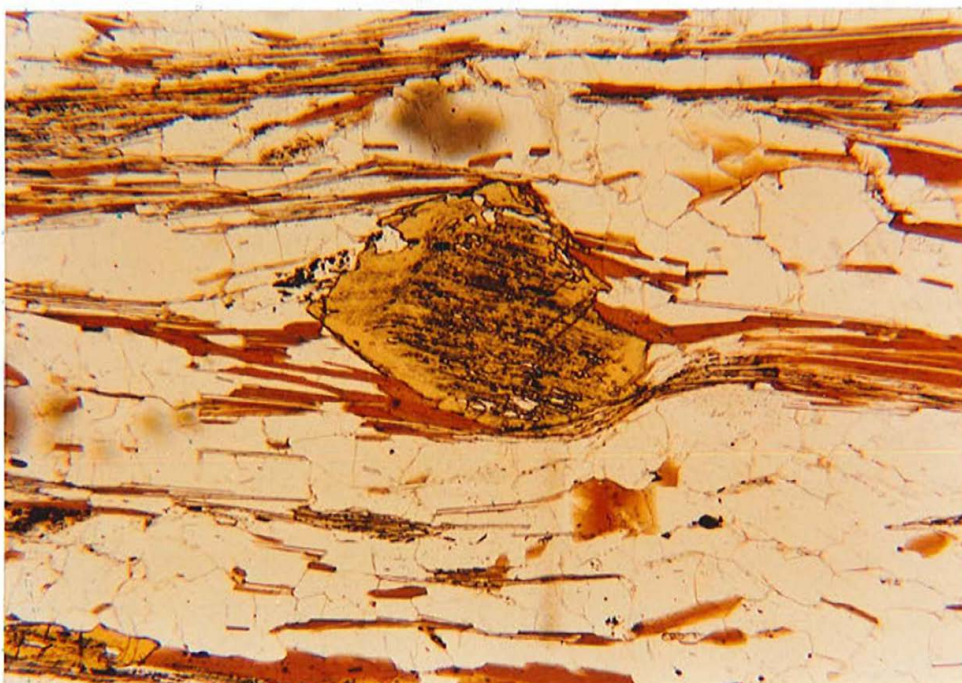
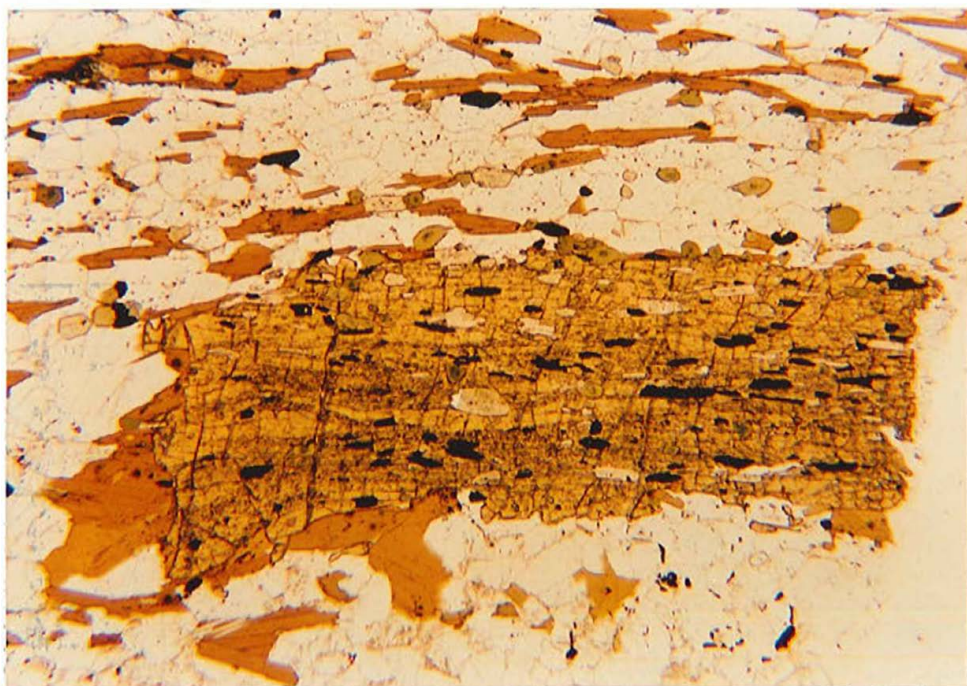




Figure 3.10 continued. Staurolites with straight inclusion trails from the northern part of the Pelham dome.

c. Staurolite with asymmetric strain shadows and a straight inclusion pattern oblique to the external foliation. Taken with plane-polarized light, field of view is 3.3 mm. across. Sample is LL2A, a lineation-parallel section, north is to the left and top is up.

straight fabrics are oriented either at high angles to the external foliation, or at a common shallow north-dipping angle ($< 30^\circ$).

In some staurolites, the inclusion fabrics run from one edge of the crystal to the other (Figure 3.9a); in others, the inclusion fabrics are truncated at an inclusion free rim. Other staurolites show a combination of these two behaviors (Figure 3.10b). The inclusion-free rims are commonly euhedral. Where the inclusion pattern is continuous to the edge of the crystal the crystal is commonly not euhedral.

The nature of inclusion trails in staurolite crystals is somewhat different than that of garnets. The number and density of inclusions present in staurolites is commonly higher than in garnet. Quartz inclusions are generally less rounded, and somewhat larger and more continuous in staurolites (Figure 3.9a). The most apparent difference from inclusions in garnet is that quartz is not always the dominant inclusion mineral. Fine opaques that are probably graphite define many of the trails (Figure 3.10a). Aligned micas, tourmalines, and coarse opaques are also present as inclusions. In most instances, the distribution of quartz and graphite inclusions within the porphyroblast echoes their distribution in the matrix around the porphyroblast.

An interesting fabric is preserved where a very large (> 7 cm.) staurolite crystal from the Littleton Formation has overgrown several small garnet crystals. Around these garnets, graphite inclusions define a relict foliation (Figure 3.11). This relict foliation is asymmetrical around the garnets. It appears that this staurolite has overgrown garnets with strain shadows and foliation asymmetries similar to those seen in other pelitic rocks. The asymmetry around the garnets is consistent with top-to-the-south sense of shear.

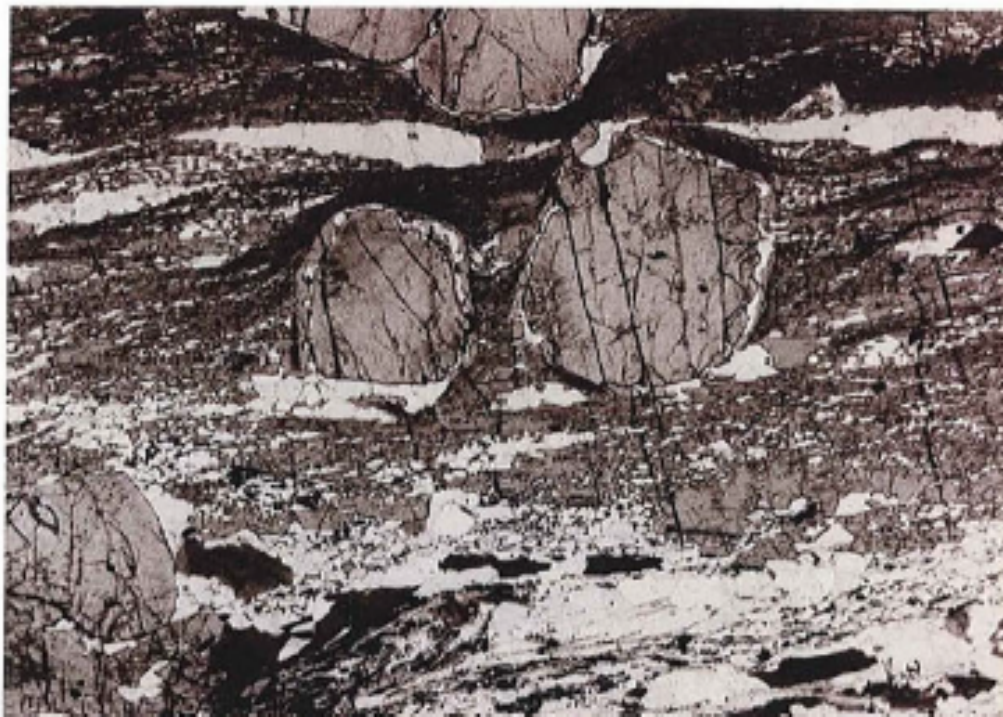


Figure 3.11. Photomicrograph of two garnets included in a large staurolite which also has fine graphite inclusion trails. Relict foliation preserved by inclusions is asymmetric around garnets, indicating top-to-the-south sense of shear. Overgrowth of staurolite over shear fabric indicates syn- to post-shearing staurolite growth. Taken with plane-polarized light, field of view is 10 mm. across. Sample is LL1B from the Littleton Formation, a lineation-parallel section, north is to the left and top is up.

The dominant matrix foliation wraps around some of the staurolites which also have strain shadows parallel to the foliation (Figures 3.9a, 3.10b, 3.10c). However, in other cases the foliation does not wrap around the staurolite (Figure 3.10a). In some samples, both of these relationships of staurolite to the foliation occur.

Fabric/Porphyroblast Relations of Kyanites

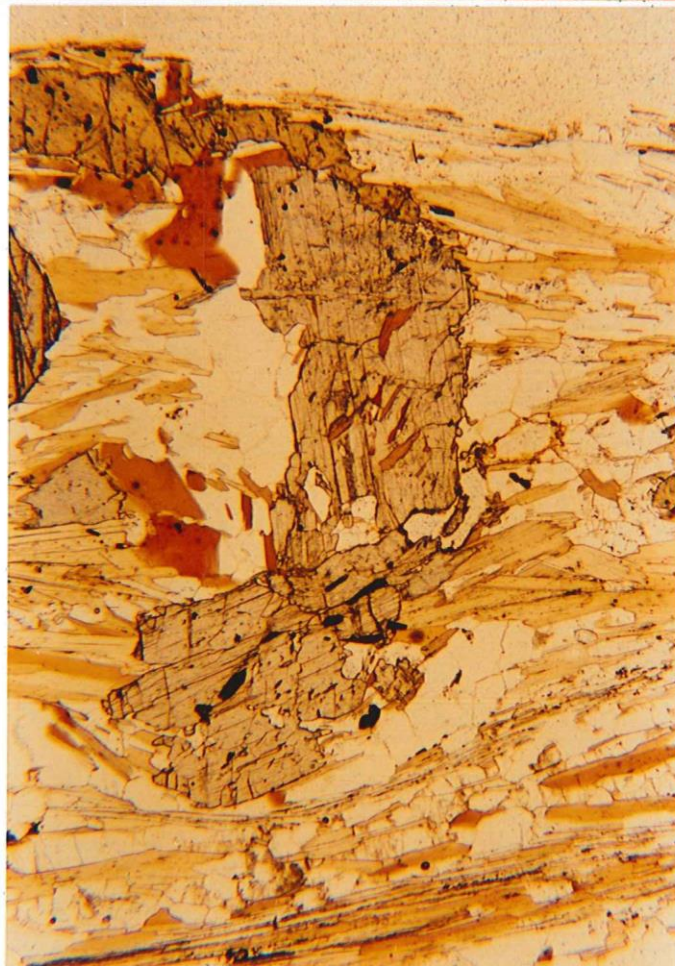
Inclusion fabrics are neither so common nor so well developed in kyanites as they are in the garnet or staurolite porphyroblasts. Where present, inclusions are mostly elongate biotites (Figure 3.12), with lesser numbers of quartz inclusions. Biotite inclusions define internal foliations, which are invariably straight. Some kyanites have biotite inclusions parallel to the regional foliation in the rocks (Figure 3.12a), whereas others have biotite inclusions that are not parallel to the external foliation, and are dipping steeply to the south (Figure 3.12b). These inclined fabrics are rare, and kyanites containing them are typically elongate at some angle to the regional fabric (Figure 3.12b). Many of the other kyanites are aligned with their long-axis and cleavage parallel to the dominant foliation. Most kyanites do not have strain shadows, and the foliation does not commonly wrap around them. Some kyanites do have strain shadows, among others, those kyanites which have inclined internal foliations typically do have strain shadows.

One kyanite shows two different directions of inclusion patterns (Figure 3.12c). One internal fabric is parallel to the external foliation, and the other is at a high angle to the external foliation. Neither one of the fabrics is particularly well-developed.

Figure 3.12. Kyanites with straight inclusion fabrics from the northern part of the Pelham dome.

a. Photomicrograph of a kyanite with inclusions parallel to the external foliation and no strain shadows. Taken with plane-polarized light, field of view is 3.3 mm. across. Sample is DR2C from the Erving Formation, a lineation parallel section, north is to the left and the top is up.

b. Photomicrograph of a kyanite elongate at angles to the external foliation showing some elongate inclusions oblique to the external foliation. Taken in plane-polarized light, field of view is 5 mm high. Sample is DR2E from the Erving Formation, lineation-parallel section, north is to the left and the top is up.



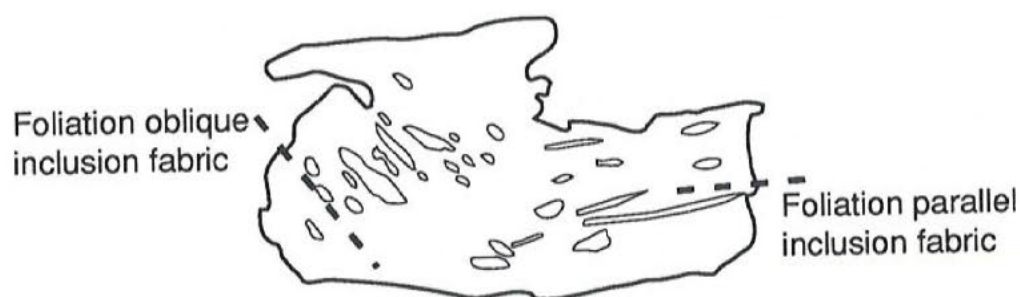


Figure 3.12 continued. Kyanites with straight inclusion fabrics from the northern part of the Pelham dome.

c. Photomicrograph and sketch of a kyanite with two separate inclusion fabrics, one parallel to the external foliation, and one at a high angle to it. Note that the fabrics do not appear to be continuous. Photomicrograph taken in plane-polarized light, photograph is 3.3 mm. across. Sample is DR2E from the Erving Formation, lineation-parallel section, north is to the left and the top is up.

The high angle fabric is in an orientation similar to straight inclusion patterns seen in some other kyanites and some staurolites and garnets, and the traces of the axial planes of the crenulated inclusions seen in other garnets. It does not appear that the two orientations are part of one curving fabric (Figure 3.12c). The relationship of this kyanite to the foliation is complex. The foliation appears to wrap around the end that has the high-angle internal fabric but is truncated where the internal fabric is parallel to the external foliation. This behavior combined with the two separate internal fabrics suggests two-stage growth.

Fabric/Porphyroblast Relations of Biotites

Large porphyroblastic biotites from one sample show a curved inclusion fabric defined by graphite inclusions (Figure 3.13). As in staurolites, the density and spacing of graphite inclusions looks very much like that seen in the surrounding matrix. The curved inclusions define a gentle sigmoidal shape which runs from one edge of the biotite to the other. The fabric is truncated on its sides along sharp boundaries. This fabric is seen in lineation-perpendicular sections, and the axial planes of these curved inclusions are generally parallel to the dominant foliation. It is interesting that the cleavage planes of the biotite are also parallel to the axial plane of the curved inclusion.

Porphyroblastic biotites with straight graphite inclusion fabrics are present in both lineation-parallel and lineation-perpendicular sections from the same sample (LL1A). These straight graphite fabrics are oriented at a high angle to the external



Figure 3.13. Photomicrograph of a biotite with crenulated graphite-inclusion pattern. The trace of the axial plane is parallel to the external foliation. Taken with plane-polarized light, field of view is 1.7 mm. across. Sample is LL1B from the Littleton Formation, lineation-perpendicular section, west is to the left and the top is up.

foliation. Thin sections in both orientations also show a few biotites with straight fabrics parallel to the dominant foliation. The composition and behavior of the inclusions is very similar to that of the crenulated inclusions.

The straight inclusion fabrics in biotite are very similar to the crenulated fabrics in composition. However, there are two orientations of straight inclusion fabrics present. It is possible, but not very likely, that one orientation represents rotated fabrics and the other orientation represents unrotated fabrics. It seems more likely that porphyroblastic biotites have overgrown two fabrics. One of these fabrics is an earlier fabric at a high angle to the foliation, possibly correlatable with the high-angle inclusion fabrics seen in other minerals. The other fabric is parallel to the external shear-related foliation and would seem to be related to it.

Fabric/Porphyroblast Relations of Plagioclases

Inclusions in plagioclase from the northern part of the Pelham dome are difficult to interpret. Mineral inclusions are rare in plagioclase from the pelitic schists of the northern part of the Pelham dome because the plagioclases present are generally not porphyroblastic. In several cases where inclusions do occur in plagioclase, the inclusions occur only in plagioclase crystals that are themselves included in staurolites. In one sample, aligned plagioclase crystals, both parallel to and oblique to the external foliation, occur as inclusions inside different staurolites. Plagioclase crystals in both orientations contain smaller muscovite inclusions with the same orientation as the surrounding plagioclase crystals. A possibly related problem with interpreting

inclusions in plagioclase is that in some samples two sets of straight muscovite inclusions seem to be superimposed on one another. Typically the two fabrics intersect at a high angle and one of the inclusion sets is commonly parallel to some other fabric present in the rock.

It is not uncommon to see inclusions in crystals that are themselves inclusions. It is less common for these two to have the same orientation. One possible explanation of this is syntectonic growth of aligned plagioclase over aligned inclusions that were then overgrown by staurolite. However, to see this in two different orientations would require that plagioclase crystals grew syntectonically during two separate deformational phases. There does not seem to be a simple overgrowth history possible for the plagioclase with two superimposed directions of inclusion fabrics. The most plausible explanation for both of these instances is that the inclusions in the plagioclase result from crystallographic control of inclusion orientation by the plagioclase. In the case of the plagioclase with two overlapping fabrics, the second fabric is probably an actual overgrowth fabric as these second fabrics are parallel to an external fabric.

Fabric/Porphyroblast Relations of Amphiboles

Porphyroblastic amphiboles are not common outside of the core gneisses, and few porphyroblasts in the core rocks contain inclusion fabrics. However, in one amphibolite from the Erving Formation (GSR1, Plate 1), hornblende crystals have plagioclase inclusions. These inclusions are common and typically occur parallel to

the cleavage planes in the hornblende. The inclusions are stubby to elongate in shape with straight sides.

The lack of a common orientation of plagioclase inclusions in hornblendes argues against them being the result of the overgrowth of a deformational fabric. The typical occurrence of plagioclases along cleavage planes in the hornblendes argues for crystallographic control of the inclusions in the hornblendes.

Some porphyroblastic hornblendes in this sample (GSR1, Plate 1) also seem to have inclusions of smaller hornblendes. It is unclear whether the included hornblendes occur along any particular crystallographic planes in the host hornblendes. However, the inclusions commonly have euhedral diamond shapes, which suggests they are oriented with their long-axis roughly perpendicular to the section.

Inclusions of crystals of a mineral in other crystals of that mineral are an uncommon phenomenon. This phenomenon may be related to two-stage growth of hornblende. A model for this instance would have hornblendes originally growing in different orientations. At a later time, conditions favored growth of hornblendes in a particular orientation. The preferentially-oriented hornblendes then overgrew those hornblendes in non-favorable orientations. Which crystals were preferred for second-stage growth was perhaps controlled by the orientation of stress.

Summary of Inclusion Fabrics

Inclusion geometries in porphyroblasts from the northern part of the Pelham dome can be broken into four basic geometries; straight (Figures 3.14a, 3.14b),

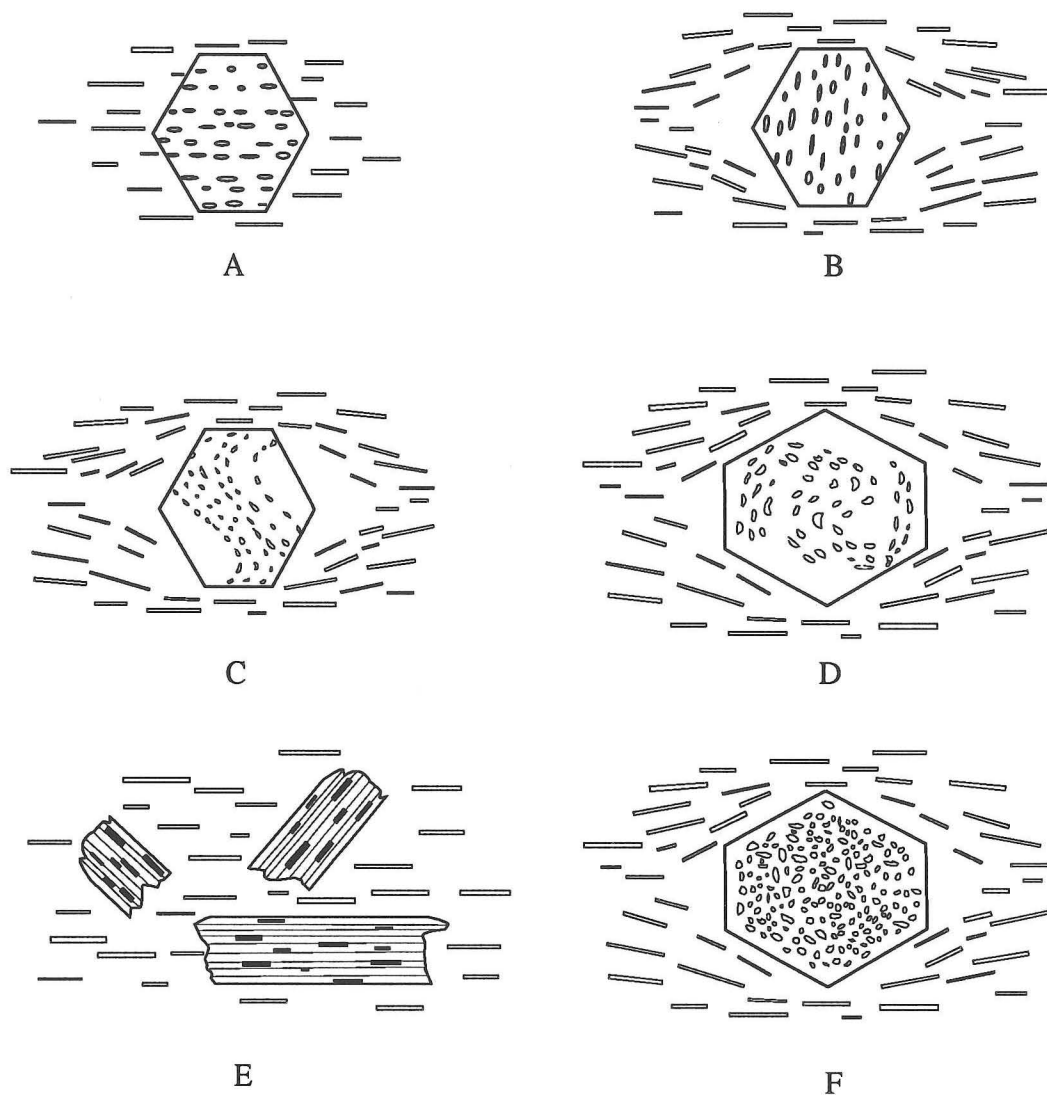


Figure 3.14. Common porphyroblast inclusion geometries seen in the northern part of the Pelham dome. A. Linear fabric parallel to the external fabric. B. Linear fabric non-parallel to the external fabric. C. Curved inclusion fabric with the trace of the axial plane parallel to the external fabric. D. Helicoidal inclusion pattern. E. Crystallographically-controlled inclusion pattern. F. One type of random pattern seen in porphyroblasts.

curved or crenulated (Figure 3.14c, 3.14d), crystallographically controlled (3.14e), and those with no apparent pattern (Figure 3.14f). Straight trails have been interpreted as the trace of planar fabrics overgrown and preserved in their original orientation. Curved trails are interpreted as resulting from porphyroblasts overgrowing microfolds. No evidence for rotation during growth has been recognized. The orientation of crystallographically controlled inclusions is established by some crystallographic feature in the host mineral, not by any pre-existing tectonic fabric. Randomly oriented fabrics have not been previously discussed although they are not uncommon in the northern part of the Pelham dome. These random fabrics do not have a coherent pattern, at least not when viewed from the particular orientation of the thin section.

Crystallographically controlled and random fabrics do not provide much opportunity for interpretation of timing relationships, but the straight and curved fabrics do. These deformation-related inclusion fabrics can be divided into four distinct groups which are preserved in the porphyroblasts. The first group includes fabrics which are associated with the current shear-related foliation (Figures 3.7a, 3.10, 3.11, 3.12a), and parallel to both the S and C directions of S-C mylonites (Lister and Snoke, 1984). These fabrics occur in some garnet, staurolite, kyanite, biotite, and possibly plagioclase crystals.

The second group includes straight fabrics at a high angle or perpendicular to the shear foliation (Figures 3.7b, 3.10c, 3.12b). These inclusion fabrics vary somewhat in orientation but are all at angles greater than 45° to the foliation. These fabrics are more common in lineation-perpendicular sections than in lineation-parallel

sections. A possible explanation of the presence of these fabrics in thin sections of both orientations is that the fabric strikes obliquely to the lineation direction. External fabrics of this orientation are not present in the rock. There are two possible interpretations for this fabric; local reorientations of the shear fabric or a planar fabric related to an earlier deformational phase. If these fabrics were related to the shear fabric, which is the final ductile strain imposed on the rock, they would probably be seen outside of porphyroblasts as well. Since these fabrics are seen only inside porphyroblasts the interpretation that they are related to an earlier deformation fabric is preferred. The high angle of intersection of these fabrics to the shear fabric and their probable relation to fabrics discussed below also support this interpretation. These fabrics occur in some biotites, staurolites, garnets, and probably in some kyanites and plagioclases.

Third are crenulated fabrics, interpreted to be transitional between the earlier foliation and the shear-related foliation (Figure 3.3). They are recognized by the trace of the axial plane being parallel to the shear-related foliation. These fabrics occur in garnets, staurolites, and biotites (Figures 3.9a, 3.9b, 3.13).

The fourth group of tectonic fabrics are crenulated fabrics with the trace of the axial plane at a very high angle to the shear foliation. This fabric is only clearly preserved in the cores of garnets (Figures 3.5, 3.6). The orientation of these crenulations is not consistent with an origin during a stage of shearing but is consistent with this fabric being transitional between the early steeply-dipping fabric described above and a previous, otherwise non-preserved, fabric (Figure 3.3).

Relative Timing of Mineral Growth

The geometry of inclusion fabrics and the relationships between the porphyroblasts and the dominant foliation can be combined to infer the relative times at which various minerals grew (Figure 3.15). Some garnets are interpreted to have grown during an earlier deformation, preserving crenulated fabrics from this deformation in their cores (Figure 3.5, 3.6). Garnets in other samples are interpreted to have overgrown the end-product foliation from this deformation (Figure 3.7b). Still other garnets have both inclusion patterns parallel to the external foliation and well developed strain shadows which indicates growth during the development of the shear-related fabric (Figure 3.7a). Several garnets cut the dominant foliation and have no strain shadows; these apparently grew after shearing ended in that particular area (Figure 3.8). The relative homogeneity of shearing in these rocks makes it likely that these garnets grew after the cessation of all shearing. The majority of garnet growth seems to have been pre- to syn-shearing (Figure 3.15). There also appears to have been additional growth on some pre-existing garnets after the end of shearing. In one example (Figure 3.16), a garnet shows an inclusion-rich core that is asymmetrically overgrown by an inclusion-free garnet rim. Close examination shows that some micas warped around the garnet truncate against this overgrowth. Micas are not truncated against the area without the overgrowth. The inclusion-free partial rim is interpreted to be a post-shearing overgrowth of the strain shadow that occurs primarily on one side of the garnet. This sort of post-deformational overgrowth seems to have occurred on many garnets, complicating interpretations of fabric relations. Microprobe analysis

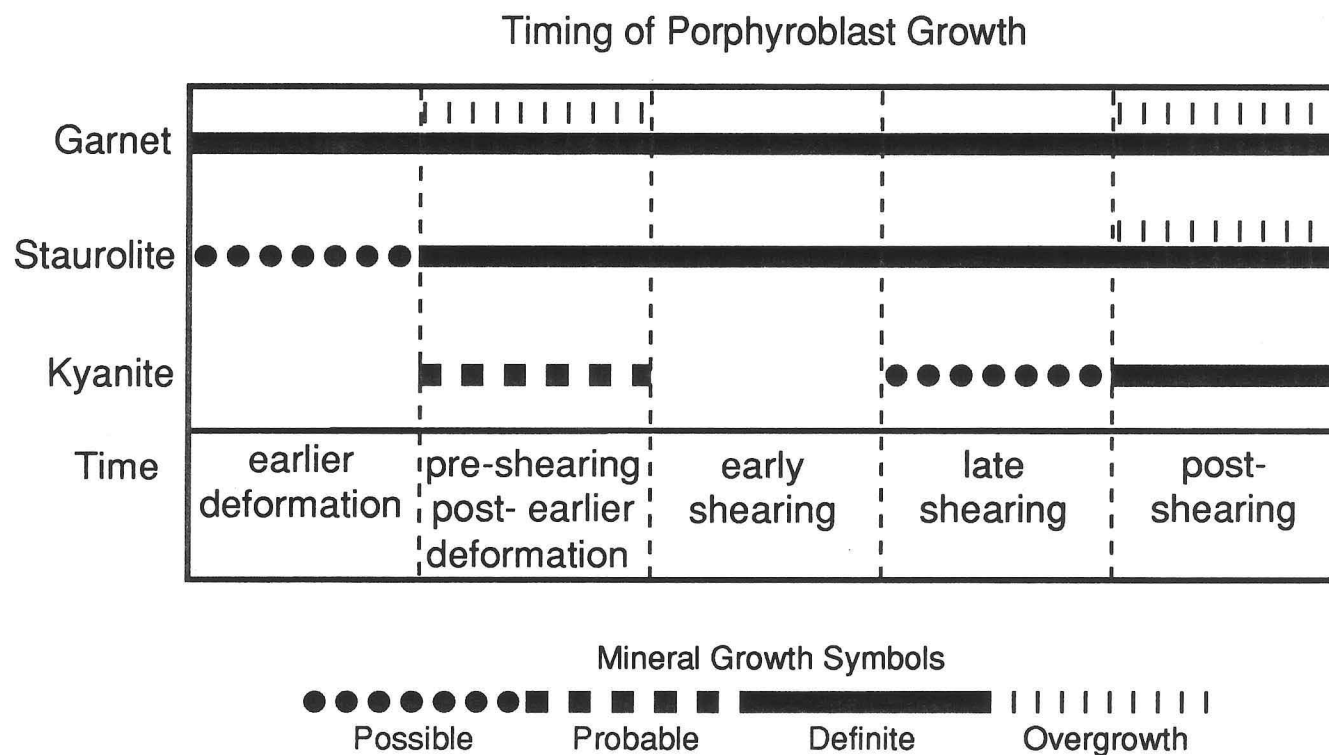


Figure 3.15. Timing of growth for major porphyroblastic minerals from pelitic rocks in the Pelham dome area. The earlier deformation referred to is the deformation that produced the high-angle inclusion fabrics in some porphyroblasts. Results indicate growth of a particular mineral in at least one sample, not necessarily in every sample. "Overgrowth" indicates that pre-existing porphyroblasts were enlarged during a particular time period.

a.



b.

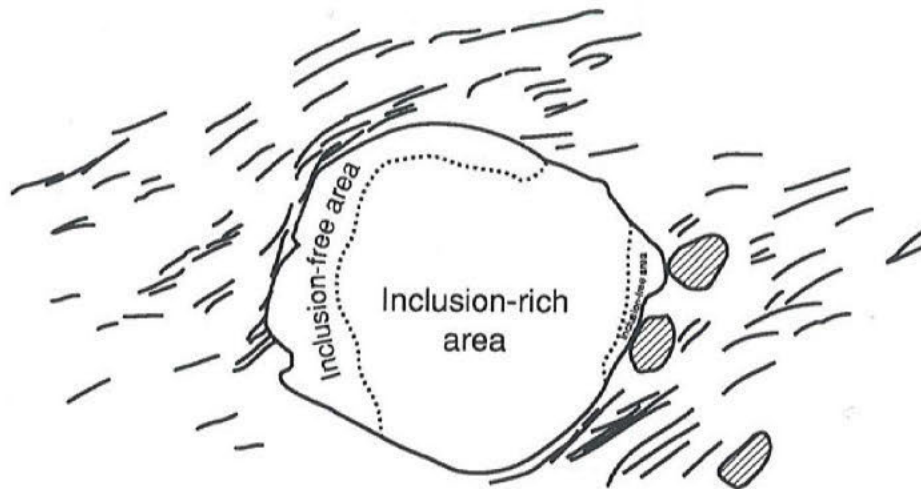


Figure 3.16. Post-shearing garnet overgrowth in the northern part of the Pelham dome. a. Photomicrograph of a garnet showing inclusion-rich core and inclusion-free partial rim indicating two possible stages of garnet growth. Note smaller garnets that clearly overgrow the foliation. Taken in cross-polarized light, field of view is 13 mm. across. Sample is MR2B, a lineation-parallel section, north is to the left and the top is up. b. Line drawing of the photomicrograph showing pertinent features. Line pattern marks small post-foliation garnets.

have not been done on the garnets in this study, but it would be interesting to compare the chemical zonation with the textures seen.

Staurolites also seem to have overgrown a variety of fabrics at a variety of times during deformation. Some staurolite crystals overgrew vertically-oriented straight fabrics that are interpreted to represent an earlier foliation (Figure 3.10c). Other staurolites overgrow crenulated fabrics which have the trace of the axial plane parallel to the dominant foliation (Figure 3.9a). Many of these staurolites also have strain shadows and thus are interpreted to have grown early during the shearing (Figure 3.15). The staurolite that overgrows shear fabrics around a garnet (Figure 3.11) clearly indicates syn- to post-shearing growth of staurolite. However, this staurolite and the numerous staurolites that overgrew straight fabrics parallel to the dominant foliation present a problem. The foliation appears to wrap around some of them suggesting syn-shearing growth (Figure 3.10b). Other staurolite porphyroblasts seem to cut straight across foliation (Figure 3.10a). This is interpreted to indicate both late syn-deformational and post-deformational staurolite growth (Figure 3.15). As with garnets there are a few staurolites that seem to have seen both pre- or syn-deformational growth followed by post-deformational overgrowth (Figure 3.15). In these cases, if growth was continuous or discontinuous is unclear.

Kyanite fabrics have proven difficult to interpret. Some kyanites without inclusions are thin and acicular and may have behaved as matrix rather than porphyroblasts during deformation. Kyanites from one sample seem to be concordant with foliation but show undulatory extinction indicating that they have been deformed. Robinson (personal communication, 1992) has seen folded kyanite crystals in the

Pelham dome area. Some kyanite crystals seen in this study show a weak straight internal fabric at an angle to the exterior fabric (Figure 3.12b), but in most of these cases it is impossible to tell whether the dominant foliation wraps around these kyanites. Few kyanites show clear strain shadows. Some kyanites show complex relationships with the foliation that suggest either two-stage growth (Figure 3.12c) or the post-deformational replacement of other minerals. It has been difficult to determine whether the kyanites that do have strain shadows grew pre- or syn-shearing or possibly both. Nevertheless, it is clear that at least some kyanite grew before the end of deformation, and that the majority of kyanites overgrew the foliation after the cessation of shearing (Figure 3.15).

Non-synchronous porphyroblast growth in different samples is not surprising. In the thinly-layered schistose units of the Erving Formation, the bulk composition of the layers varies widely even on the scale of a thin section. Similar variations occur in the Littleton Formation, although on a larger scale. In particular the amount of graphite present in pelitic rocks varies widely. These chemical variations are enough so that all the pelitic units do not necessarily have the same mineral assemblages (Figure 3.1), and more importantly that porphyroblastic minerals apparently grew during different deformational phases in different rocks. This variation in chemistry has contributed to the observed wide diversity in inclusion fabrics.

Relationship of Inclusion Fabrics to Deformational Events

It should be possible to correlate the four different tectonic inclusion fabrics (Figure 3.14) with the established regional deformational sequence (Figure 1.5).

Three possible regional deformational phases can be correlated with fabrics; nappe stage, backfold stage, and dome stage (the shearing event).

Straight inclusion fabrics that are parallel to the external foliation and are in many cases continuous with it, imply a relationship between the internal and external foliation. Because the dominant foliation in the rocks is interpreted to be related to a shearing event (Chapter 2), the internal fabric is also interpreted to be related to the shearing event.

Some crenulated inclusion fabrics have their axial plane traces parallel to the external shear fabric. It was discussed earlier how crenulated fabrics are formed as one foliation is progressively recrystallized to form another foliation (Figure 3.3). If such fabrics formed during the development of the shear-related foliation the crenulations would have the same orientation as the crenulated fabrics being discussed. On the basis of this similarity in orientation, these crenulated fabrics are interpreted to be related to earlier stages of the development of the shear-related fabric.

It is more difficult to assign a deformational event to the oblique inclusion fabrics. As previously stated, there is some variation in the inclination of these fabrics. In lineation-parallel sections, inclined fabrics are typically subvertical but they can dip either to the north or the south. A similar variation is seen in the orientation of the trace of the axial plane of crenulations in the cores of early garnets, but in this

case most of the traces dip to the south. In lineation-perpendicular sections, inclined fabrics are typically subvertical but can dip either to the east or west.

This diversity of orientation is a slight problem. No single exclusively planar foliation could account for all these orientations. Either more than one deformational event is preserved in these fabrics or the fabric is non-homogeneous. The fabric is interpreted as being non-homogeneous. Slight variations in foliation attitude and/or small folds in a generally vertical fabric with a strike at an angle to north-south could have produced the differences in fabric orientation. Another way to produce slight variations in foliation attitude would be by reorientation of early fabrics. In some situations instead of being recrystallized, parts of early fabrics are reoriented into near parallelism with the new fabric being formed. In this case, such reorientation along with the new subvertical foliation could account for the variation in fabric.

It is difficult to constrain the timing of the deformation that is being correlated with the pre-shearing high angle fabrics. Several lines of evidence may be significant. The upright orientation of the internal foliation would fit well with the backfold stage of deformation (Figure 1.5). The angles which these fabrics make with the shear-related foliation are far too steep for them to be relict S-surfaces related to early stages of shearing. The strike of this fabric is oblique to the dominant foliation which also suggests that it is unrelated to shearing. Secondly, this fabric seems to have immediately preceded the shearing, which also supports correlation of it to the backfold stage of Acadian deformation. However, it also is possible that the fabric is related to some early dome stage event that is not clearly evident elsewhere.

Peak of Metamorphism

Previous workers in central Massachusetts have attempted to constrain the relative timing of the peak of the dominant regional metamorphism (Schumacher and others, 1989; Berry, 1989). The peak was generally defined on the basis of the highest temperature mineral assemblage in pelitic rocks and tied to some phase of regional deformation. This peak point was generally taken to be the maximum temperature point on the P-T path, and is probably close to the 580°C and 5.5 kilobars pressure and temperature calculated for the assemblage (Tracy and others, 1976).

Defining a "peak" of regional metamorphism is difficult in the northern part of the Pelham dome. The "peak" metamorphic assemblage in pelitic rocks seems to consist of garnet-staurolite-kyanite-biotite. The one earlier deformation recognizable from inclusion fabrics took place at conditions at least conducive to the growth of garnet and probably the growth of staurolite. Staurolite was stable before the initiation of the main shearing event, and there is some evidence that kyanite also may have been stable at this point. Kyanite, staurolite and garnet all grew both during and after shearing but most kyanite appears to have grown post-deformationally and has been locally retrograded to muscovite.

From these relationships similar conditions seem to have existed from at least the end of the earlier deformation represented by inclusion fabrics to after the cessation of shearing. If the peak is defined on the highest grade index mineral, the growth of the majority of the kyanite after shearing seems to indicate that the peak occurred post-deformationally. This differs from earlier work (Schumacher and

others, 1989) northeast of the Pelham dome which shows peak metamorphism occurring prior to the backfold stage. This suggests a fundamental difference in the histories of the Pelham dome and the area studied by Schumacher and others (1989).

In any case, the last two phases of deformation seem to have taken place at or near the regional grade of metamorphism. This relationship is not unique to the northern part of the Pelham dome. Work further east in the Bronson Hill anticlinorium has documented similar relationships (Peterson, 1992; Peterson and Robinson, 1993) in sillimanite grade rocks, where two orthogonal lineations are present.

Timing of Other Metamorphic Events

Relict Sillimanite-Potassium Feldspar Metamorphism

Work in the southern part of the Pelham dome, in areas with the relict high-grade metamorphism, indicates that the high-grade metamorphism preceded the development of the now dominant shear-related fabrics (Roll, 1987). However, for the northern part of the Pelham dome, it is not clear whether the bulk of the rock was still comprised of these high-grade metamorphic assemblages when shearing began or whether the rocks were retrograded in an earlier deformation.

There is one sample of rock from this study (JHR3*A) which provides somewhat ambiguous clues about how the metamorphic events related to the dominant shearing deformation. In a calc-silicate pod from the Poplar Mountain Quartzite there is a large garnet that shows both asymmetric strain shadows and a partial reaction rim

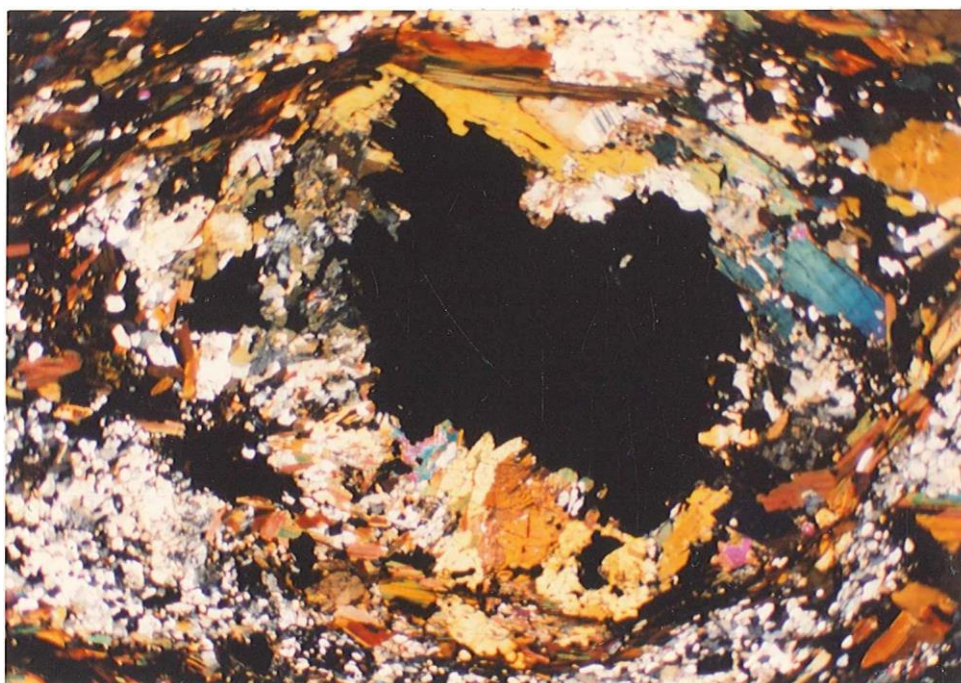


Figure 3.17. Photomicrograph of a garnet from a calc-silicate pod from the Poplar Mountain Quartzite. Garnet appears to have undergone retrograde reaction to epidote and hornblende. Note that foliation wraps around both garnet and retrograde products. Taken with in cross-polarized light, field of view is 13 mm. wide. Sample is JH3*A, a lineation parallel section, north is to the left and top is up.

of epidote (Figure 3.17). Compositional analyses have not been made, but considering the composition of the pod and the pale color of the garnet, the garnet probably has a significant grossular component. The reaction involved is probably; garnet + anorthite + water reacting to form epidote + quartz. In general, reactions that involve conversion of non-hydrous phases to hydrous phases are retrograde in nature. Reaction rims also seem to be more common for retrograde reactions.

Interpreting the timing relations of this retrograde reaction has been extremely difficult. The minerals formed by hydration are large well formed crystals, not the fine-grained intergrown crystals that form in many retrograde reactions. No chlorite was formed in this retrograde reaction. The epidote formed is clinozoisite which tends to form at higher temperature than pistacite (Laird and Albee, 1981). These observations suggest the retrograde reaction was not at very low temperatures.

Determining the relationship of the foliation to the garnet and the epidote is difficult. The foliation wraps around the epidote and the garnet, but it is not entirely clear that the epidote reaction rim was present when the foliation formed. This is complicated by the fact that the biotite that defines the foliation around the garnet has undergone a degree of recrystallization.

Based on the appearance of the minerals, the most likely interpretation of this reaction is as follows. The garnet is part of the high grade metamorphic assemblage. The reaction rim is a lower amphibolite-grade retrograde reaction. Fabric relations are not entirely clear, but the reaction probably occurred prior to shearing.

Retrograde Metamorphism

Evidence for the timing of retrograde metamorphism is much more pervasive than evidence for the early high-grade metamorphism. There are two styles of retrograde metamorphism. One style is the non-oriented growth of large, subhedral to euhedral grains of muscovite or chlorite. Many samples contain isolated randomly-oriented grains of chlorite. In other samples, chlorite replaces staurolite along its margins. In some samples, foliated biotites have been converted to chlorite. In one sample (DR2A, Plate 1), the replacement pattern is clearly related to localized fluid access. The foliated texture of this rock is overprinted by branching areas in which biotite has been converted to chlorite. These branching areas are interpreted to mark fluid pathways within the rock.

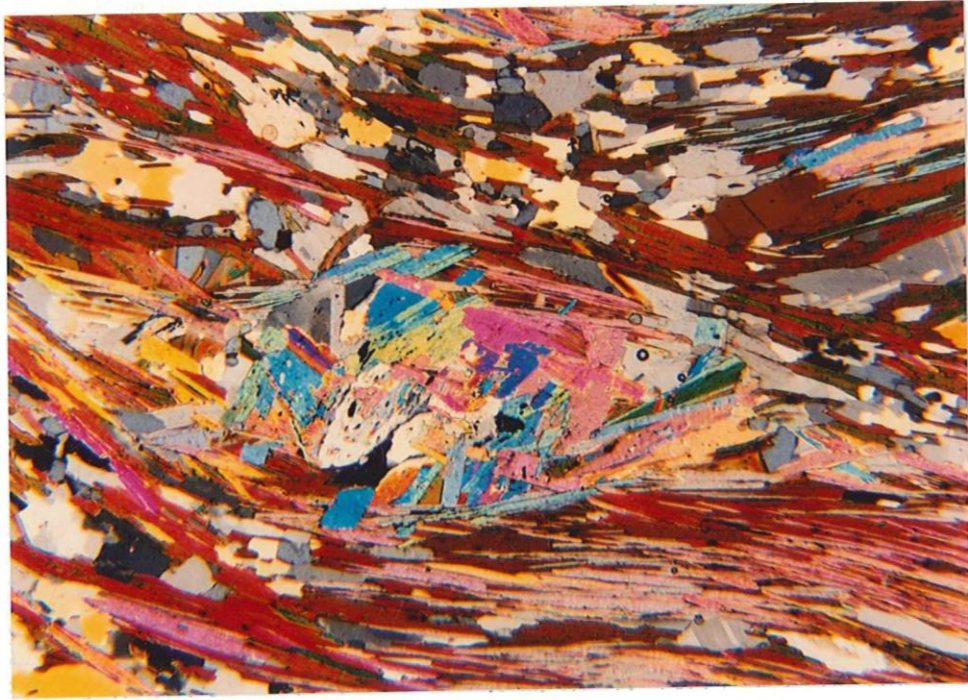
An interesting feature of the isolated retrograde chlorites is that some are kinked, even though other minerals in the thin section appear unaffected by the kinking. The kinking of the chlorites without an accompanying foliation, could best be explained by a slight, syn- to probably post-retrograde, deformation.

Large oval areas of unoriented muscovite crystals are present in a sample of the Littleton Formation from the eastern margin of the Pelham dome. While these muscovites are themselves undeformed and not aligned, the matrix foliation clearly wraps around them (Figure 3.18a). Close examination of the muscovites shows trails of graphite inclusions that cut across individual grains (Figure 3.18b). These trails are similar to inclusion fabrics seen in staurolites in other pelitic rocks from nearby. Some of these muscovite patches contain small remnants of kyanite or staurolite. The

Figure 3.18. Muscovite replacing a staurolite? porphyroblast in the Littleton Formation from the northern part of the Pelham dome.

a. Photomicrograph of a pod of randomly-oriented muscovite with strain shadows. An ECC has reoriented the foliation in the vicinity of the pod, but notice the non-aligned nature of the muscovite that makes up the pod. Taken in cross-polarized light, field of view is 5 mm. across. Sample is LLR4, north is to the left and the top is up.

b. Close up of non-aligned muscovite pod showing faint, upright, straight, opaque inclusion fabric that cuts across muscovite boundaries. This inclusion fabric is very similar to that seen in staurolites in the area. Some similar muscovite pods in this sample show small amounts of relict staurolite in the pods. This situation is being interpreted as replacement of the staurolite by muscovite after shearing. Taken with plane-polarized light, field of view is 3.3 mm. across. Sample is LLR4, north is to the left and the top is up.



muscovites appear to have replaced porphyroblasts of these minerals and the inclusion geometries have been preserved.

These muscovite pods were probably produced by retrograde metamorphism controlled by local access of metamorphic fluid. It is fairly widespread throughout the rocks and varies widely in intensity. This retrogression is possibly related to the retrograde metamorphism described near New Salem, Mass. (Figure 1.2) by Hollocher (1981).

While the exact timing of this metamorphism cannot be determined, it is possible to determine relative timing with respect to other features present in the rock. The new minerals formed overprint the shear fabric and the minerals being hydrated are part of the dominant regional metamorphic assemblage. A few of the chlorites are kinked, but for the most part the muscovites and chlorites are unoriented and undeformed, indicating growth after the cessation of large-scale deformation. It has not proven possible to determine the timing of this retrograde metamorphism relative to Mesozoic brittle faulting, so a minimum age cannot be constrained.

The second style of retrograde metamorphism involves alteration to very fine-grained white micas that seem to be associated with local brittle deformation. Two samples show evidence for localized micro-faulting with a slight ductile component expressed as the bending of micas near the fault (Figure 2.14). Retrograde metamorphism is associated with these micro-faults. This deformation is interpreted to be related to brittle faults formed by early Mesozoic extension in the area and the metamorphism to fluids moving along these micro-faults.

CHAPTER 4

FORMATION MECHANISM OF THE PELHAM DOME

Introduction

The domes of the Bronson Hill anticlinorium having long been described as "mantled gneiss domes" (Eskola, 1949; Robinson, 1963; Thompson and others, 1968; Dixon, 1974). Despite this, there are certain features of the Pelham dome which may not be compatible with the genetic implications of some current definitions of a mantled gneiss dome. In this chapter, the observed physical characteristics of the Pelham dome have been compared with the expected characteristics of various dome-formation models. The strengths and weaknesses of the various models have been evaluated in an effort to resolve a logical formation method.

Definition of a Mantled Gneiss Dome

Eskola (1949) first used the term "mantled gneiss dome" to refer to a series of oval-shaped exposures of basement gneiss surrounded by metamorphosed sedimentary and volcanic rocks in Finland. He further applied the term to basement gneiss exposures in Maryland and, based on the descriptions of others, to the domes of the Bronson Hill anticlinorium (Eskola, 1949). The original definition may have been purely descriptive, but the term is commonly given genetic implications. Eskola

interpreted mantled gneiss domes as forming by the injection of granitic magma into previously deformed gneisses. He suggested that the injection of magma lowered the viscosity of the gneiss and allowed it to rise upward into the denser mantling metamorphic rocks. The increased volume combined with the rise of the gneiss created the domal structure. The general concept of mobilization and gravitational rise has persisted, although in many current interpretations (Dixon, 1987) injection of new granitic material is not an essential component of the model. The current edition of the Glossary of Geology (Bates and Jackson, 1987) defines a mantled gneiss dome as: " ... a dome in metamorphic terrains that has a core of gneiss that was remobilized from an original basement and has risen through a cover of younger rocks, also metamorphosed. The gneiss is surrounded by a concordant sheath of the basal part of the overlying metamorphic sequence."¹¹

The Pelham dome fits most of the descriptive part of this definition but not necessarily the genetic part. The Pelham dome does consist of a gneissic core surrounded by mantling metamorphosed sedimentary and volcanic rocks (Figure 1.4). It is oval in shape, if a somewhat elongate oval (Figure 1.1). The foliation forms a gentle doubly-plunging arch which is generally parallel to layering or bedding.

However, the above definition also states that the gneiss has been "remobilized" and has "risen through a cover of younger rocks". This specifies a gravitational mechanism for the formation of mantled gneiss domes which may be inconsistent with the structural characteristics of the Pelham dome.

Relationship of Ductile Shearing and Dome Formation in the Pelham Dome

The relationship between ductile shearing and dome formation is of fundamental importance for understanding the origin of the Pelham gneiss dome. It is critical to establish if the ductile shearing is an integral part of the dome formation mechanism or if it preceded or succeeded the formation of the dome.

Previous workers (Onasch, 1973; Laird, 1974) have correlated the dominant subhorizontal mineral lineation and the dominant domal foliation with the main phase of dome formation. The foliation defines the dome, so the correlation is obvious. The mineral lineation occurs within the foliation and is generally parallel to the long-axis of the dome. This orientation suggests an association with dome formation. These same workers have assigned asymmetric folds seen in the dome to the late stages of dome formation. This was partially based on the fact that these folds commonly deform both the foliation and the mineral lineation.

Evidence from this study suggests that the dominant foliation, the mineral lineation, and the asymmetric folds were all formed during the ductile shearing. The ductile shearing event is interpreted as being of sufficient duration to allow the foliation and lineation to form early and then be folded. This correlation of the dome-defining foliation with the shearing constrains dome formation to be syn- or post-shearing.

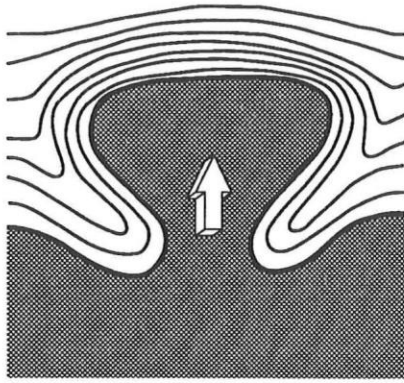
Nevertheless, it could be possible that the shear-related foliation was reactivated (Bell, 1985) by a later doming phase. However, there is no real evidence that any major deformation post-dated the shearing. If the foliation was reactivated in

a later event it seems likely that there would be some evidence of this and shear fabrics would be overprinted. The few places where the shear fabric is disturbed are very minor and can be interpreted in more than one way. It seems unlikely that doming post-dated the shearing.

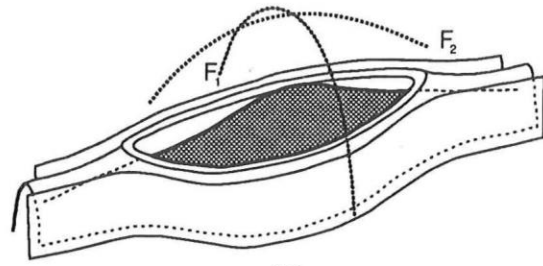
Dome Formation Mechanisms

The related processes of diapirism and buoyancy caused by density inversion (Figure 4.1a) remain the primary models used to explain the formation of mantled gneiss domes (Dixon, 1987). However; several other processes have been suggested for the formation of gneiss domes in some regions. Some gneiss domes have been interpreted (Naylor, 1969; Brun, 1983; Bleeker and Westra, 1987) to represent interference between two generations of folds (Ramsay, 1967) with roughly perpendicular and nearly vertical axial planes (Figure 4.1b). Coward (1981) and Brun (1983) proposed that gneiss domes may be surface exposures of elongate sheath folds that have formed in very large shear zones (Figure 4.1d). Schreurs and Westra (1986) suggested that some domes in Finland may be mega-boudins formed during extension (Figure 4.1e). Lastly, some basement domes in the southern Appalachians are thought to have formed above duplexes (Figure 4.1c) associated with basement thrusts (Hatcher, 1983; Hatcher and others, 1986).

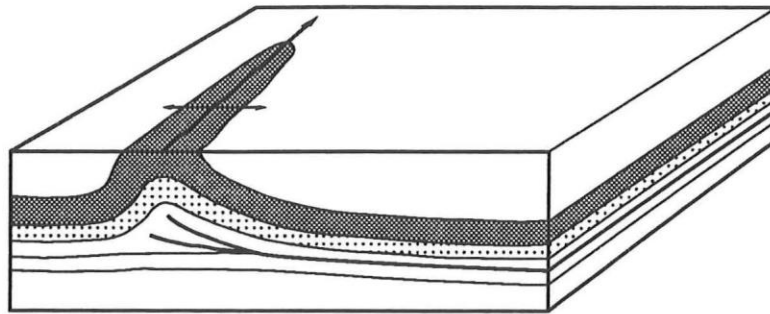
Figure 4.1. Some possible mechanisms of dome formation. In all cases heavy stippled pattern indicates gneiss. a) Solid-state buoyancy-driven formation of a gneiss dome, arrow indicates direction of gneiss movement. (redrawn from Brun, 1983) b) Refolded fold mechanism for dome formation. c) One possible way of forming a dome in association with a buried thrust fault. d) Formation of a gneiss dome by the development of a large sheath fold; arrows indicate direction of shearing. (redrawn from Brun, 1983) e) Formation of oval "dome" structures by extensional boudinage of a gneissic body.



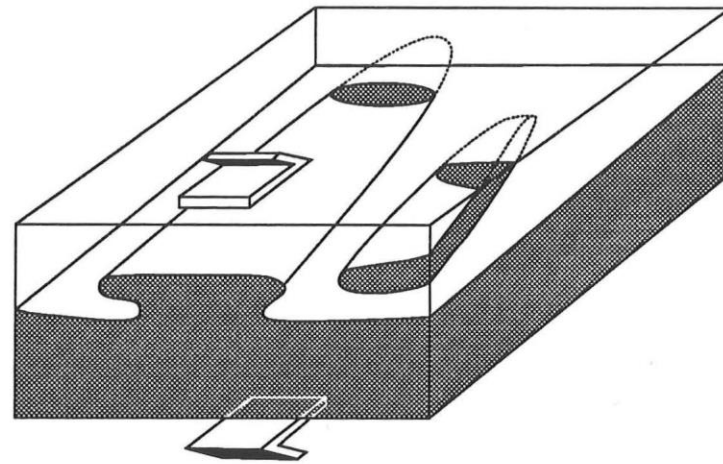
A



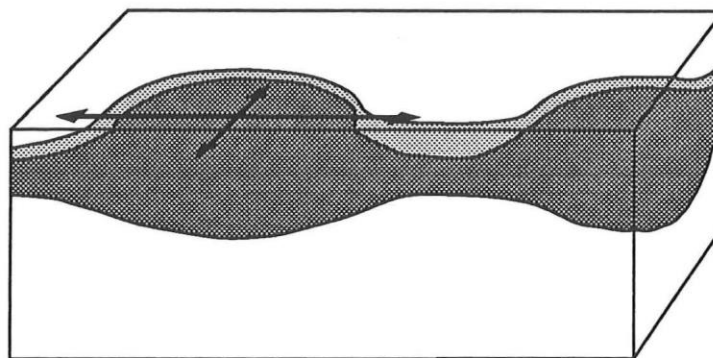
B



C



D



E

Solid-State Gravitational Models

The popularity of solid-state buoyancy-driven models for gneiss dome formation has contributed to the large amount of research on the physical characteristics of the process. Solid-state rise of the gneissic core is driven by gravitational instability between it and the overlying metamorphosed sedimentary and volcanic rocks (Ramberg, 1968). The core gneiss is generally 0.1 to 0.5 g/cm^3 less dense than the average density of the cover rocks (Dixon, 1987). Such density inversions are interpreted to cause the gravitational instabilities which lead to the less dense gneissic rock rising into the more dense mantling rocks.

A gneiss dome formed solely by buoyancy processes with no other active deformation is characterized by a radial lineation pattern (Dixon, 1987). The principle stretching direction is predicted to be vertical in the stem and subhorizontal across the expanding top of the dome (Figure 4.2). If a regional strain field was superimposed on the rising gneiss, the lineation pattern may be modified to some extent. However, in the Mustio gneiss dome of Finland, the formation mechanism is thought to be a combination of refolding and diapiric processes (Bleeker and Westra, 1987) and this gneiss dome has a radial lineation pattern. For the radial lineation pattern to be completely obscured the magnitude of the regional strain field would have to greatly exceed the gravitational forces. If a dome was produced in such a situation the formation mechanism would be more directly related to the regional stress field. The mineral lineation present in the Pelham dome is not even slightly radial, it consistently

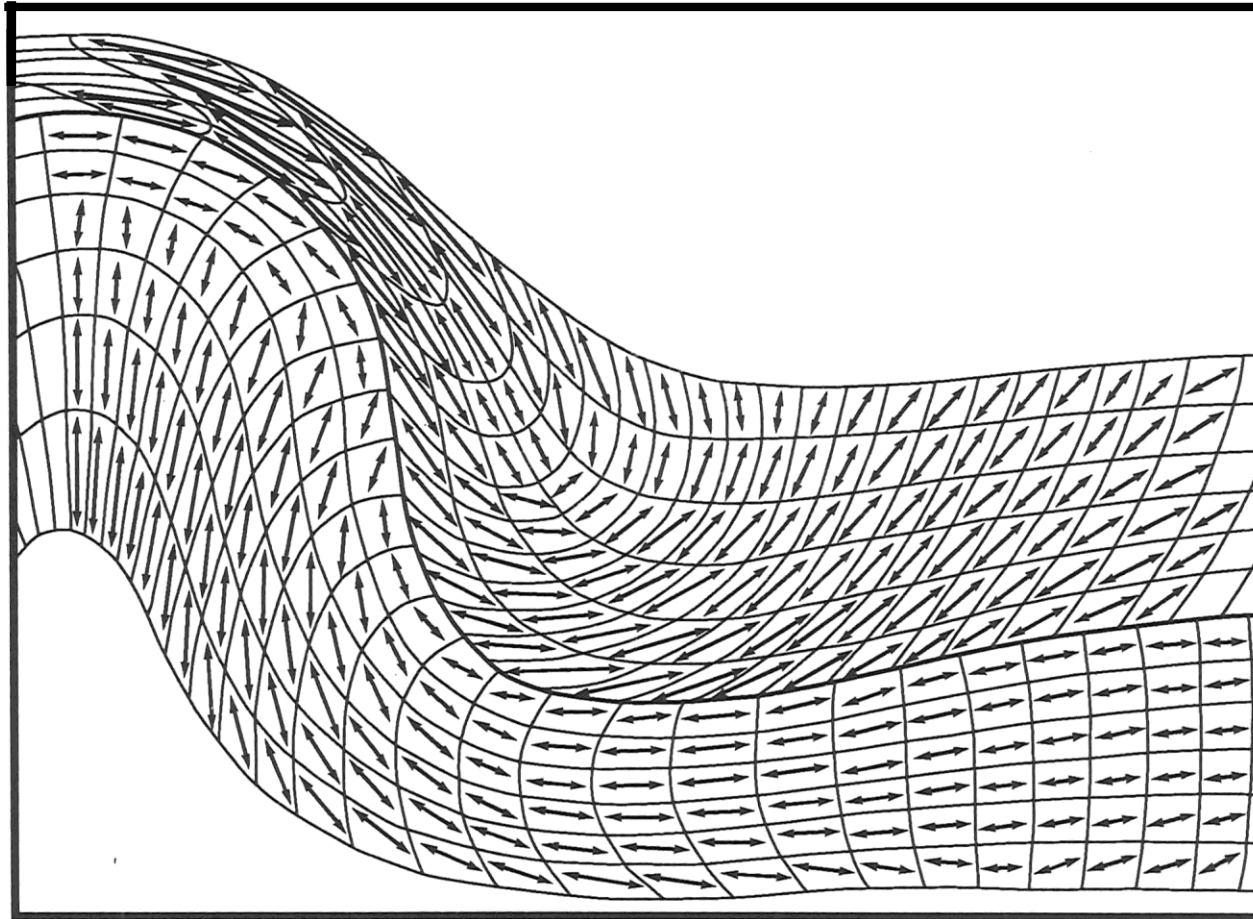


Figure 4.2 Cross-section of an experimentally-derived strain grid for an immature diapiric structure model. The arrows represent the orientations and relative magnitudes of the long axes of strain ellipses calculated for each element. (Redrawn from Dixon, 1974)

trends north-south, sub-horizontal, and roughly parallel to the long-axis of the dome (Figure 2.1).

No microfabric evidence of vertical motion has been found in the dome. As previously discussed, even in the deepest exposures of the dome structure the mineral lineation and thus the transport direction is subhorizontal. This could be interpreted to represent the horizontal extension at the top of a immature diapiric body (Figure 4.2). However, theoretically this sort of extension should be pure shear and radially oriented. The actual shear seen throughout the exposed parts of the Pelham dome is dominated by simple shear with a consistent north-south direction and a top-to-the-south sense.

Some of these problems have been previously noted (c.f. Dixon, 1987). The anomalous lineation and lack of vertical motion have been explained by later deformation superimposed on the gneiss domes. This explanation is unsatisfying. While none of the points against buoyancy-driven mechanisms are completely conclusive, they are sufficient to warrant examining other theories of dome formation. These other mechanisms may fit the observed features better than this one.

Refolded Folds

Domal structures can be formed by the superposition of two folds (Ramsay, 1967; Figure 4.1b). To produce the Pelham dome, it would be necessary to have two large orthogonal folds. One fold would have to be a subhorizontal upright fold and strike approximately north-south; the other fold would have to be a subhorizontal

upright fold striking approximately east-west. Folds with the first orientation were in fact formed during the "backfold stage" of Acadian deformation (Robinson, 1979; Figure 1.5). Planar fabrics possibly related to this event have been preserved in porphyroblasts in the cover rocks (Figures 3.7b, 3.10c, 3.12b). No foliation or any minor folds that correspond with the second fold generation have been recognized. Further, the subhorizontal shear, pervasive throughout the Pelham dome, would have to be incorporated into this refolding model.

Sheath Folds

Discussions of very large sheath folds have become more common in the geologic literature (Volmer, 1988; Goscombe, 1991), and the possibility that sheath folds could form dome-like gneiss structures has been suggested (Coward, 1981; Brun, 1988). In fact, the possibility that the Pelham dome represents part of a large sheath fold has been suggested by Robinson and others (1989). Folds which seem to be sheath folds, one of which is quite large, have been described in the Pelham dome (see Figure 20 in Ashenden, 1973; and Figures 5 and 9 in Onasch, 1973).

A large tubular sheath fold with a shallow-dipping axial plane could have an oval outcrop shape elongate in the direction of shear, a consistent sense of shear throughout, and a lineation parallel to the long-axis of the oval (Figure 4.3a), similar to the Pelham dome. In such a case, the long-dimension of the fold cross-section (Y-Z section) must be vertical (Figure 4.3a) to produce an oval outcrop shape that is elongate in the direction of shear. Almost any slice through such a fold (Figure 4.3b)

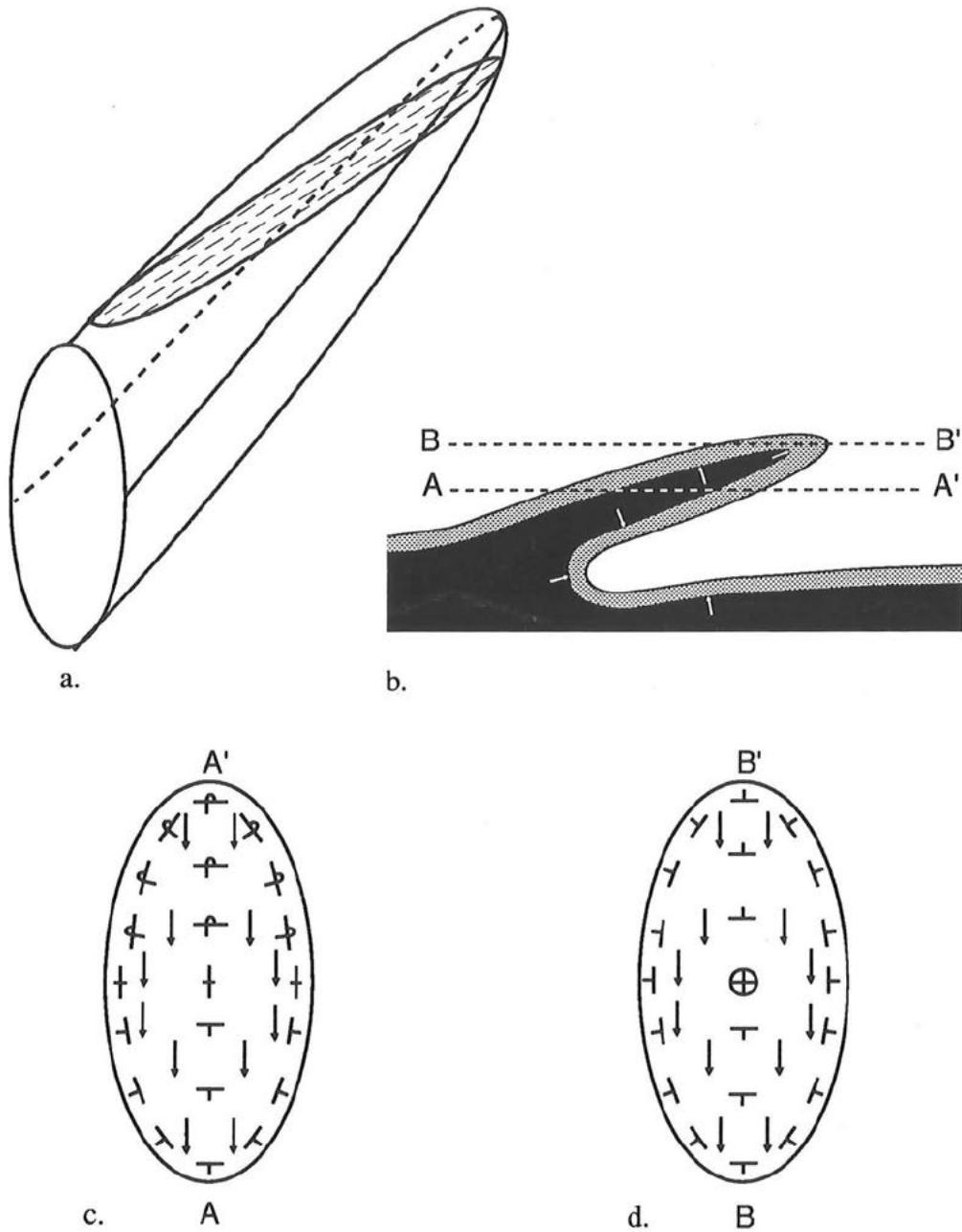


Figure 4.3. Structural features of a large sheath fold forming a domal structure in outcrop. a. How an elongate sheath fold can have an oval outcrop pattern with the long axes parallel to the direction of shear and the stretching lineation. b. Two cuts through the profile of such a sheath fold, A -A' is a complete section while B-B' is a partial section. Arrows indicate younging direction. c. and d. How the stretching lineation and strike and dip of bedding or layering would look for the respective cuts shown in b.

would necessarily expose overturned bedding. Even in a strongly asymmetric sheath fold the overturned area would have to be at least as thick as the complete section involved in the folding. If the left half of Figure 4.3c corresponds with the northern part of the Pelham dome where the mantle units are not overturned, then the southern part of the Pelham dome would be predicted to be overturned. The majority of layering and bedding in the southern half of the Pelham dome have not been reported to be overturned (Zen and others, 1983), so it seems unlikely that the Pelham dome represents a complete section through a sheath fold.

An alternative to a complete slice through a sheath fold is a section through the upper parts of the fold that truncates the top of the fold nose (**B-B'**, Figure 4.3b). In map view, such a cut would have a dome geometry, would be elongate in the direction of shear, and could have a consistent sense of shear (Figure 4.3d). Problems do exist with this scenario, however.

One important problem concerns the orientation of foliation. A review of the literature has shown that two types of foliations are generally present in sheath folds. There is a foliation, typically a compositional layering, that defines the sheath fold and which has been reoriented by shearing. A second foliation noted in some cases is an axial planar foliation that is commonly parallel to the compositional layering but cross-cuts the compositional layering in the hinges of the fold (Goscombe, 1991; Volmer, 1988; Skjernaa, 1989). This foliation is typically defined by the alignment of platy minerals (Goscombe, 1991) and is generally subparallel to the XY plane of the shear strain that formed the sheath fold (Skjernaa, 1989). Only one foliation is generally seen in the northern part of the Pelham dome, and it is typically parallel to layering.

A foliation formed by the shearing seen should be subhorizontal and planar, not arched as the foliation is in the northern part of the Pelham dome. The foliation seen in the northern part of the Pelham dome seems inconsistent with what would be expected in a large sheath fold.

Another problem with interpreting the Pelham dome as a partial section through a large sheath fold is a matter of scale. The exposed part of the Pelham dome is almost forty kilometers long and depending on the exact shape of the sheath fold the amplitude of the complete fold would have to be at least twice that length and probably even longer. The development of such a large sheath fold would require large amounts of shear. As discussed earlier, it is difficult to make a truly quantitative assessment of the amount of shear that has occurred in the Pelham dome. However, the evidence available indicates that it is probably not of the magnitude necessary to produce such a large sheath fold.

Still, it is not yet possible to rule out a sheath fold origin for the Pelham dome as a whole. Mapping in the southern part of the dome has mostly been at a reconnaissance level. Structural interpretation has recently been complicated by the reinterpretation of the former Proterozoic Mt. Mineral Formation as an infold of Paleozoic rocks (Robinson and Tucker, 1991). Further mapping may support the possibility that the southern end of the Pelham dome is the nose of a large sheath fold. A sheath fold with a curved axial plane might fit the characteristics better, but this would require an explanation for the curvature of the axial plane, such as refolding of the sheath fold.

Thrust Fault Associated Folding

It has been proposed (Hatcher, 1983; Hatcher and others, 1986) that it is possible to produce a dome by ductile deformation above a buried thrust fault (Figure 4.1c). A fold forms in front of the buried thrust and with a relatively short fault length the surface expression of such a fold could be a dome. In such a scenario, the dome should be elongate perpendicular to the direction of transport and parallel to the length of the thrust. The transport of material in the Pelham dome is parallel to the direction of transport and perpendicular to the direction of thrusting in the Bronson Hill anticlinorium (c.f. Robinson and others, 1991). Also thrust faulting seen in the Bronson Hill anticlinorium is earlier in the deformational history (Figure 1.5), and most thrust faults are clearly contorted around latter dome-stage structures (Thompson and others, 1968). The diffuse ductile deformation seen in the Pelham dome is incompatible with the generally more brittle focussed deformation occurring in thrust sheets.

Gates (1987) has suggested that a combination of a refolded fold mechanism and the thrust duplex mechanism explains domes in the Virginia Piedmont. The domes are suggested to have formed by a combination of fold superposition and thrust faulting in a transpressional shear zone. The proposed structure has similarities to a positive flower structure. The area studied by Gates (1987) differs from the Pelham dome in two important respects: 1) two generations of orthogonal folds are present, and 2) shear zones occur along the dome margins and shear is vertically oriented. While this model may work well in the Virginia Piedmont, the differences in the shear

distribution and direction make it highly unlikely that this model should be applied to the Pelham dome.

Mega-Boudinage

Schreurs and Westra (1986) suggest that domes can form through the boudinage of large gneissic bodies surrounded by schists (Figure 4.1e). Such a model for the Pelham dome would explain the subhorizontal fabric and the reorientation of the shear sense with the foliation along the sides of the dome structure. However, the sense of shear seen in purely extensional boudins should be opposite at either end and null at some point in the middle (Figure 4.4). This pattern does not fit with reconnaissance work by the author and by V. DelloRusso (personal communication, 1989) that shows the same north-over-south sense of shear in the southern part of the Pelham dome as in the northern part. Schreurs and Westra (1986) documented "pinch and swell" structures near mega-boudin domes in Finland that show flow into mega-boudin necks. Similar structures are not present in the cover rocks at the extreme northern end of the Pelham dome (Figure 1.3). The en-echelon alignment of domes in the Bronson Hill anticlinorium also does not fit well with a simple symmetric boudinage model as the boudinaged domes should be in linear arrays in such a model.

The evidence discussed above makes it unlikely that the Pelham dome is a purely extensional boudin. However, there exists the possibility that the Pelham dome is a large asymmetric boudin or lower strain domain formed in a shear zone. Bell and Hammond (1984) described the geometric relationships expected to characterize

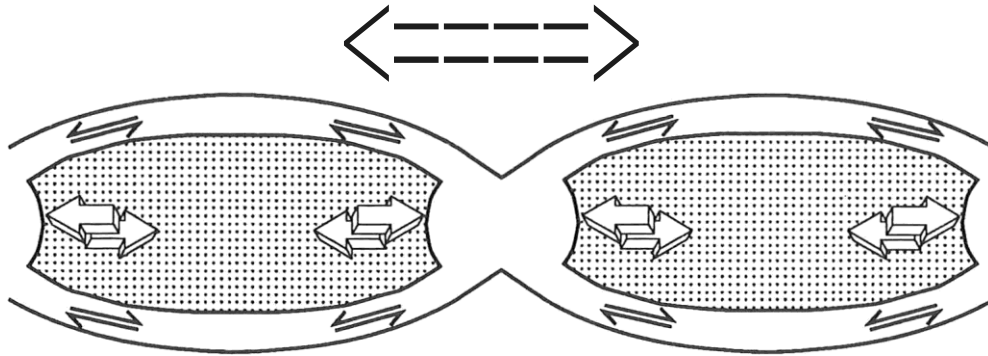


Figure 4.4. Shear senses along the edges of boudins during extension or pure shear. Note the opposite sense of shear on opposite ends of the boudins.

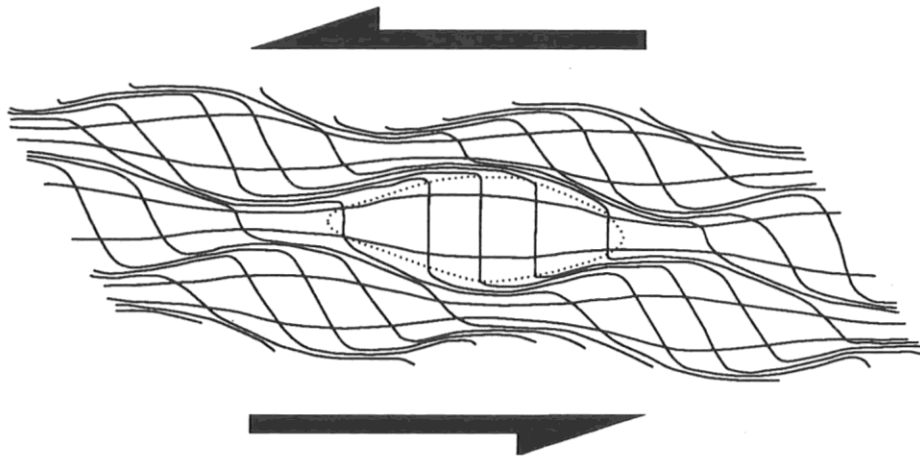


Figure 4.5. Patterns of strain in a rock undergoing heterogeneous shear with the development of low-strain pods and shear-dominated high strain zones. Redrawn from Bell (1985).

heterogeneous shearing. Strain is partitioned such that domains of high strain anastomose around a series of pods dominated by pure shear histories (Figure 4.5). These pods are generally oval in shape with a consistent sense of shear along the sides. In applying this model to the Pelham dome, the mantling metamorphosed sedimentary and volcanic rocks would be expected to have strain partitioned into them. The gneisses would be sheared along the margins and take up progressively less shearing strain toward the center of the pod. A section through the upper part of such a pod would consist of an oval gneissic body surrounded by less gneissic rocks. The foliation would wrap around the pod and be arched over the top, the lineation would be parallel to the length and subhorizontal. The sense of shear could be consistent along the length of a "dome" formed by this method. While the rest of these criteria fit the Pelham dome a decrease in shear intensity with exposure depth has been suggested, but not unequivocally demonstrated.

Another problem with this model has to do with the three-dimensional shape of the Pelham dome. This shear model would work best if strain could be partitioned both over and under the dome. There are some interpretations that show the Proterozoic gneiss as being part of an early thrust slice that overlies metamorphosed sedimentary rocks (see cross-section D-D', Zen and others, 1983). This would facilitate the partitioning of strain under the dome because the gneisses would be underlain by more easily deformable metamorphosed sedimentary rocks.

Summary and Conclusions

There are several areas of study that would help to constrain a genetic model for the Pelham dome. In particular, further study is needed in the southern part of the dome. Information on the orientation of layering and foliation, and kinematic data would be helpful in evaluating the applicability of the sheath-fold dome model.

Structural studies in the other domes of the Bronson Hill anticlinorium are necessary if the correlation between ductile shearing and dome formation is to be continued. Most of the suggested models that associate shearing and dome formation would suggest a similar association in the surrounding domes. Although the Pelham dome is the only dome in the Bronson Hill anticlinorium to expose Proterozoic rocks, no one has suggested that different models are needed for its formation.

Work that has been done on other domes in the Bronson Hill anticlinorium has complicated the structural interpretation. Work in the northern part of the Warwick dome (DelloRusso and Robinson, 1989) showed poorly-developed kinematic indicators with shear senses inconsistent with those in the Pelham dome. However, in the present study, cover rocks almost to the southwestern edge of the Warwick dome (Plate 1) were sampled and analyzed, and all of them indicate a sense of shear similar to that seen in the Pelham dome. This inconsistency in shear strain from different areas suggests heterogeneous strain distribution in the Warwick dome. Microfabric work has not yet been done on other nearby domes and it remains to be seen if shearing similar to that in the Pelham dome is present.

The geometry and correlation of late-stage strain in the Bronson Hill anticlinorium is a problem. In the Pelham dome, shearing seems to be generally parallel to foliation and compositional layering. On the eastern edge of the Bronson Hill anticlinorium where the bedding is steeply inclined, the mineral lineations have a subhorizontal orientation, but the foliation is near vertical. Kinematic indicators suggest a dextral sense of shear (Peterson, 1989, 1992; Peterson and Robinson, 1993). Despite similarities in deformation style and movement direction, it remains unclear whether this shearing is related to that seen in the Pelham dome. In particular, isotopic work (Robinson and Tucker, 1991) suggests different ages for the two areas. However, as discussed earlier, it is possible that shearing occurs in major parts of the Bronson Hill anticlinorium. Whether the bulk strain is top-to-the-south subhorizontal shear on a subhorizontal shear plane or dextral sub-horizontal shear on a subvertical shear plane will be important in figuring out which model best fits formation of the domes of the Bronson Hill anticlinorium.

None of the models discussed for dome formation seems completely satisfying at this time. Models involving formation of the dome through thrust-related processes, refolding, and purely extensional boudinage have flaws that remove them from serious consideration. A model involving formation of the dome through solely gravitational processes fails to adequately explain the apparently shear-related fabrics present. Incomplete information on the southern part of the dome creates difficulty evaluating important aspect of the suggestion that the dome has a sheath fold geometry. Nevertheless, this model has serious problems. The model describing the dome as a

"sheared boudin" or a pod-shaped low-strain domain in a shear zone seems to fit the observed characteristics best.

Consideration here has been primarily of simple versions of these models. In fact, the real mechanism may be a complex combination of two or more of the models examined. However, more structural information on the southern part of the Pelham dome would be needed to effectively evaluate this idea.

CHAPTER 5

REGIONAL TECTONICS

Timing of Deformation

Until recently the tectonic events influencing the study area and most of the Bronson Hill anticlinorium were thought to be primarily Acadian in age (Figure 1.5) with an unknown but probably minor Taconian component (Robinson and Hall, 1980). However, recent geochronologic work with several isotopic systems (Tucker and others, 1988; Gromet and Robinson, 1990; Robinson and Tucker, 1991) has complicated the interpretation of how major orogen-parallel shear fits into the tectonic evolution of central New England. The isotopic age determinations have revealed that there probably is a large amount of post-Acadian deformation in the area. In particular, Gromet and Robinson (1990) have used a relatively new radiometric dating technique that purports to date the fabric present in the rocks by using metamorphic mineral isochrons. A number of radiometric dates of Pennsylvanian age (≈ 290 Ma) have been obtained. While complete data on that study has not yet been published, there is a high probability that the shearing documented in the northern part of the Pelham dome is in fact Pennsylvanian in age. Pennsylvanian ages are slightly older than those typically given for Alleghanian deformation in the Hope Valley terrane of southeastern New England (Getty, 1990), but well within Alleghanian ages for the Appalachian orogen as a whole (Hatcher and others, 1989).

Suggested Correlations with Avalonian and Alleghanian Events

Possible Correlation with Avalonian Rocks

It has been proposed (Robinson, 1986; Gromet, 1989; Getty, 1990) that the Proterozoic gneisses of the Pelham dome are related to Avalonian gneisses of the Hope Valley terrane (Figure 5.1) exposed in eastern Connecticut and Rhode Island. Both groups of gneisses have approximately the same late Proterozoic ages (≈ 600 Ma). Rock types are similar and geochemical studies (Hodgkins, 1985) have shown a likely, though not certain, correlation.

While this proposal has merit as a lithological comparison, tectonic interpretations that accompany it are more questionable. One aspect of this interpretation is a suggestion that the Avalonian basement gneisses were not involved in Acadian deformation (Gromet, 1989). While this structural interpretation may prove true for rocks in the Willimantic dome (Getty, 1990), it fails to account for pre-shearing folds of Proterozoic gneisses in the Pelham dome that are correlated with Acadian deformation (Robinson, 1979). This difference in Acadian history suggests that the two Proterozoic gneiss groups may not be directly correlatable. Yet, this lithological correlation is the basis of structural models showing a continuous, relatively-flat Avalonian basement underlying all of southern New England (Gromet, 1989; Getty, 1990).

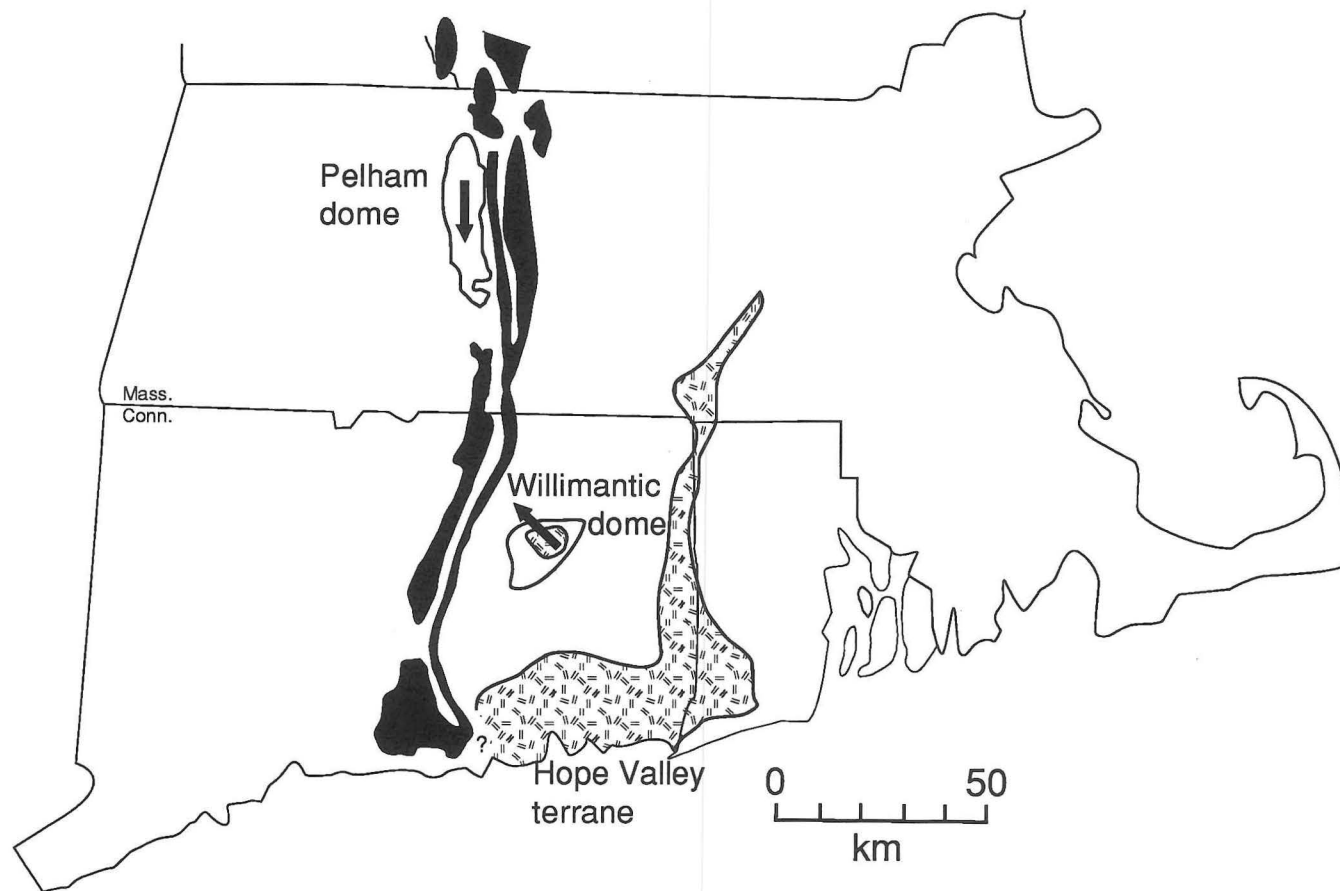


Figure 5.1. Direction of shearing within the Pelham and Willimantic domes. Arrows indicate the direction of movement of the cover rocks in the two domes, note the difference in the directions. Patterned areas indicate presence of correlated Proterozoic rocks within the Hope Valley terrane and the Willimantic dome. Domes of the Bronson Hill anticlinorium are shown in black.

Suggested Deformational Correlation with the Willimantic dome

Various workers (Gromet, 1989; Getty, 1990), have attempted to correlate deformation in the Proterozoic (Avalonian) rocks of the Pelham dome with that seen in the Willimantic dome (Figure 5.1). Deformation in the Willimantic dome involves subhorizontal shearing with a top-to-the-northwest sense, and is concentrated into a mylonitic shear zone developed at the boundary between Proterozoic rocks and Paleozoic pelitic cover rocks (Getty, 1990). The main mylonite zone at the basement-cover contact is accompanied by synthetic extensional shear zones with a normal sense of movement that are developed in the cover rocks (Getty, 1990). This contrasts sharply with the shearing that is seen in the Pelham dome. Shearing in the Pelham dome is homogeneous and pervades the 2 kilometer thick exposed section. No concentration of deformation exists either at the boundary between Proterozoic and Paleozoic rocks, or at the separate boundary between core gneisses and cover rocks. Other characteristics of the deformation are also different. As previously mentioned, there seems to be a slight E-W compressional element to deformation in the northern part of the Pelham dome. This contrasts with the purely extensional deformation seen in the Willimantic dome (Getty, 1990).

Even more importantly, in the Pelham dome, there is a top-to-the-south sense of shear which is markedly different than the top-to-the-northwest shear seen in the Willimantic dome (Figure 5.1) (Getty, 1990). How two shears of markedly different direction of motion can be directly correlated is unclear.

Brittle faulting in the Willimantic dome has similar orientations and movement directions to the normal shear zones present there (Getty, 1990). The brittle deformation in and around the Pelham dome is early Mesozoic in age and does not have a movement sense or an orientation similar to that of ductile deformation. In fact, brittle deformation in the Pelham dome does not appear to be related in any way to earlier ductile deformation.

Ages given for deformation in the Pelham dome (Gromet and Robinson, 1990; Tucker and Robinson, 1991) are around 290 Ma. Ages for deformation at the basement cover contact given by Getty (1990) are ≈ 270 Ma. Deformation in the Avalonian gneisses below the basement/cover contact at Willimantic is dated at ≈ 290 Ma (Getty, 1990), but the orientation and significance of this deformation is unclear. While these objections do not argue against an Alleghanian age for the deformation in the Pelham dome, they do rule out structural models that attempt to directly correlate deformation in the Pelham dome with deformation in the Willimantic dome.

Absolute Timing of Deformation: Evidence From Fabrics

There are observations about the absolute timing of deformation in and around the Pelham dome that do not fit neatly with an Alleghanian age for deformation. Included in this are observations from this study about the relative timing of metamorphism and deformation (Chapter 3). This study has shown that the shearing and the earlier deformation which produced some of the inclusion fabrics seen in porphyroblasts took place at approximately the same metamorphic grade. Tentative

correlations have been made between this relict fabric and the backfold stage of Acadian deformation. There are several possible ways that this problem could be resolved. It is possible that the earlier deformation should not be correlated with the backfold stage of Acadian deformation. This could necessitate an additional phase of Alleghanian deformation before the shearing. It is also possible that the rocks that were to form the Pelham dome were either kept at the same metamorphic grade from the end of the Acadian deformation until the beginning of the Alleghanian, or that approximately equal metamorphic grades were reached in both orogenies. Further work will need to be done before these problems can be resolved.

Another problem involves possible continuation of top-to-the-south shearing outside the Pelham dome. A sill of the Belchertown intrusive complex intrudes the northern part of the Pelham dome (Hodgkins, 1985) and shows a north-south trending, stretching lineation and evidence for subhorizontal shearing. A strong north-south lineation is also seen in the contact metamorphosed rocks in and around the Belchertown intrusive complex (Figure 2.16). On this basis, it was earlier suggested that shearing continued south of the Pelham dome into the Belchertown complex. However, if contact metamorphic minerals are lineated this seems to require that the deformation took place at roughly the same time as the intrusion. If the rocks were deformed at the regional lower amphibolite facies grade after contact metamorphism, there would have been significant retrogression and the contact metamorphic minerals would not be lineated. The Belchertown intrusion has been dated at 380 ± 5 Ma and is interpreted as a syn-tectonic intrusion (Ashwal and others, 1979).

There are several possibilities for resolving this discrepancy. It is possible that the lineation associated with the shearing may be unrelated to the lineation seen in the Belchertown complex. It is also slightly possible the area has seen two major orogen-parallel deformational events at different times but at the same metamorphic grade. If the rocks around the Pelham dome were tectonically undisturbed and in isostatic equilibrium between the Acadian and Alleghanian orogenies, the rocks might have been deformed at similar metamorphic conditions. If two deformations with similar movement directions have occurred it is necessary that the second one did not greatly effect the Belchertown intrusive complex because this would have retrograded the contact metamorphic aureole.

Work on the eastern margin of the Bronson Hill anticlinorium has documented orogen parallel shearing from an area with consistent Acadian isotopic ages (Peterson and others, 1990; Peterson, 1992; Peterson and Robinson, 1993). These rocks also contain evidence for a deformational event that directly preceded the shearing event at the same metamorphic conditions. In order to separate this shearing and lineation from that seen in the Pelham dome, Robinson and Tucker (1991) have proposed a major metamorphic and structural discontinuity in the Bronson Hill anticlinorium. This discontinuity would divide rocks that have seen significant Alleghanian deformation from those that have not. This discontinuity is proposed to trend north-south in the Bronson Hill anticlinorium and to be marked by zones of retrograde metamorphism (Figure 1.2) and by reorientation of the N-S lineation (Figure 2.1).

Possible Alleghanian Tectonic Correlations

It is not clear how a major orogen parallel shear fits with deformation in the Alleghanian orogeny. Correlations of the shear with late-stage orogenic collapse in the Acadian orogeny (Peterson and others, 1990) make more sense from a purely mechanical standpoint. The 290 Ma age of deformation (Gromet and Robinson, 1990; Robinson and Tucker, 1991) is at a time when the dominant Alleghanian deformational pattern in New England is suggested to be compressional (Hatcher and others, 1989). Later in the orogeny, incidents of both dextral and sinistral shear have been described (Hatcher and others, 1989). A strike-slip environment would be more likely to produce an orogen-parallel shear such as that seen in the Pelham dome, but the timing is wrong.

It is obvious that there are a number of unresolved problems relating to Alleghanian deformation in New England. The observations in this study will need to be incorporated into any future tectonic models. However, solution of some of the discrepancies raised in this chapter will be necessary before a coherent tectonic model can be developed. Further microstructural and isotopic work in the area will be necessary to resolve the discrepancies.

CHAPTER 6

CONCLUSIONS

1) The northern part of the Pelham dome is pervasively deformed by relatively homogeneous, subhorizontal shear with a top-to-the-south shear sense. The direction of shear is indicated by both microstructural and outcrop-scale kinematic indicators including: asymmetric winged porphyroclasts, asymmetric pressure shadows, S-C fabrics, asymmetric folds, and asymmetrically boudinaged pegmatites.

2) The deformation seen in the Pelham dome has several distinctive characteristics. The shear is parallel to a well-developed stretching lineation and shear is distributed homogeneously, only in rare instances forming discrete shear zones. Easily visible variations in shear intensity are associated with changes in rock type and are probably the result of strain partitioning due to differences in strength between the rock types. The shear plane is reoriented along the margins of the dome, staying perpendicular to compositional layering.

3) Based on reconnaissance geology by the author and others (V. DelloRusso, personal communication, 1989; P. Robinson, personal communication, 1992), and the presence of a strong stretching lineation throughout the Pelham dome (Figure 2.1), it appears that this top-to-the-south shearing is present throughout the central and southern part of the Pelham dome as well. Evidence for this shearing may also exist farther south in the Belchertown intrusive complex (Figure 1.1). Evidence for this includes; lineation data (Figure 2.16), and the presence of shear fabrics (Ashwal,

1974). There are other areas within the Bronson Hill anticlinorium with a N-S stretching lineation that also seem to have a significant component of ductile shear (Peterson, 1992). However, recent geochronologic work (Tucker and Robinson, 1991) suggests that the eastern part of the Bronson Hill anticlinorium was deformed at an earlier time than the western parts. However, it remains possible that many areas within the western Bronson Hill anticlinorium may have been deformed in a manner similar to the Pelham dome. All of the domes of the Bronson Hill anticlinorium should be examined to see if this top-to-the-south shearing is present.

4) Scarcity of strain markers has made it difficult to measure quantitatively the amount of strain seen in the Pelham dome. A sheared pegmatite from the Dry Hill Formation gives a 34° angular shear parallel to the lineation and perpendicular to the foliation (Figure 2.17). If this is accepted as a valid minimum for the entire exposed section, it suggests a minimum transport of 1.25 kilometers across the shear zone. Reconstruction of objects pulled apart by shearing has given extensions ranging from 0.08 to 1.32. The minimum angular shear necessary to produce the maximum measured extension in the Pelham dome converts to 2.6 kilometers of transport across the shear zone.

5) Textural criteria in samples from the upper and lower exposures of the Poplar Mountain Gneiss suggest that the shear strain decreases slightly with depth in the dome. An attempt to compare textural criteria between quartzites from the cover rocks and from the core gneisses was inconclusive, partially due to the presence of primary recrystallization. However, extremely similar textures are seen in quartzites from the core and cover suggesting similar magnitudes of shear. Robinson (personal

communication, 1992) has suggested that this conclusion is supported by an increased variation in the trend of fold axes with depth, implying that pre-shearing folds have been less reoriented by shearing with depth.

6) Some previously interpreted "late shears of reversed sense" (Onasch, 1973) are probably related to the interaction of shearing and folding (Figure 2.21). Other evidence given for supposed top-to-the-north shearing (Onasch, 1973) is a misinterpretation of the kinematic development of feldspar pods with asymmetric tails (Figure 2.19). Whether the "late-flattening and extension" proposed by Onasch (1973) is also related to shearing is less clear, but also likely. All the boudins seen in this study seem to be related to disaggregation of pegmatites during shearing, and not a separate phase of "late flattening and extension".

7) Evidence for two phases of deformation and probably a third has been found in porphyroblast inclusion fabrics from the cover rocks of the Pelham dome. One of these fabrics is clearly related to the dominant shear-related fabric present in the matrix. Some porphyroblasts preserve an included foliation at a high angle to the shear foliation with very steep dips to the north or to the south. The strike of this foliation is oblique to the stretching lineation because the fabric appears in thin sections oriented both parallel and perpendicular to the lineation. The orientation and timing of this fabric suggest that it is probably related to a pre-shearing deformation, possibly the back-fold stage of Acadian deformation (Figure 1.5) and not an early phase of shearing. Previous studies (Ashenden, 1973, Onasch, 1973; Laird, 1974) have shown evidence for folding that probably relates to this relict foliation. Unfortunately, porphyroblasts from the core gneisses typically lack inclusion fabrics

and therefore show microfabric evidence only of the shearing. The only fabric evidence for earlier events is an example of a possible pre-shearing retrograde reaction (Figure 3.17).

8) Both deformations represented by microfabrics in the rocks took place at roughly the same metamorphic grades. The peak metamorphic assemblage in pelitic rocks (staurolite-kyanite-biotite-garnet) was stable during and after shearing, and possibly during the preceding phase of deformation. Most of the kyanite seen in the pelitic rocks formed after shearing (Figure 3.15).

9) Two highly-localized phases of retrograde metamorphism occurred after the end of shearing. The first phase was controlled by fluid access and may be related to the New Salem retrograde zone (Figure 1.2). The second phase was typically very minor and seems to be related to brittle faults that cut the region in the early Mesozoic.

10) Despite an extensive examination, no evidence has been found in the cover rocks of the relict high-grade metamorphism seen in recently recognized Paleozoic rocks (Robinson and Tucker, 1991) infolded into the core rocks of the southern part of the Pelham dome (Roll, 1987). Possible evidence for this metamorphic event in the basement rocks of the northern part of the Pelham dome is confined to one instance of a garnet in a calc-silicate pod undergoing a retrograde reaction to epidote (Figure 3.17). The lack of evidence in the basement gneisses is not surprising in that the mineral assemblages of the gneisses, quartzites, and semi-pelitic rocks that make up the Proterozoic units are not particularly sensitive to metamorphic conditions.

11) The previously suggested (Robinson, 1963; Thompson and others, 1968; Dixon, 1974) density-driven solid-state buoyancy mechanism proposed for formation of domes in the Bronson Hill anticlinorium fails to account for the stretching lineation and the shear seen within the Pelham dome. Formation of the Pelham dome by superposition of orthogonal folds, thrust-fault processes, or symmetrical boudinage requires features not seen in the Pelham dome, and/or fails to explain all the microstructural features. It has been proposed (Robinson and others, 1989) that the Pelham dome may be the surface expression of a subhorizontally-oriented sheath fold. This explanation could account for the shearing, the elongate oval shape, and the mineral lineation if the shape of the sheath fold is narrowly constrained. However, a sheath fold mechanism fails to account for the orientation of the foliation, and could require some radical revisions to the mapping done in the southern end of the dome. The mechanism that best fits the requirements is a newly proposed one, that the Pelham dome is the result of partitioning of strain around a large pod within a very large shear zone.

12) On the basis of evidence from this study, previous suggestions that deformation in the Pelham dome may be related to deformation in the Willimantic dome (Gromet, 1989; Getty, 1990) seem to be incorrect. Deformation in the Willimantic dome is subhorizontal shear with a top-to-the-northwest sense (Getty, 1990), while the shear seen in the Pelham dome has a top-to-the-south sense. Deformation in the Willimantic dome is in discrete shear zones which are concentrated at the boundary between Proterozoic rocks and Paleozoic pelitic cover rocks (Getty, 1990). Deformation in the Pelham dome is diffuse, with no such concentration of deformation either at the boundary between Proterozoic and younger rocks, or at the

boundary between core gneisses and cover rocks. Deformation in the Willimantic dome is clearly of an extensional nature and shows a transition from ductile to brittle (Getty, 1990). Deformation in the Pelham dome probably has an E-W compressional component in addition to shearing. Brittle deformation seen in the Pelham dome does not appear to be related in any way to earlier ductile deformation. An isotopic technique that is supposed to yield radiometric ages for deformation fabrics (Gromet and Robinson, 1990; Getty, 1990), gives ages of approximately 290 Ma for deformation in the Pelham dome (Gromet and Robinson, 1990); while the same method in the Willimantic dome gives dominantly ages of approximately 270 Ma (Getty, 1990).

13) The shearing seen in the northern part of the Pelham dome does not clearly fit with models proposed for the Alleghanian orogeny in central New England (Hatcher and others, 1989; Getty, 1990). Much more will have to be known about microfabrics and ages of deformation in the Bronson Hill anticlinorium before the discrepancies can be resolved.

BIBLIOGRAPHY

- Ashenden, D.D. (1973) Stratigraphy and structure, northern portion of the Pelham dome, north-central Massachusetts, Contribution no. 16 (M.S. thesis), 132 p. Department of Geology and Geography, University of Massachusetts, Amherst.
- Ashwal, L.D. (1974) Metamorphic hydration of augite-orthopyroxene monzodiorite to hornblende granodiorite gneiss, Belchertown batholith, west-central Massachusetts, Contribution no. 18 (Ph.D. thesis), 124 p. Department of Geology and Geography, University of Massachusetts, Amherst.
- Ashwal, L.D., Leo, G.W., Robinson, Peter, Zartman, R.E. and Hall, D.J. (1979) The Belchertown quartz monzodiorite pluton, west-central Massachusetts: A syntectonic Acadian intrusion. *American Journal of Science*, 279, 936-969.
- Balk, R. (1956a) Bedrock geology of the Miller's Falls quadrangle, Massachusetts. U.S. Geological Survey Quadrangle map G.Q. 93.
- Balk, R. (1956b) Bedrock geology of the Massachusetts's portion of the Northfield quadrangle. U.S. Geological Survey Quadrangle map. G.Q. 92.
- Bates, R.L. and Jackson, J.A. (1987) Glossary of geology (3rd edition). American Geological Institute, Alexandria, Va.
- Bell, T.H. (1985) Deformation partitioning and porphyroblast rotation in metamorphic rocks: a radical reinterpretation. *Journal of Metamorphic Geology*, 3, 109-118.
- Bell, T.H. (1986) Foliation development and refraction in metamorphic rocks: reactivation of earlier foliations and decrenulation due to shifting patterns of deformation partitioning. *Journal of Metamorphic Geology*, 4, 421-444.
- Bell, T.H., Fleming, P.D. and Rubenach, M.J. (1986) Porphyroblast nucleation, growth and dissolution in regional metamorphic rocks as a function of deformation partitioning during foliation development. *Journal of Metamorphic Geology*, 4, 37-67.
- Bell, T.H., and Hammond, R.L. (1984) On the internal geometry of mylonite zones. *Journal of Geology*, 92, 667-686.
- Bell, T.H. and Johnson, S.E. (1989) Porphyroblast inclusion trails: the key to orogenesis. *Journal of Metamorphic Petrology*, 7, 279-310.

- Bell, T.H. and Johnson, S.E. (1990) Rotation of relatively large rigid obstructions during ductile deformation: Well established fact or intuitive prejudice? *Australian Journal of Earth Sciences*, 37, 441-446.
- Bell, T.H. and Rubenach, M.J. (1984) Sequential porphyroblast growth and crenulation cleavage development during progressive deformation. *Tectonophysics*, 92, 171-194.
- Berry, H.N., IV (1989) A new stratigraphic and structural interpretation of granulite-facies metamorphic rocks, Brimfield-Sturbridge area, Massachusetts and Connecticut. Ph.D. dissertation, Department of Geology and Geography, University of Massachusetts, Amherst, Massachusetts.
- Billings, M.P. (1937) Regional metamorphism of the Littleton-Moosilauke area, New Hampshire. *Geological Society of America Bulletin*, 48, 463-566.
- Billings, M.P. (1956) The geology of New Hampshire, Part II: Bedrock geology, 203 p. New Hampshire State Planning and Development Commission, Concord, N.H.
- Bleeker, W. and Westra, L. (1987) The evolution of the Mustio gneiss dome, Svecofennides of SW Finland. *Precambrian Research*, 36, 227-240.
- Bradley, D.C. (1983) Tectonics of the Acadian orogeny in New England and adjacent Canada. *Journal of Geology*, 91, 381-400.
- Brun, J.P. (1983) L'origine des dômes gneissiques: modèles et tests. *Bulletin de la Societe Geologique de France*, 25, 2, 219-228.
- Coward, M.P. (1981) Pan African gneiss domes, diapirs, and sheath folds. *Journal of Structural Geology*, 3, 1, 91.
- DelloRusso, V. and Robinson, Peter (1989) Late-Acadian elongation lineation in the gneiss domes of the Bronson Hill anticlinorium and the problem of the Great Swirl. *Geological Society of America Abstracts with Programs*, 21, 6, A264.
- Dixon, J.M. (1974) Experimental studies of strain in diapirs, with application to the mantled gneiss domes of New England, 204 p. Ph.D. dissertation, University of Connecticut, Storrs.
- Dixon, J.M. (1987) Mantled gneiss domes. In C.K. Seyfert, Ed., *The Encyclopedia of Structural Geology and Plate Tectonics*, p. 398-412. Van Norstrand Reinhold Company, New York.

- Emerson, B.K. (1898) Geology of Old Hampshire county, Massachusetts. U.S. Geological Survey Monograph, 29, 790 p.
- Eskola, P.E. (1949) The problem of mantled gneiss domes. Geological Society of London Quarterly Journal, 54, 4, 461-476.
- Etchecopar, A. (1977) A plane kinematic model of progressive deformation in a polycrystalline aggregate. Tectonophysics 39, 121-139.
- Field, M.T. (1975) Bedrock geology of the Ware area, central Massachusetts, 186 p. Ph.D. thesis, University of Massachusetts, Amherst, Massachusetts.
- Flinn, D. (1965) On the symmetry principle and the deformation ellipsoid. Geological Magazine, 102, 36-45.
- Gates, A.E. (1987) Transpressional dome formation in the southwest Virginia Piedmont. American Journal of Science, 287, 927-949.
- Getty, S.R. (1990) Late Paleozoic tectonism in the northern Appalachian orogen; insights from studies in southern New England, 191 p. Ph.D. dissertation, Brown University, Providence, R.I.
- Goldstein, A.G. (1988) Factors affecting the kinematic interpretation of asymmetric boudinage in shear zones. Journal of Structural Geology, 10, 7, 707-715.
- Goscombe, B. (1991) Intense non-coaxial shear and the development of mega-scale sheath folds in the Arunta Block, central Australia. Journal of Structural Geology, 13, 3, 299-318.
- Gromet, L.P. (1989) Avalonian terranes and late Paleozoic tectonism in southeastern New England: Constraints and problems. In R.D. Dallymeyer, Ed., Terranes in the circum-Atlantic Paleozoic orogen, Geological Society of America Special Paper 230, 193-211.
- Gromet, L.P. and Robinson, Peter (1990) Isotope evidence for late Paleozoic gneissic deformation and recrystallization in the core of the Pelham dome, Massachusetts. Geological Society of America Abstracts with Programs, 22, 7, A368.
- Guthrie, J.O. (1972) Geology of the northern portion of the Belchertown intrusive complex, west-central Massachusetts, Contribution no. 8 (M.S. thesis), 110 p. Department of Geology and Geography, University of Massachusetts, Amherst.
- Hanmer, S. (1986) Asymmetrical pull-aparts and foliation fish as kinematic indicators. Journal of Structural Geology, 8, 111-122.

- Hanmer, S. and Passchier, C. (1991) Shear-sense indicators: a review. Geological Survey of Canada Paper 90-17, 72 p.
- Hatch, N., Zen, E., Goldsmith, R., Ratcliffe, N.M., Robinson, Peter, Stanley, R.S., and Wones, D.R. (1984) Lithotectonic assemblages as portrayed on the new bedrock geologic map of Massachusetts. *American Journal of Science*, 284, 9, 1026-1034.
- Hatcher, R.D., Jr. (1983) Basement massifs in the Appalachians: their role in deformation during the Appalachian Orogenies. *Geological Journal*, 18, 225-265.
- Hatcher, R.D., Jr. (1989) Tectonic synthesis of the U.S. Appalachians. In R.D. Hatcher Jr., W.A. Thomas, and G.W. Viele, Eds., *The Appalachian-Ouachita Orogen in the United States*, Boulder, Colorado, Geological Society of America, *The Geology of North America*, v. F-2, 511-535.
- Hatcher, R.D., Jr., Thomas, W.A., Geiser, P.A., Snoke, A.W., Mosher, S., and Wiltschko, D.V. (1989) Alleghanian orogen. In R.D. Hatcher Jr., W.A. Thomas, and G.W. Viele, Eds., *The Appalachian-Ouachita Orogen in the United States*, Boulder, Colorado, Geological Society of America, *The Geology of North America*, v. F-2, 233-318.
- Hatcher, R.D., Jr., Williams, R.T., Coruh, C. and Costain, J.C. (1986) ADCOH seismic reflection data: evidence for a new subthrust platform duplex mechanism for dome formation in crystalline thrust sheets. *Geological Society of America Abstracts with Programs*, 18, 6, 631.
- Hodgkins, C.E. (1985) Geochemistry and Petrology of the Dry Hill Gneiss and related gneisses, Pelham dome, central Massachusetts, Contribution no. 48 (M.S. thesis), 137 p. Department of Geology and Geography, University of Massachusetts, Amherst.
- Hollocher, K. (1981) Retrograde metamorphism of the lower Devonian Littleton Formation, New Salem area, west-central Massachusetts, Contribution no. 37 (M.S. thesis), 268 p. Department of Geology and Geography, University of Massachusetts, Amherst.
- Johnson, S.E. (1990) Lack of porphyroblast rotation in the Otago Schists, New Zealand: implications for crenulation cleavage development, folding and deformation partitioning. *Journal of Metamorphic Geology*, 8, 13-30.
- Laird, H.S. (1974) Geology of the Pelham dome near Montague, west-central Massachusetts, Contribution no. 14 (M.S. thesis), 84 p. Department of Geology and Geography, University of Massachusetts, Amherst.

- Laird, J. and Albee, A.L. (1981) Pressure, temperature, and time indicators in mafic schist: their application to reconstructing the polymetamorphic history of Vermont. *American Journal of Science*, 284, 376-413.
- Leo, G.W. (1985) Trondhjemite and metamorphosed quartz keratophyre tuff of the Ammonoosuc Volcanics, western New Hampshire and adjacent Vermont and Massachusetts. *Geological Society of America Bulletin*, 96, 1493-1507.
- Lister, G.S. and Snoke, A.W. (1984) S-C mylonites. *Journal of Structural Geology*, 6, 679-690.
- Michener, S.R. (1983) Bedrock geology of the Pelham-Shutesbury syncline, Pelham dome, west-central Massachusetts, Contribution no. 43 (M.S. thesis), 101 p. Department of Geology and Geography, University of Massachusetts, Amherst.
- Naylor, R.S. (1969) Age and origin of the Oliverian domes, central-western New Hampshire. *Geological Society of America Bulletin*, 80, 405-428.
- Naylor, R.S., Boone, G.M., Boudette, E.L., Ashenden, D.D., and Robinson, Peter (1973) Pre-Ordovician rocks in the Bronson Hill and Boundary Mountain anticlinoria, New England, U.S.A. (abs.) *Transcripts of the American Geophysical Union*, 54, 495.
- Onasch, C.M. (1973) Analysis of the minor structural features in the north-central portion of the Pelham dome, Contribution no. 12 (M.S. thesis), 87 p. Department of Geology and Geography, University of Massachusetts, Amherst.
- Osberg, P.H., Tull, J.F., Robinson, Peter, Hon, R., and Butler, J.R., 1989, The Acadian orogen. In R.D. Hatcher, Jr., W.A. Thomas, and G.W. Viele, Eds., *The Appalachian-Ouachita Orogen in the United States*, Boulder, Colorado, Geological Society of America, *The Geology of North America*, v. F-2.
- Passchier, C.W. and Simpson, C. (1986) Porphyroclast systems as kinematic indicators. *Journal of Structural Geology*, 8, 831-843.
- Peterson, V.L. (1984) Structure and stratigraphy of the bedrock geology in the Ashburnham-Ashby area, north-central Massachusetts, Contribution no. 47 (M.S. thesis), 182 p. Department of Geology and Geography, University of Massachusetts, Amherst.
- Peterson, V.L. (1989) Orthogonal sillimanite lineations and two phases of shearing within a shear zone in upper amphibolite-granulite facies rocks, south-central Massachusetts. *Geological Society of America Abstracts with Programs*, 21, 6, A263.

- Peterson, V.L. (1992) Structure, petrology, and tectonic implications of highly strained rocks along the west margin of the Acadian granulite-facies high, south-central Massachusetts, 283 p. Ph.D. dissertation, University of Massachusetts, Amherst.
- Peterson, V.L., and Robinson, Peter (1992) Progressive evolution from uplift to orogen-parallel transport in a late-Acadian, upper amphibolite- to granulite-facies shear zone, south-central Massachusetts. *Tectonics*, in press.
- Peterson, V.L., and Thomson, J.A. (1991) The western margin of the Acadian metamorphic high, south-central Massachusetts. *Geological Society of America Abstracts with Programs*, 23, 114.
- Peterson, V.L., Williams, M.L., Robinson, Peter, and Reed, R.M. (1990) Late orogen-parallel extension: an example and kinematic implications from the Bronson Hill anticlinorium, central New England. *Geological Society of America Abstracts with Programs*, 22, 7, A368.
- Pike, T.M. (1968) Structural geology of the Tully body of Monson Gneiss, 48 p. M.S. thesis, University of Massachusetts, Amherst.
- Platt, J.P., and Vissers, R.L. (1980) Extensional structures in anisotropic rocks. *Journal of Structural Geology*, 2, 397-410.
- Poirier, J.-P. (1985) Creep of crystals, high-temperature deformation processes in metals, ceramics, and minerals, 260 p. Cambridge University Press, Cambridge.
- Poirier, J.-P., and Guillope, M. (1979) Deformation-induced recrystallization of minerals. *Bulletin de Mineralogie*, 102, 67-74.
- Poirier, J.-P., and Nicolas, A. (1975) Deformation-induced recrystallization by progressive misorientation of subgrain-boundaries, with special reference to mantle peridotites. *Journal of Geology*, 83, 707-720.
- Ramberg, H. (1968) Instability of layered systems in the field of gravity, I and II. *Physics Earth and Planetary Interiors*, 1, 427-474.
- Ramsay, J.G. (1962) The geometry and mechanics of formation of 'similar' type folds. *Journal of Geology*, 70, 309-327.
- Ramsay, J.G. (1967) Folding and fracturing in rocks, 508 p. McGraw-Hill, New York.

- Reed, Robert M. (1990) Relative timing of microfabric deformational phases and metamorphism, northern portion of the Pelham dome, north-central Massachusetts. Geological Society of America Abstracts with Programs, 22, 2, A64.
- Reed, Robert M., and Williams, Michael, L. (1989) Petrofabric kinematic indicators in the northern portion of the Pelham dome, western Bronson Hill Anticlinorium, central Massachusetts. Geological Society of America Abstracts with Programs, 21, 2, 60.
- Robinson, Peter (1963) Gneiss domes of the Orange area, Massachusetts and New Hampshire, 253 p., separate volume of tables and appendices, portfolio of 16 plates. Ph.D. dissertation, Harvard University, Cambridge, Massachusetts.
- Robinson, Peter (1967) Gneiss domes and recumbent folds of the Orange area, west-central Massachusetts. In Peter Robinson, Ed., Guidebook for Field Trips in the Connecticut Valley of Massachusetts: 59th annual meeting of the New England Intercollegiate Geological Conference, Amherst, Massachusetts, 17-47.
- Robinson, Peter (1979) Bronson Hill anticlinorium and Merrimack synclinorium in central Massachusetts. In J.W. Skehan and P.H. Osberg, Eds., The Caledonides in the U.S.A.: geological excursions in the northeast Appalachians, IGCP Project 21, Caledonide orogen, p. 126-150. Weston Observatory, Weston, Massachusetts.
- Robinson, Peter (1983) Realms of regional metamorphism in southern New England, with emphasis on the eastern Acadian metamorphic high. In P.E. Schenk, Ed., Regional trends in the geology of the Appalachian-Caledonian-Hercynian-Mauritanide orogen, p. 249-258. Reidel Press, Holland.
- Robinson, Peter (1986) Introduction. In Peter Robinson and D.C. Elbert, Eds., Field Trip Guidebook: Regional metamorphism and metamorphic phase relations in northwestern and central New England, Contribution No. 59, p. 1-10. Department of Geology and Geography, University of Massachusetts, Amherst.
- Robinson, Peter and Hall, L. (1980) Tectonic synthesis of southern New England. In D.R. Wones, Ed., Proceedings, The Caledonides in the U.S.A., IGCP Project 27: Caledonide orogen, p. 73-82. Virginia Polytechnic University, Blacksburg, Va.

- Robinson, Peter, Tracy, R.J., Hollocher, K., Schumacher, J.C., and Berry, H.N., IV (1986) The central Massachusetts metamorphic high. In Peter Robinson and D.C. Elbert, Eds., *Field Trip Guidebook: Regional metamorphism and metamorphic phase relations in northwestern and central New England*, Contribution No. 59, p. 145-194. Department of Geology and Geography, University of Massachusetts, Amherst.
- Robinson, Peter, Tracy, R.J., Hollocher, K., Berry, H.N., IV, and Thomson, J.A. (1989) Basement and Cover in the Acadian metamorphic high of central Massachusetts. In C.P. Chamberlain and Peter Robinson, Eds., *Styles of Metamorphism with depth in the central Acadian high, New England (A field trip honoring J.B. Thompson Jr.)*, p.69-140. University of Massachusetts, Amherst.
- Robinson, Peter, Thompson, P.J., and Elbert, D.C. (1991) The nappe theory in the Connecticut Valley region: Thirty-five years since Jim Thompson's first proposal. *American Mineralogist*, 76, 689-712.
- Robinson, Peter and Tucker, R.D. (1991) Implications of new U-Pb zircon and monazite ages in the Bronson Hill anticlinorium, Massachusetts: Proterozoic source regions, a major overthrust, and Acadian versus Carboniferous metamorphism. *Geological Society of America Abstracts with Programs*, 23, 5, A310.
- Roll, M.A. (1987) Effects of Acadian kyanite-zone metamorphism on relict granulite-facies assemblages, Mount Mineral formation, Pelham dome, Massachusetts, Contribution no. 60 (M.S. thesis), 202 p. Department of Geology and Geography, University of Massachusetts, Amherst.
- Rosenfeld, J. (1968) Garnet rotations due to the major Paleozoic deformations in Southeast Vermont. In E. Zen, W.S. White, J.B., Hadley and J.B. Thompson Jr., Eds., *Studies of Appalachian geology: Northern and maritime*: p. 85-202. Interscience Publishers, New York, N.Y.
- Rosenfeld, J. (1970) Rotated garnets in metamorphic rocks. *Geological Society of America Special Paper* 129, 102 p.
- Schoneveld, C. (1977) A study of some typical inclusion patterns in strongly paracrystalline rotated garnets. *Tectonophysics*, 39, 453-471.
- Schreurs, J. and Westra, L. (1986) The thermotectonic evolution of a Proterozoic, low pressure granulite dome, West Uusimaa, SW Finland. *Contributions to Mineralogy and Petrology*, 93, 236-250.

- Schumacher, J.C. (1988) Stratigraphy and geochemistry of the Ammonoosuc Volcanics, central Massachusetts and southwestern New Hampshire. *American Journal of Science*, 288, 619-663.
- Schumacher, J.C., Schumacher, R., and Robinson, Peter (1989) Acadian metamorphism in central Massachusetts and south-western New Hampshire: evidence for contrasting P-T trajectories. In J.S. Daly, R.A. Cliff and B.W.D. Yardley, Eds., *Evolution of metamorphic belts*, Geological Society Special Publication no. 43, 453-460.
- Simpson, C. and Schmid, S.M. (1983) An evaluation of criteria to deduce the sense of movement in sheared rocks. *Geological Society of America Bulletin*, 94, 1281-1288.
- Simpson, C. and Wintsch, R.P. (1989) Evidence for deformation-induced K-feldspar replacement by myrmekite. *Journal of Metamorphic Geology*, 7, 261-275.
- Skjernaa, L. (1989) Tubular folds and sheath folds: definitions and conceptual models for their development, with examples from the Grapesvare area, northern Sweden. *Journal of Structural Geology*, 11, 6, 689-703.
- Smith, J.V. and Brown, W.L. (1988) *Feldspar Minerals, Vol. 1, Crystal Structures, Physical, Chemical and Microtextural Properties*, 828 p. Springer-Verlag, Berlin.
- Springston, G.C. (1990) Stratigraphy and structural geology of the Royalston-Richmond area, Massachusetts-New Hampshire, 100 p. M.S. thesis, University of Massachusetts, Amherst.
- Spry, A. (1969) *Metamorphic Textures*, 350 p. Pergamon Press, Oxford.
- Stanley, R.S. and Ratcliffe, N.M. (1985) Tectonic synthesis of the Taconian orogeny in western New England. *Geological Society of America Bulletin*, 96, 1227-1250.
- Steinhardt, C.K. (1989) Lack of porphyroblast rotation in non-coaxially deformed schists from Petrel Cove, South Australia, and its implications. *Tectonophysics*, 158, 127-140.
- Thompson, J.B., Jr., Robinson, Peter, Clifford, T.N., and Trask, N.J., Jr., (1968) Nappes and gneiss domes in west-central New England. In E. Zen, W.S. White, J.B. Hadley and J.B. Thompson Jr., Eds., *Studies of Appalachian geology: Northern and maritime*, p. 203-218. New York, Interscience Publishers.

- Thompson, P.J., Elbert, D.C., and Robinson, Peter (1987) Thrust nappes superimposed on fold nappes: A major component of early Acadian tectonics in the central Connecticut Valley region, New England. Geological Society of America Abstracts with Programs, 19, 868.
- Tracy, R.J., Robinson, Peter and Thompson, A.B. (1976) Garnet composition and zoning in the determination of temperature and pressure of metamorphism, central Massachusetts. American Mineralogist, 61, 762-775.
- Trouw, R. (1973) Structural geology of the Marsfjallen area, Caledonides of Vasterbotten, Sweden. Svergies Geologiske Undersokning, Series C, 689, 1-115.
- Tucker, R.D. (1977) Bedrock geology of the Barre area, central Massachusetts, Contribution no. 30 (M.S. thesis), 132 p. Department of Geology and Geography, University of Massachusetts, Amherst.
- Tucker, R.D., Robinson, Peter and Hollocher, K.T. (1988) U-Pb zircon, titanite, and monazite dating in "basement" rocks of the Bronson Hill anticlinorium, central Massachusetts. Geological Society of America Abstracts with Programs, 20, 7, A216.
- Tucker, R.D., and Robinson, Peter (1990) Age and setting of the Bronson Hill magmatic arc: A re-evaluation based on U-Pb zircon ages in southern New England, Geological Society of America Bulletin, 102, 1404-1419.
- Tucker, R.D. and Robinson, Peter (1991) Age of inherited components in composite, single zircons from the Dry Hill Gneiss, central Massachusetts: evidence concerning the "basement" of the Bronson Hill magmatic arc. Geological Society of America Abstracts with Programs, 23, 1, 141.
- Tullis, J. (1983) Deformation of Feldspars. In P.H. Ribbe, Ed., Feldspar Mineralogy, Mineralogical Society of America short course notes, 2, 297-323.
- Urai, J.L., Means, W.D. and Lister, G.S. (1985) Dynamic recrystallization of minerals. In B.E. Hobbs and H.C. Heard, Eds., Mineral and rock deformation: Laboratory studies, Geophysical Monograph 36, p. 161-199.
- Vernon, R.H. (1987) A microstructural indicator of shear sense in volcanic rocks and its relationship to porphyroblast rotation in metamorphic rocks. Tectonophysics, 95, 127-133.
- Vernon, R.H. (1988) Microstructural evidence of rotation and non-rotation of mica porphyroblasts. Journal of Metamorphic Geology, 6, 595-660.

- Vernon, R.H. (1989) Porphyroblast-matrix microstructural relationships: recent approaches and problems. In J.S. Daly, R.A. Cliff and B.W.D. Yardley, Eds., *Evolution of Metamorphic Belts*, Geological Society Special Publication No. 43, p. 83-102.
- Vernon, R.H. (1991) Questions about myrmekite in deformed rocks. *Journal of Structural Geology*, 13, 9, 979-985.
- Vollmer, F.W. (1988) A computer model of sheath-nappes formed during crustal shear in the Western Gneiss Region, central Norwegian Caledonides. *Journal of Structural Geology*, 10, 7, 735-743.
- Webster, J.R. and Wintsch, R.P. (1987) Geochemistry and origin of the Killingworth dome rocks, Bronson Hill anticlinorium, south-central Connecticut. *Geological Society of America Bulletin*, 98, 465-474.
- White, S.H., Burrows, S.E., Carreras, J., Shaw, N.D., and Humphreys, F.J. (1980) On mylonites in ductile shear zones. *Journal of Structural Geology*, 2, 23-47.
- Zartman, R.E. and Naylor, R.S. (1984) Structural implications of some radiometric ages of igneous rocks in southeastern New England. *Geological Society of America Bulletin*, 95, 522-539.
- Zen, E-an, Ed., Goldsmith, R., Ratcliffe, N.M., Robinson, Peter, and Stanley, R.S., Compilers, (1983) *Bedrock geological map of Massachusetts*. U.S. Geological Survey, scale 1:250,000, 3 sheets.
- Zwart, H.J. (1962) On the determination of polymetamorphic minerals associations, and its application to the Bosost area (Coastal Pyrenees). *Geologische Rundschau*, 52, 38-65.

Plate 1. Sample Locations and Geologic Map of Metamorphic Rocks: Northern Part of the Pelham Dome

Metamorphic Rock Units

Lower Devonian Erving Fm. Deg: interlayered granular feldspar-biotite rock and biotite-garnet-staurolite-kyanite schist Dea: epidote amphibolite

Lower Devonian Littleton Fm. D1: graphitic muscovite-biotite-garnet-staurolite schist

Silurian Clough Quartzite Sc: muscovitic quartzite, commonly conglomeratic

Ordovician Partridge Fm. Ops: rusty-weathering quartz-biotite-muscovite-garnet schist with minor quartzite and felsic gneiss Opa: medium-grained hornblende amphibolite, not differentiated in all areas.

Ordovician Four Mile Gneiss Ofm: biotite-quartz-feldspar and hornblende-plagioclase gneisses

Late Proterozoic Poplar Mountain Gneiss Zpmg: gneiss member, gray feldspar-quartz-biotite gneiss with large microcline megacrysts Zpmq: quartzite member basal feldspathic quartzite Zpmjh: Jerusalem Hill member, pink felsic gneiss with hornblende and feldspar megacrysts Zpmg: zone of interlayered gneiss member and quartzite

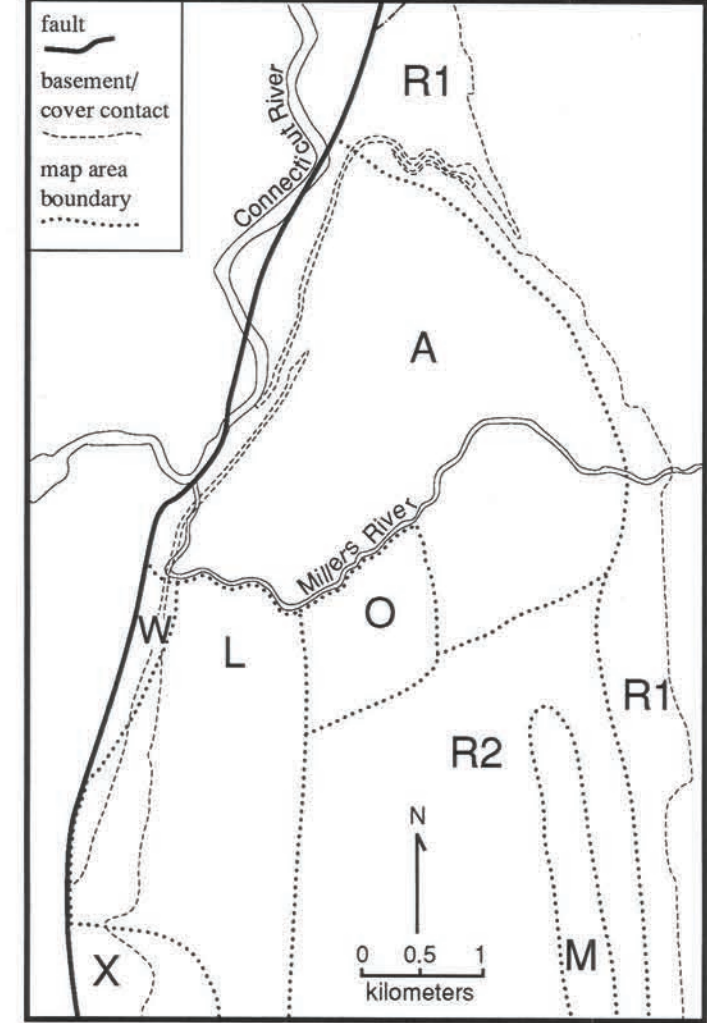
Late Proterozoic ? Mount Mineral Fm. Zmm: Zpmg was previously correlated with Zmm: quartz-biotite-garnet-aluminosilicate schist with amphibolite and quartzite, but recent reassignment of part of this formation to the Silurian has made southern extension of the Zpmg uncertain.

Late Proterozoic Dry Hill Gneiss Zdh: hornblende member, foliated pink quartz-feldspar-hornblende gneiss, with feldspar megacrysts and biotite Zdb: biotite member, foliated pink quartz-feldspar-biotite gneiss, with feldspar megacrysts Zpq: Pelham quartzite member, feldspathic quartzite with actinolite Zdq: other impure quartzites within the Dry Hill gneiss

Symbols

Fault --- Contact - - - - -

Sources for Geological Contacts Shown



- A mapped by Ashenden (1973)
- L mapped by Laird (1974)
- M mapped by Michener (1984)
- O mapped by Onasch (1973)
- R1 mapped by Robinson (1963)
- R2 mapped by Robinson (unpublished)
- W mapped by Willard (1952)
- X student mapping projects for the University of Massachusetts (1963-1964)

For highest accuracy of contact locations consult original sources

